Estimation of Pressuremeter Modulus

From Shear Wave Velocity

In the Sonoran Desert

by

Ashley Elizabeth Evans

A Dissertation Presented in Partial Fulfillment
of the Requirements for the Degree
Doctor of Philosophy

Approved July 2018 by the
Graduate Supervisory Committee:

Sandra Houston, Co-Chair
Claudia Zapata, Co-Chair
Leon van Paassen

ARIZONA STATE UNIVERSITY

August 2018

ABSTRACT

Laterally-loaded short rigid drilled shaft foundations are the primary foundation used within the electric power transmission line industry. Performance of these laterally loaded foundations is dependent on modulus of the subsurface, which is directly measured by the Pressuremeter (PMT). The PMT test provides the lateral shear modulus at intermediate strains, an equivalent elastic modulus for lateral loading, which mimics the reaction of transmission line foundations within the elastic range of motion. The PMT test, however, is expensive to conduct and rarely performed. Correlations of PMT to blow counts and other index properties have been developed but these correlations have high variability and may result in unconservative foundation design. Variability in correlations is due, in part, because difference of the direction of the applied load and strain level between the correlated properties and the PMT. The geophysical shear wave velocity (S-wave velocity) as measured through refraction microtremor (ReMi) methods can be used as a measure of the small strain, shear modulus in the lateral direction. In theory, the intermediate strain modulus of the PMT is proportional to the small strain modulus of S-wave velocity. A correlation between intermediate strain and low strain moduli is developed here, based on geophysical surveys conducted at fourteen previous PMT testing locations throughout the Sonoran Desert of central Arizona. Additionally, seasonal variability in S-wave velocity of unsaturated soils is explored and impacts are identified for the use of the PMT correlation in transmission line foundation design.

ACKNOWLEDGMENTS

I would like to thank all the people who helped and supported me through my dissertation. This dissertation has taken me on an interesting journey, one that I would not trade for the world.

I would like to thank my committee for guiding me through and helping me find my place as an engineer.

I would like to thank my daughter for sleeping just long enough so that I can write, hopefully I can live up to her title of "doctor of the dirt". This endeavor would not be possible without the love and support of my fiancé, who has helped me through every stage of the project.

This project would not be possible without the years of research conducted by Peter Kandaris, Mike Rucker, and Jim Adams. I am grateful that they were so willing to pass on data and help direct me in research, hopefully I can return the favor for a future student.

A very special thank you is for Tiana Rasmussen who taught me how to swing a sledge hammer, put up with my never-ending questions about geophysics, and made sure the data was collected and interpreted correctly.

I would like to acknowledge the contributions made by DiGioia Gray, Amec Foster Wheeler, and the Salt River Project for providing the resources, mentorship, and support for this research.

TABLE OF CONTENTS

LIST OF TABLES

Table Page

LIST OF FIGURES

Figure Page

Figure Page

Figure Page

Figure Page

CHAPTER 1

FOUNDATION DESIGN IN THE SONORAN DESERT USING MODULUS

To meet the increased demand from renewable energy sources and increased infrastructure requirements, the electric utility industry is undergoing a wave of construction of new transmission lines and retrofitting of exiting transmission lines. Design improvements for transmission line structures (monopoles, lattice towers and H-frame structures) have reduced the cost of construction, but there has been little improvement to the design of foundations for these structures. Currently, there are no standards in the electric utility industry for foundation design (Kandaris et al. 2017). Foundation design is largely based on local practice and limited guideline documents. Without standards, foundation design in the electric utility industry tends to be overly conservative and limited understanding of foundation design has driven up the cost, construction and schedule for transmission line projects. Improvements in foundation design, therefore, have the potential for large cost savings.

Nearly every transmission line (69kV to 500kV) is supported by, drilled shaft, deep foundations loaded primarily in the lateral direction. These tall transmission structures transfer large overturning reactions generated from line tension and wind load to the foundation. To meet clearance requirements set by the North American Electric Reliability Corporation (NERC), the top of foundation rotation is restricted (Boland et al., 2015; Kandaris et al. 2012). Full scale testing of transmission line foundations has identified the fundamental behavior as a rigid shaft, where the elastic modulus of the foundation is assumed constant (EPRI EL-2197, 1982) (see Chapter 6). These rigid shaft foundations are also considered short, with typical depth to diameter ratios of less than 10 to 1 (e.g. Broms, 1964). Due to the rotation limit, the rigidity and the short embedment, the foundation element remains in the elastic range of motion.

The major factor that controls the performance of transmission line foundation then is the stress-strain behavior of subgrade material subjected to lateral pressure by the foundation, which is known in the industry as the deformation modulus. Direct measurement of the deformation modulus is done through down hole pressuremeter (PMT) testing (e.g. Mendard, 1975; Briaud, 1992). The PMT measures the stress-strain response of the subsurface in the horizontal direction. The PMT has been widely used for transmission line foundation design models (e.g. Briaud et al., 1984; EPRI 1982; Kalaga and Yenumula, 2017; Budhu, 1987). Theoretically, the way the PMT loads the soil is similar to how transmission line foundations load the soil. Thus, the deformation modulus determined in this fashion is thought to be more relevant to foundation behavior than an elastic modulus determined from a laboratory test wherein specimens are loaded vertically, or through correlations based on such laboratory tests. Furthermore, field testing minimizes sampling disturbance associated with laboratory test results. As a result, the primary commercially available foundation design model in the electric utility industry requires the deformation modulus from PMT testing as an input (EPRI, 1982).

The cost of PMT testing is high compared to other forms of subsurface testing and is rarely conducted in practice. Direct-subsurface sampling is limited, as it is common practice in the electric utility industry to only have a single boring for every 10 structures. For a recent 191-mile transmission line in Iowa, only 114 auger borings, 38 cone penetrometer tests and 14 pressuremeter tests were conducted for the design of over 1000 monopole structures (Kandaris et al., 2017). In cases like these, the rough and highly variable terrain that transmission lines cross further limit the ability to directly test the subsurface (CEATI, 2017). As a result, correlations to PMT modulus based on less expensive and easier field tests (e.g. SPT, geophysical

methods) are used to design foundations (Kandaris, 1994; Briaud et al., 1982; Duncan and Bursey, 2014). A number of global correlations between PMT modulus and other field tests are available, but have wide scatter and require refinement for specific geologic conditions (Kulhawy and Mayne, 1990).

In the desert setting, correlations to soil index properties are further complicated due to unsaturated and cemented soil conditions. In addition, the large cobble deposits that form alluvial terraces create challenges for direct subsurface sampling (Durkee et al., 2007). Previous correlations in the central Arizona have found a direct correlation between increased cementation and PMT modulus (Kandaris, 1994). Likewise, previous laboratory and field testing conducted by others indicate that the degree of matric suction has a significant influence on the PMT modulus (Massarasch, 2004; Miller and Muraleetharan, 2000; Pereira et al., 2003). As a result, any correlations to PMT modulus should account for both the degree of cementation and the effects of matric suction in unsaturated soil conditions. Changes in soil matric suction are of most concern at shallow depths, because, it is the shallow depth soil response that dominates the pier rotation.

Recent advances in seismic refraction have allowed for more nuanced interpretation of soil properties including estimates of cementation and matric suction (Robertson and Ferreira, 1993; Duncan and Bursey, 2014; Rucker and Fergason, 2006; Rucker, 2008; Whalley, 2012; Grelle and Guadagno, 2009). Unlike other testing methods, seismic refraction analyses produce a direct measure of the low strain elastic modulus of soil mass, based on wave speed and wave propagation (Grelle et al., 2009). The shear wave velocity (S-wave velocity) can be obtained from refraction microtremor (ReMi) survey and used to calculate low-strain shear modulus. In theory, the low strain (dynamic) shear modulus from S-wave velocity is proportional to the intermediate strain (static) shear modulus from PMT testing, as

both are measures of lateral resistance of the subsurface. However, nonlinearity of modulus over the stress-strain range of interest brings into question this proportionality assumption, particularly for unsaturated and cemented soils.

The goal of the following research is to define the relationship between low and high strain shear modulus to allow for use of S-wave velocity for calculation of the PMT modulus (Figure 1). By developing a correlation that accounts for the effects of cementation and matric suction, as well as differences in strain level, foundation design may be improved. Furthermore, the following research suggests that modulus of unsaturated and cemented soils is underestimated by traditional correlations resulting in conservativeness of transmission line foundation design.

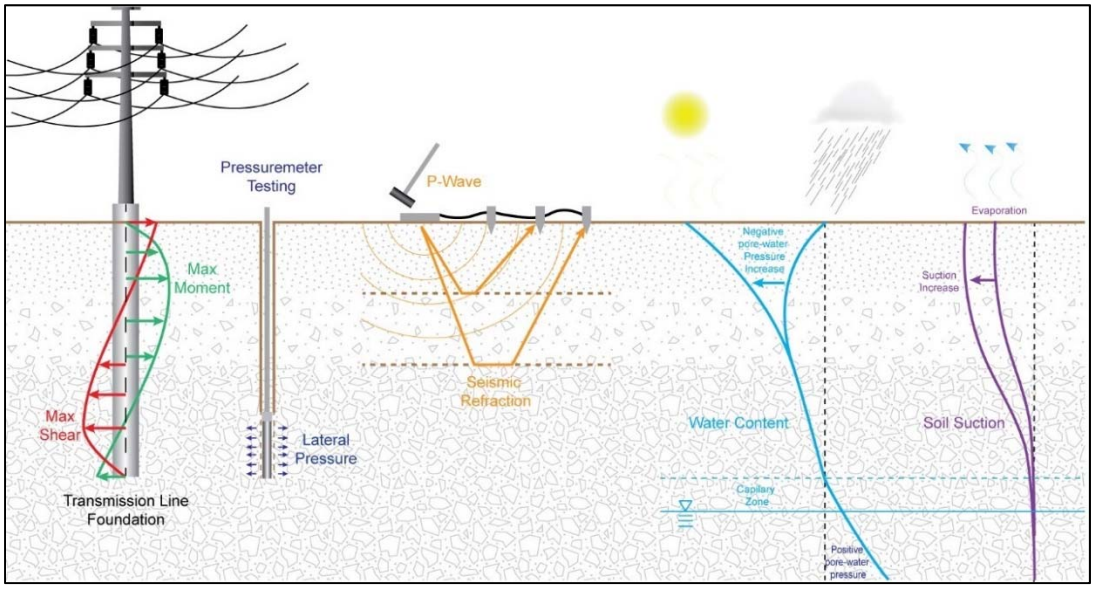

Figure 1. Illustration of relationship of laterally loaded foundation, subsurface testing and unsaturated soil mechanics

Several different datasets with PMT tests, standard penetration tests, and geophysical surveys were used to evaluate the existing trends in PMT modulus, account for variation in S-wave velocity, and develop a correlation between PMT modulus and S-wave velocity. Additional geophysical surveys were conducted as part

of this research to expand the existing datasets. All datasets are from testing sites located across the Sonoran Desert of central Arizona (Figure 2).

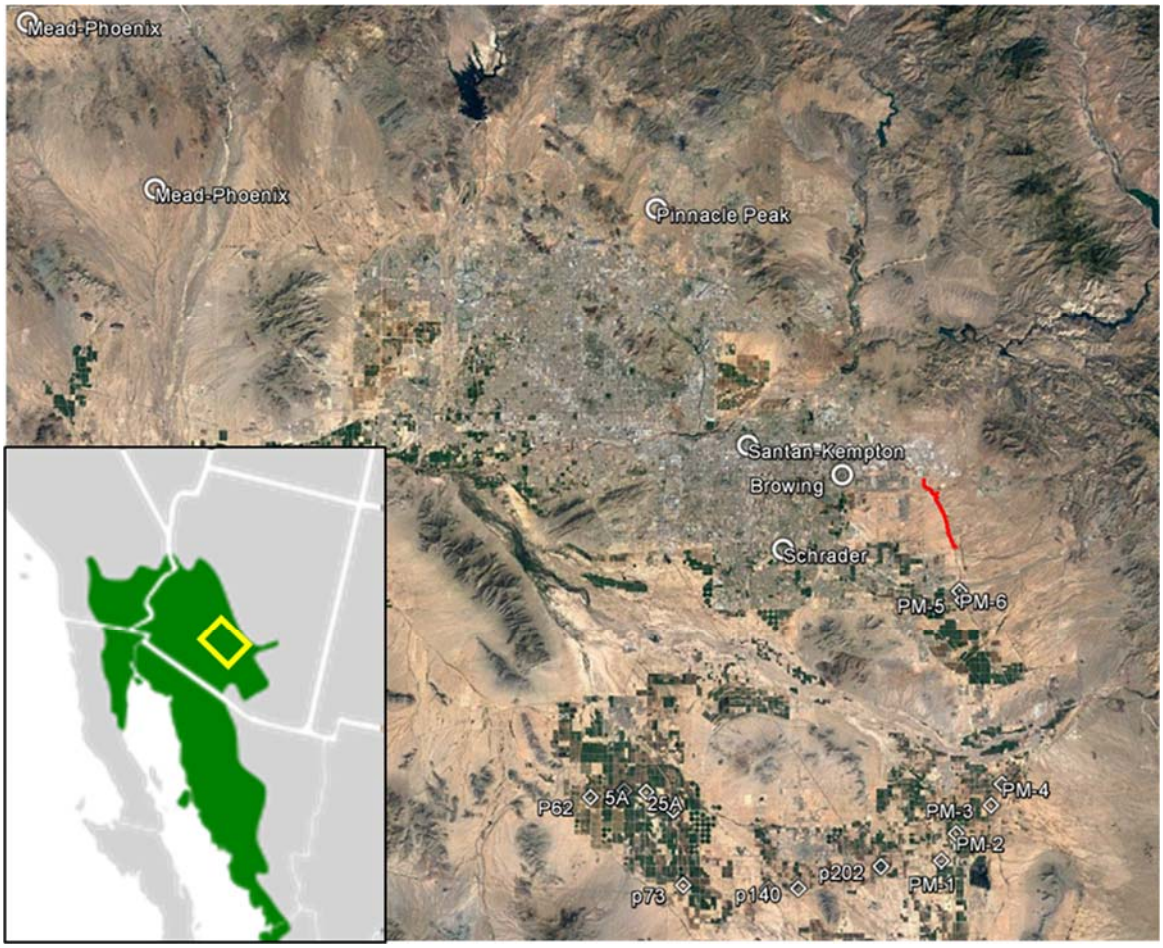

Figure 2. Map of testing locations in the Sonoran Desert (PMT and SPT locations at circle markers; PMT with SPT and seismic refraction survey at diamond markers; geophysical survey at red line)

The development of the PMT modulus correlation for transmission line foundation design is split into separate chapters as follows:

Chapter 2: Provides the background literature review for the correlation between PMT modulus and S-wave velocity.

Chapter 3: The variability and limitations of existing correlations of PMT modulus with standard penetration testing (SPT) blow count values are evaluated. Additional PMT testing data was provided from the Salt River Project (SRP) that increased the number of PMT testing

site across central Arizona. New correlations are proposed to refine SPT to PMT correlations.

Chapter 4: The variability in geophysical refraction wave velocity measurements is evaluated along flood retention structure sites in the Sonoran Desert. A database of geophysical survey lines and borings was provided by AMEC Foster Wheeler along the length of the Vineyard and Powerline Chanel flood retention structures. An additional six surveys were performed as part of the current analysis to evaluate seasonal variability is wave velocity measurements.

Chapter 5: Describes the development of a PMT modulus correlation to S-wave velocity for the Sonoran Desert. The correlation is based on existing PMT sites, at which additional geophysical survey was conducted. The correlation includes an estimation of a degradation factor between the intermediate strain and low strain modulus for use if Poisson's ratio and density are known. Additional correlations are provided which account for density and Poisson's ratio, as to estimate the PMT modulus directly from seismic refraction survey.

Chapter 6: The effects of using the proposed PMT correlation on transmission line foundation design is evaluated. The PMT sites are located near exiting transmission line foundations. Re-analysis of the foundation designs using the PMT modulus values and the estimated PMT modulus form S-wave velocity is shown to have minimal effect on foundation design.

Chapter 7: Provides a discussion on the limitations of the proposed modulus correlation, the use of correlations in transmission line foundation design, and recommendations for future research.

CHAPTER 2

WHAT IS MODULUS?

DEFINITION OF MODULUS

The word modulus simply means a ratio. In engineering terms, a modulus is a single ratio used to define the stress-strain characteristics of a material. In geotechnical engineering terms, modulus is a representation of the deformation behavior of the subsurface. Modulus is a property of the subsurface material and is largely a function of stress state, because this property is nonlinear and stress dependent (Kulhawy and Mayne, 1990). The stress state of soil in broad terms is affected by the direction of loading, packing of particles, degree of saturation, matric suction, stress history and degree of cementation (e.g. Duncan et al., 2013).

As the modulus is a function of stress state, researchers have defined modulus by type of loading, direction of loading, and confining conditions (Table 1). The directionality of applied forces, area of analysis, size of strain and duration of loading all impact the measurement of modulus (Briaud 2013). When defining modulus, the directionality of the applied forces and reactions matter because of the anisotropy of the soil mass. In practice, engineers separate vertical soil reactions from horizontal soil reactions to describe different loading conditions. This research focuses on PMT modulus (E_{PMT}), which is a deformation modulus that is calculated using the Poission's ratio (ν) to convert the measured static shear modulus (G). Poisson's ratio is the ratio of radial strain to axial strain and is typically measured with triaxial test in the laboratory or through geophysical wave velocity measurements. The static shear modulus, as measured during PMT testing, is the shear stress to shear strain relationship from horizontal loading under static conditions. Similarly, the shear modulus (G_d) as derived from ReMi S-wave velocity

is a measurement of shear stress to shear strain from a shear wave (V_s) traveling nearly horizontally through the soil of a given density (ρ) under dynamic conditions.

Table 1

Modulus parameters (adapted from Hunt 1983, Table 3.34)

Parameter	Stress-Strain Relationship	Correlation Equation	Description
Static Modulus			
Young's Modulus	$E_y = \sigma/\varepsilon$	$E_y = \mathrm{G}(2 + 2\upsilon)$	Uniaxial stress to axial strain
Shear Modulus (rigidity)	$G = \tau_{zx}/\gamma_{zx}$	$G = E_y/(2 + 2\upsilon)$	Shear stress to shear strain
Bulk Modulus (incompressibility)	$B = \sigma_o/\varepsilon_v$	$B = E_y/(3 - 6\,\upsilon)$	Multi-axial stress to volumetric strain
Constrained Modulus (confined)	$M = \sigma_a/\varepsilon_a$	$M = \frac{E_y(1-\upsilon)}{(1+\upsilon)(1-2\upsilon)}$	Uniaxial stress to uniaxial strain
Pressuremeter Modulus (deformation)	$E_{PMT} = \sigma_z/\varepsilon_z$	$E_{PMT} = G * (2 + 2\upsilon)$ $E_{PMT} = E_y * a$	Horizontal stress to strain
Dynamic Modulus			
Dynamic Young's Modulus	$E_{yd} = \sigma/\varepsilon$	$E_{yd} = \frac{G_d(3M_d - 4G_d)}{M_d - G_d}$	Dynamic normal stress to strain
Dynamic Shear Modulus	$G_d = \tau/\gamma$	$G_d = \rho\left(V_s{}^2\right)$	Dynamic shear to shear strain
Dynamic Constrained Modulus	$M_d = \sigma/\varepsilon$	$M_d = \rho\left(V_p{}^2\right)$	Dynamic uniaxial stress to uniaxial strain

Researchers have found that the stress-strain relationship of soil can often be represented as a hyperbolic function (Vucetic and Dobry, 1991; Duncan and Chang, 1970; Kulhawy et al., 1969). For foundation design the complex stress-strain function is often reduced to a linear relationship (i.e. tangent modulus, secant modulus, Young's modulus). A single ratio or linear approximation is only accurate for a material that is linearly elastic, which is not the case for most subsurface materials. This is particularly true of soils, which have a highly non-linear stress-strain response. As a result, numerous different moduli have been defined depending on which points are selected on a stress-strain curve (Figure 3). The simple

conceptualization of modulus as a given slope of a materials stress-strain characteristics is only correct for a limited set of conditions (Briaud, 2001).

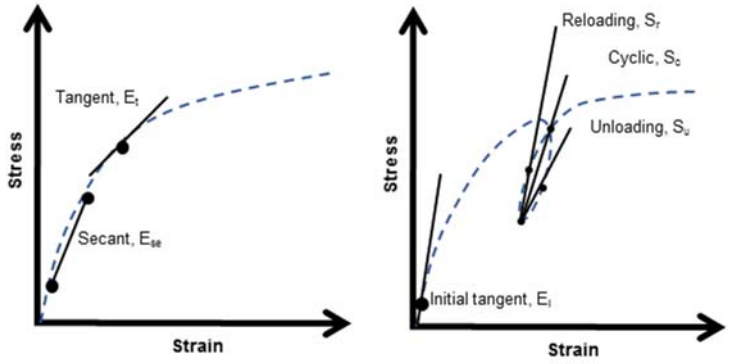

Figure 3. Different forms of moduli (adapted from Briaud, 2001)

This research focuses on the PMT modulus which is a secant modulus and the seismic refraction velocity based shear modulus is an initial tangent. The secant is a line that intersects a curve at two points and the tangent is the derivative of a single point on a curve (Figure 3). Several authors propose a method that relate the low strain modulus to the high strain modulus by comparison with the reloading modulus, which is thought to be a good approximation of the initial modulus (Massarsch, 2004; Hammam and Eliwa, 2012; Robertson and Ferreira, 1993; Robbins, 2013; Rucker, 2008).

The magnitude, direction and duration of strain affect the interpretation of modulus (Figure 4). At small strains the soil is loaded within the elastic range of motion, where incremental loading and unloading produce small changes in deflection. At large strains, the soil is loaded in the plastic range of motion, where incremental loading and unloading produce large changes in deflection. "Soil is commonly considered essentially linear elastic at small strains" (Hardin, 1978; Jardine et al., 1984; Robertson and Ferreira, 1993); where large strains are influenced by stress path, strain rate effects and state boundary conditions

(Robertson and Ferreira, 1993). Several researchers have defined the relationship between small shear strain (dynamic) and large shear strain (static) modulus (Seed et al., 1984; Hammam and Eliwa, 2012; Robertson and Ferreira, 1993). The small shear strain modulus is considered a maximum (steeper slope on the stress-strain curve) compared to the large strain moduli (flatter slope on the stress-strain curve). There are currently no devices that can determine both the small strain and large strain modulus. Instead, researchers have obtained small strain modulus from geophysical velocity measurements, used PMT testing to obtain intermediate strains modulus, and used standard penetration testing or laboratory tests to obtain large strain modulus (e.g. Robbins, 2013; Hammam and Eliwa, 2012; Rucker, 2008).

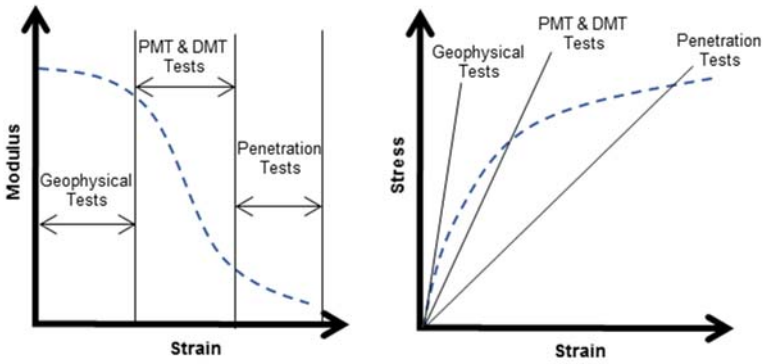

Figure 4. Range of modulus and stress for different test methods

The relationship between intermediate strain (static) and low-strain (dynamic) moduli is complicated by unsaturated soil mechanics. Where the simple strain-strain relationship is expanded to include matric suction and effects both the net normal and suction stress state variables, as follows:

$$E = \frac{(\sigma_y - u_w) - \nu(\sigma_x - \sigma_z - 2u_w)}{\varepsilon_y - (u_a - u_w)/H} \quad (1)$$

Where ν is the Poisson's ratio, σ is the total normal stress, E is the modulus, and H is the modulus of elasticity for the soil structure with respect to change in matric suction $(u_a - u_w)$, u_w is the porewater pressure, an u_a is pore air pressure (equation

rearranged from Fredlund et al. 2012, equation 13.13). The measurement of modulus then is directly affected by matric suction. The matric suction can be related to the water content of the soil by use of the soil-water character curve, which is a hyperbolic curve that typically relates decreasing volumetric water content with soil suction, depending on the degree of saturation and the particle grain size. In general, laboratory tests have shown that as pore water pressure increases (corresponding to low water content) the strength and stiffness of a soil mass increases, where the resulting moduli of an unsaturated soil then increases with increasing suction. The matric suction has been found to have a significant influence on the modulus (Miller and Muraleetharan 2000; Whalley et al. 2012). Likewise, as soil ages as identified by increased cementation, the strength and stiffness of a soil also increases (Duncan et al. 2013; Montoya and DeJong 2015). Therefore, any correlation between moduli should also account for factors of unsaturated soils including both matric suction and cementation.

The following is a discussion on the methods of measuring modulus and how factors of stress state, particularly those of unsaturated soils, affect the moduli.

MEASURING MODULUS

To measure lateral modulus, researchers have used back calculations from full scale load tests (Poulos and Davis, 1980; Callanan and Kulhawy, 1985; EPRI 1982; Ohya et al., 1982; Mayne and Frost, 1989); used cone penetration tests to directly measure at depth reactions (Mayne and Frost, 1989); correlated modulus with standard penetration tests (Goh et al., 2012 ; Ohya et al., 1982; D'Appolonia et al., 1970; Schmerttmann, 1970; Davidson, 1982; Kandaris, 2006; Bellana, 2009); and conducted detailed analysis in the laboratory using triaxial tests (Massarsch, 2004). The direct measurement of modulus in the field is limited and correlations are primarily used in practice due to the cost of direct measurements. Duncan et al.

(2014) evaluates several modulus correlations and notes that correlations should be based on appropriate soil modulus and testing conditions that relate to the material response under investigation. For the case of laterally loaded foundations, the PMT test is the most appropriate method of measurement as it mimics the loading of the subgrade, although the test only evaluates a small increment within the subsurface. Alternatively, measurement of shear modulus from S-wave velocity also provides a measure of horizontal stress-strain properties but provides an average of the subsurface. The following discussion describes the background behind PMT testing, measurement of shear modulus using geophysical survey, and correlations available between the two properties.

Intermediate strain modulus

The PMT test is the gold standard to determine the in-situ horizonal stress-strain behavior of soil (Anderson et al., 2003). The PMT test was developed by Menard (1957) and is used to calculate the PMT modulus (E_{PMT}) which is a function of the measurement of the ratio of shear pressure to volumetric strain. The details of PMT have been outlined in standards (ASTM D4719) and by numerous researchers (e.g. Briaud 2013; Kandaris, 1994). In summary, the PMT measures the shear stress and volume change of the soil by using an inflatable cylindrical probe placed in a pre-drilled borehole and the probe is expanded radially. Measurement is taken of the volume and pressure in the probe, as the probe is either inflated under equal pressure or equal volume increments. Typically, the test is stopped as measurements exceed the elastic range of motion and yielding occurs. Calibration of the devise is done to account for rigidity of the probe walls and compressibility of the fluid (also called hydrostatic pressure), as follows:

$$P = P_{reading} + P_{water} - P_{membrane} \; where \; P_{water} = \left(z + G_{height}\right) * \gamma_{water} \quad (2)$$

where the P is a function of the pressure reading, the fluid pressure, and the membrane, z is depth, G is gauge height, γ is the unit weight of water.

The secant line to the linear-elastic portion of the shear stress-volume change curve is used to calculate the intermediate strain shear modulus (G_{PMT}). The shear modulus is then converted to the confined lateral (E_{PMT}) modulus by use of the Poisson's ratio. The resulting equation for PMT modulus is as follows,

$$E_{PMT} = 2(1 + \upsilon)\, G_{PMT} \quad (3)$$

$$G_{PMT} = (V_o + V_m)\frac{\Delta P}{\Delta V} \quad (4)$$

where υ is Poisson's ratio, V_o is the zero-volume reading, V_m is the corrected volume reading, ΔP is the change in corrected pressure, ΔV is the change in corrected volume.

Relationship with Young's Modulus

The PMT modulus is not the Young's modulus; however, they are correlated by an alpha factor (α) (Menard, 1957; Gabin et al., 1996; Biarez et al., 1998). This factor has been found to be a function of material type, with values ranging from 0 to 1 (Mendard, 1957). Fawaz et al. (2014) identified the influence of cohesion and friction in defining material types on the alpha value, from field testing. Additional analysis was conducted on the relationship between limit pressure (the maximum pressure reading from PMT) to both elastic modulus and shear strength, by empirical modeling. Their study did not directly account for unsaturated soil properties and they found the greatest variation in alpha in sand (0.25 to 1), suggesting matric suction may be a factor in the correlation.

Relationship with Poisson's Ratio

The PMT modulus equation shows that the measurement is a direct measure of shear modulus and relies heavily on the Poisson's ratio (υ). Typically, an engineer selects a single value for the Poisson's ratio when calculating PMT modulus. For a given geologic setting the variability in Poisson's ratio is assumed to be small, with a

common used value of 0.33 for unsaturated soils and 0.2 for cemented soils in previous studies conducted in Arizona (SRP 2010, 2011, 2012a, 2012b). This variation is thought to be minimal compared to the measurement of modulus and in practice is considered a constant (Kulhawy et al., 1969). The Poisson's ratio, however, can range from 0.1 to 0.5 for clays and from 0.25 to 0.35 for sands (Karray and Lefebvre, 2008).

Poisson's ratio is a ratio of horizontal strain and vertical strain under uniaxial loading conditions. The coefficient of at rest earth pressure (K_o) is the ratio of horizontal stress and vertical stress relationship. As the PMT modulus is the ratio of stress to strain, holding the Poisson's ratio constant results in greater variability in the stress side of the equation (Equation 5), because Poisson's ratio is likely to change as the ratio of lateral to vertical strain changes. In theory, the elastic modulus can be related to both Poisson's ratio and the coefficient of at rest earth pressure (Equation 6 to 7). The modulus, however, is dependent on the direction of forces and the relative size of strain and these need to be comparable to create a true correlation (see Briaud, 2013).

$$E = f\left(\frac{\sigma}{\varepsilon}\right) \rightarrow E = f\left(\frac{k_o}{\nu}\right) \quad (5)$$

$$k_o = \nu/(1-\nu) \quad (6)$$

$$E = f(k_o/\upsilon) \rightarrow E = 1/(1-\nu) \quad (7)$$

Relationship to Strain

PMT can cover a wide range of strains (10^{-1} to 10^{-5} %). Some researchers have used PMT to measure the plastic range of motion (Duncan et al, 2003). The PMT, however, is not good at estimating very small strain reactions (Robertson and Ferreira, 1993). In practice, PMT testing typically covers the range of intermediate to large strain response (Figure 4). In the following discussion PMT is assumed to

provide the intermediate strain modulus as defined within the elastic range of motion.

Issues of Disturbance

The quality of the PMT test is highly dependent on the stability of the bore hole and the ability to maintain a tight clearance with the probe (ASTM D4719). Disturbance in the borehole is more common in conditions of soft clay and loose sands. Unique methods have been developed to account for hole stability issues (Durkee et al., 2005). Reduced quality of the PMT results may be indefinable in the test results, where there is a large offset form the origin (Figure 5). New methods of direct push PMT have been developed minimize sidewall instability. The following research focuses on the use of pre-drilled borehole PMT sampling. All PMT values that showed side wall stability issues were excluded from the analysis.

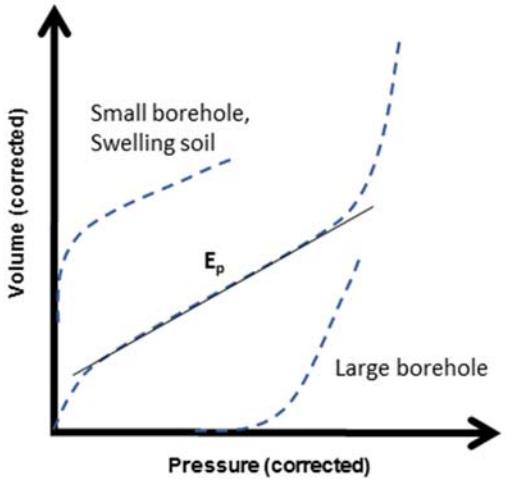

Figure 5. Variation in quality of testing

Correlations to Blow Counts

Previous research into PMT modulus have focused on providing correlations to standard penetration tests (SPT). The correlation widely used in the transmissions line industry was developed by Electric Power Research Institute (EPRI) for cohesive soils and granular soils (Figure 6) (EPRI, 1982). These correlations have a wide scatter in the data, which were largely obtained from on glacial till deposits. More recently, correlations have focused on the variability in granular soils (Duncan et al., 2013; Kandaris, 1994). Research has shown that these correlations are highly affected by grainsize and degree of cementation (Figure 7). Chapter 3 provides a detailed comparison of SPT to PMT modulus for the Sonoran Desert by adding testing sites to the existing database developed by Kandaris (1994).

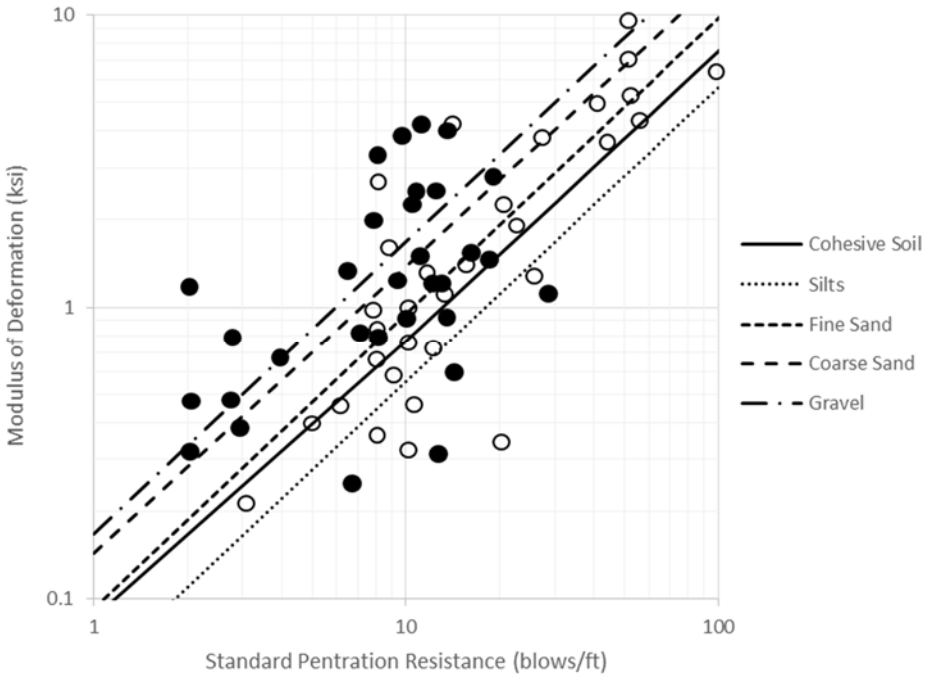

Figure 6. Correlation of PMT modulus to blow count, adapted from EPRI (1982)

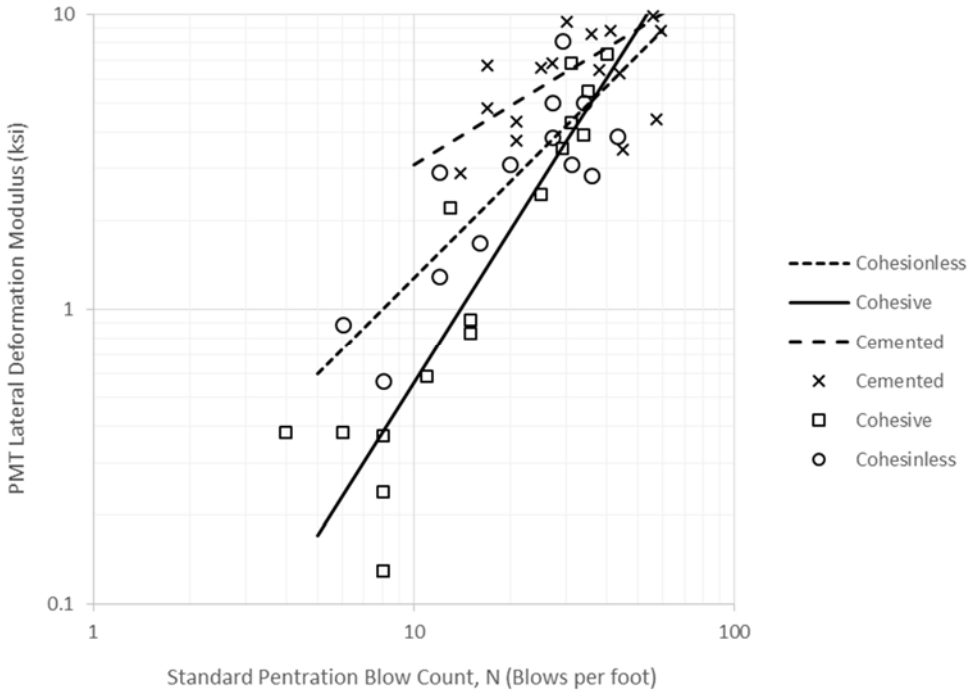

Figure 7. Correlation of PMT modulus to blow count, adapted from Kandaris (1994)

The correlations between SPT and PMT deformation modulus are variable because of the difference in directionality of the applied loads and the difference in the strain rate during loading (Figure 8). As a result, correlations between SPT and PMT modulus are highly dependent on the coefficient of at rest earth pressure (K_o) and Poission's ratio. Chapter 3 proposes correlations to account for the variation in loading and strain level between SPT to PMT modulus for the unsaturated soils in the Sonoran Desert.

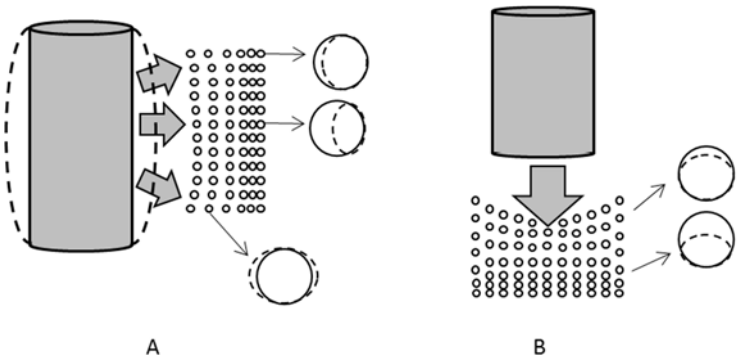

Figure 8. Illustration of forces on soil particles from PMT (A) and SPT (B)

Unsaturated Soil Conditions

Several authors have indicated a strong correlation between increased PMT modulus and suction (Pereira et al., 2003; George, 2004). This holds true, however, only for large pressure variations (deviatoric stress) because there is a threshold at which suction does not trigger a large strain response, although the threshold limit is highly debatable and a function of confining pressure. Miller and Muraleetharan (2000) estimated the effect of PMT modulus responses at different soil moisture conditions for cohesive soils; in which a decrease in saturation corresponded to an increase in matric suction and, therefore, correspond to an increase in PMT modulus. This relationship is supported by the theoretical relationship of modulus and stress states of unsaturated soils (Equation 1). A correlation then of PMT modulus to any other modulus measurement should be highly dependent on matric suction.

Full-scale Back Calculation of Lateral Modulus

For drilled shaft foundations, only full-scale testing provides a better measure than the PMT of soil-structure interaction, as a full-scale test directly incorporates the stress-strain reaction of the field soil and soil-structure interaction aspects of the foundation system (Duncan 2013). Full scale testing of laterally loaded short, rigid shaft foundations, typical of the transmission line industry are limited. The tests are largely conducted on an as needed basis and results are used for the design of a particular structure. A large regional study of multiple full scale foundation tests was conducted by the Electric Power Research Institute (EPRI 1982) and the PMT results were used to model subgrade reactions. A similar approach was used by Briaud et al. (1984) that "uses finite difference approach to the solution of the governing differential equations and relies on soil reaction curves (p-y) obtained from the PMT curve." Both approaches use a layered subgrade with corresponding PMT values to estimate the reaction of an entire laterally loaded foundation. These approaches

assumes that the individual PMT values can be used to estimate the entire subgrade reaction.

The EPRI (1982) research found the load-deflection curve to have a hyperbolic shape. Others have found that the lateral load-deflection shape is a Weibull curve (e.g. Shirito et al. 2009) (Equation 8).

$$p = p_{ult}\, e^{(-\frac{y}{\alpha})^{\beta}} \qquad (8)$$

Where p is the lateral pressure multiplied by the pier diameter, y is the horizontal deflection, α and β are curve fitting functions. The beta (β) value corresponds to a point at the end of the elastic range of motion and the alpha (α) value is a function of modulus, depth and diameter.

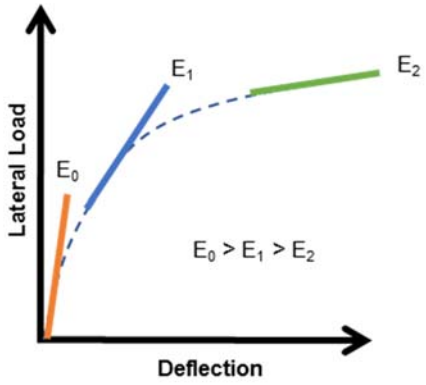

Figure 9. Relationship from full-scale testing and PMT

Low Strain Modulus Measurements

The general Weibull shape of the p-y curve indicates that the modulus decreases with increasing load; with the design deflection for a laterally loaded foundation limited to the elastic range of motion at intermediate strains. For a rigid shaft foundation, the subsurface layer with the smallest, near surface, modulus typically controls the design. The PMT values are considered relatively low modulus (E_1, Figure 9) and dynamic shear modulus are considered maxima (Briaud, 1992). A more accurate model then of a laterally loaded foundation within the elastic range of

motion, might consider measurement of the very small strain modulus, such as that obtained geophysical measurement of S-wave velocity.

Compression Wave Velocity

Seismic refraction is based on the physics of wave propagation and speed, where the velocity of a wave is a function of the wavelength and frequency. Snell-Descartes law governs how a wave refracts in different media. Therefore, as an induced wave travels through the subgrade the refraction time and distance is measured. The velocity will vary depending on the density of the subgrade.

Traditional near-surface seismic refraction surveys are used to evaluate the thickness of overburden soils and depth to rock or rock-like materials by measuring compression waves (P-waves) (Hunt, 1984; Thornburgh, 1930). The compression wave travels at a constant speed, which is dependent on the density and constrained modulus of the material (Robbins, 2013) (Figure 10). Where the constrained modulus is defined as follows:

$$M_d = \rho(V_p^{\,2}) \qquad (9)$$

where, M_d is the dynamic constrained modulus, ρ is the density, V_p is the compression wave velocity (P-wave velocity). Until recently, the use of seismic refraction has been limited because P-wave velocity measurements can only increase with depth, therefore "hiding" soil layers of lower density materials. As a result, traditional compression wave studies are often un-conservative in their layer identification.

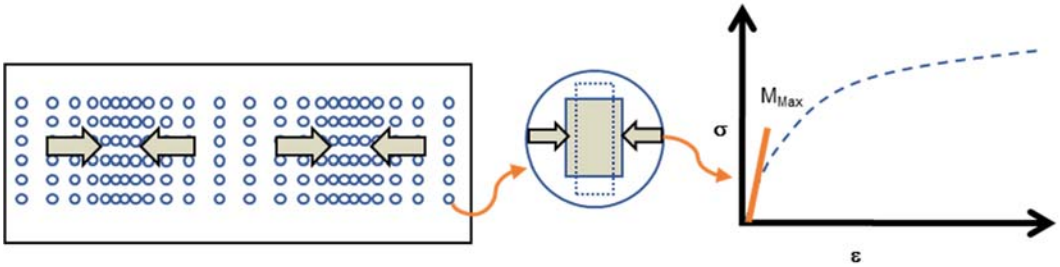

Figure 10. Relationship between compression wave (a), particle forces (b), and constrained modulus (c) (adapted from Karray and Hussien, 2016)

Shear Wave Velocity

To identify lower velocity layers that might be hiding, refraction microtremor (ReMi) surveys use surface wave methods for measuring Rayleigh-waves (Louie, 2001; Rucker, 2003; Robbins, 2013). ReMi surveys provide an indirect measure of S-wave velocity by taking the inverse of the dispersive Rayleigh wave, which is a body wave (Louie, 2001) (Figure 11). The resulting profiles identify "hidden" lower velocity layers (also known as velocity reversals). Note that the curve fitting of ReMi data is a non-unique result and variation at depth can be caused by near surface variability in both saturation and inclination of subgrade horizons. To account for near surface anomalies, the S-wave velocity should be used in conjunction to evaluate the dispersion curve and the S-wave velocity profiles.

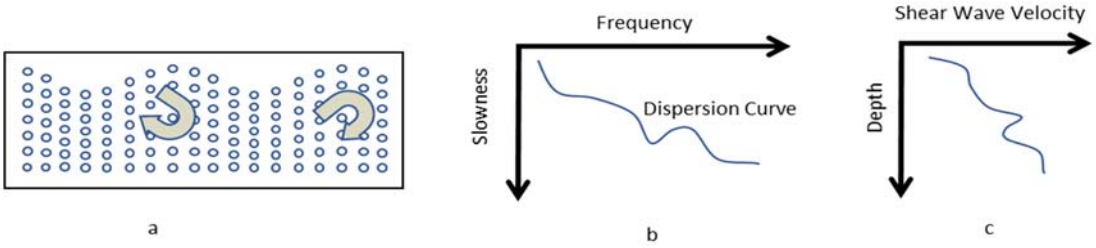

Figure 11. Conversion of Rayleigh Wave (a) to dispersion curve (b) to shear wave velocity profile (c)

The calculated S-wave velocity then can be used as a measurement of dynamic shear modulus by accounting for density (Figure 12).

$$G_d = \rho(V_s^2) \qquad (10)$$

where G_d is the dynamic shear modulus, ρ is the density, V_s is the shear wave velocity. Where the dynamic shear modulus is largely a function of density of the soil skeleton, as shear waves are impeded by water. By comparing the S-wave and P-wave velocity the water table can also be identified (Grelle and Guadagno, 2009).

The dynamic shear modulus is a function of very low strain and is often referred to as a maximum modulus, whereas large strain modulus such as form a PMT is considered a minimum or static modulus (Robertson and Ferreira, 1992) (Figure 4 and Figure 9). The typical range of strain level associated with S-wave velocity are on the order of 10^{-4} to 10^{-6} %.

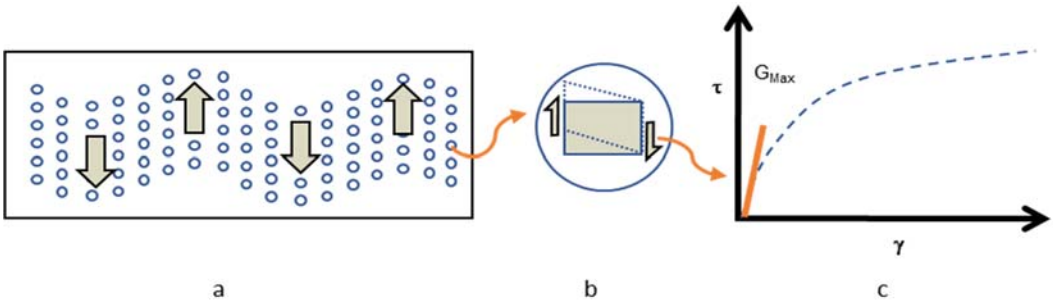

Figure 12. Relationship between shear wave (a), particle forces (b), and constrained modulus (c) (adapted from Karray and Hussien, 2016)

Relationship with Poison's Ratio

As with intermediate strain modulus, low strain modulus has a direct relationship to Poisson's ratio (see correlation equations in Table 1). Poisson's ratio is often expressed as a complex ratio of S-wave and P-wave velocity, however these velocities are dependent on the directionality of the wave, as they are a measure of different strains in the soil mass. To get a true Poisson's ratio, the directions of the waves need to be orthogonally oriented, which requires adjustment of the geophone alignment and direction of applied forces between measurement of S-wave and P-wave velocities. Depending on the setup of geophysical wave survey the ratio of shear to compression wave may not be an appropriate estimate of Poisson's ratio (Grelle et al. 2009; Karry and Lefebvre, 2008). Assuming the orthogonal relationship of compression to shear wave then,

$$\nu = \frac{2V_p^2 - V_s^2}{2\left(V_s^2 - V_p^2\right)} \qquad (11)$$

where υ is the Poisson's ratio, V_p is the compression wave velocity, and V_s is the shear wave velocity. When the Poisson's ratio is 0.33 then the S-wave velocity is about half of the P-wave velocity.

The setup of the geophones, directionality of the imparting force, and directionality of the waves affects the geophysical interpretation. The following research uses the same alignment in of geophones for both the S-wave velocity and P-wave velocity measurement, with the direction of force of the compression wave imparted perpendicular to the geophone alignment. The geometric relationship of waves as defined for Equation 11 is not appropriate for comparing surface ReMi based S-wave velocity measurements with P-wave velocity, using the same geophone alignment, due to the similar directionality in the compression and Rayleigh waves. However, the variation in wave velocities between S-waves (derived from ReMi Rayleigh waves) and the P-waves may be useful for estimating other parameters.

Relationship to Strain

Unlike the PMT testing, direct measurement of the strain is difficult for seismic refraction velocity testing outside of the laboratory. High strain shear modulus is expected to be on the order of 10^{-3} % of low strain modulus (Seed et al., 1984). This is because the slope of the shear stress-strain curve is steeper at small, dynamic strains than at intermediate, static strains (Figure 4, Figure 9). As strain increases, there is a point where dynamic and static modulus ratio are equal to each other, which likely occurs in dense rock materials (Rucker, 2008).

Correlations to Standard Penetration Test

The correlation between standard penetration test (SPT) blow count (N) with shear wave velocity is commonly used in earthquake related designs (Karray and

Hussien, 2016). These correlations are typically used as an estimate for seismic site hazard classifications. The general form of most of these relationships is as follows,

$$V_s = a * N^b \quad (12)$$

where N is the corrected blow count, a and b are from a statistical regression of the dataset. For use in this relationship, the blow count is not typically corrected for overburden pressure but for hammer energy, rod length, and sampler diameter. In this formula alpha controls the amplitude and beta controls the curvature. In particular, the void ratio and relative density directly influence the alpha and beta factor. The correlations between V_s and N, are geologically specific and highly dependent on material type. Chapter 3 provides an estimate of the correlation between S-wave velocity and N for the Sonoran desert samples.

Relationship to Porosity

Granular materials do not have a true linear-elastic response like most rock (Rucker and Fergason, 2006; Rucker, 1998). Rucker's (2008) research points to a non-linearity when calculating the dynamic shear modulus of granular soils (Figure 13). He proposes the use of a percolation theory to calculate the velocity measurements from seismic refraction data with modulus behavior. Percolation theory assumes that rocks and cohesive soils act as chemical gels, whereas granular soils and fractured rock act as physical gels. Percolation theory models both the density (packing of particles) and elasticity (interconnectedness) of the subsurface materials.

$$E_{Max} = k\,(P_c - P)^f \quad (13)$$

where E_{Max} is the low stain modulus, P_c is the percolation threshold porosity, P is the material porosity, k is a proportionality constant, and the exponent f is a parameter based on modulus behavior.

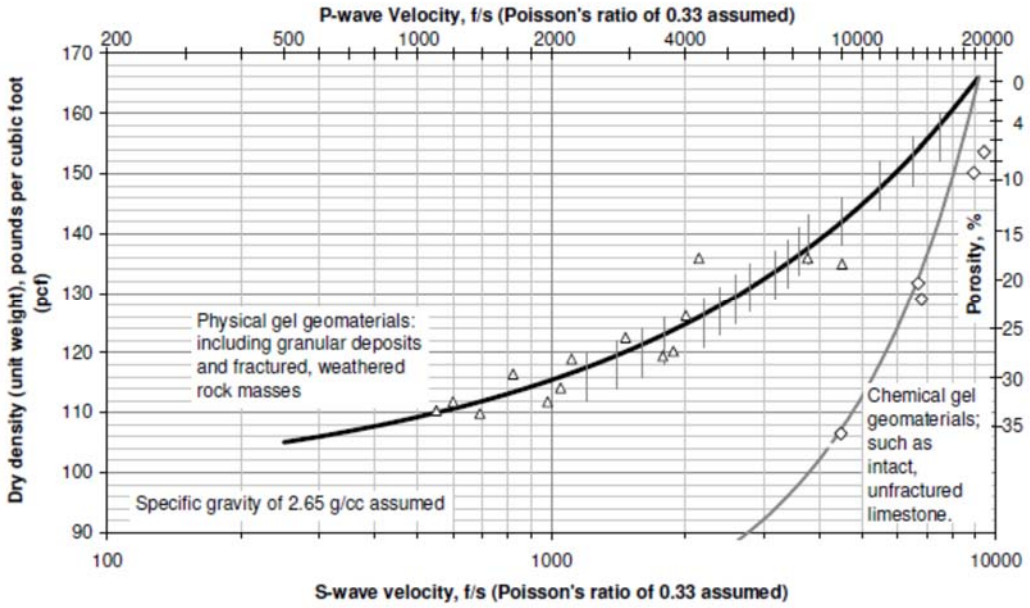

Figure 13. Non-linear relationship of various soil cases between low strain modulus (E) and porosity (Rucker, 2008)

The application of unsaturated soil mechanics and consideration of cementation, arising both from soil suction and other forms of particle bonding such as calcium carbonate and other salts, to the interpretation of seismic refraction may account for this variation between the physical gel and chemical gel models (Figure 13). Whereas the stress state of unsaturated soils depends on matric suction as well as confining stress and cementation in granular materials is affected by soil age.

Effects of Degree of Cementation

Rucker and Fergason (2006) developed a correlation between cementation stage and the P-wave velocity (Table 2). Basically, soils with P-wave velocity greater than 2000 feet per second, should have a visible identifier of cementation in the form of clast coatings. With increased coatings and cemented particles, then the modulus is also expected to increase as there is more angularity and surface area to resist stress and strain, in addition to increased matric suction of fine grains. A trend of increased PMT modulus was found with degree of cementation by Kandaris (1994) for soils located in central Arizona (Figure 7). The parent material, type of

cementation, and degree of cementation all have been found to influence the S-wave velocity and, therefore, the modulus (van Paassen et al., 2010). In general, the relationship between Young's Modulus and calcium carbonate content is an exponential relationship. Measuring calcium carbonate content in the field, however, is uncommon.

Table 2

Relationship of Cementation to Compression Wave Velocity (adapted from Rucker and Fergason, 2006)

Cementation Stage	V_p (ft/s)	Description
I	0-2000	Few filaments or coatings
II	2000-3000	Clast coating
III	3000-4000	Continuity of fabric high in carbonate
IV	4000+	Partly or entirely cemented

In Arizona, a form of cementation called caliche is commonly found, which forms when calcium carbonate precipitates in dry soils. Caliche can form from a range in parent materials including sands and clays. Due to how caliche forms there can be high variability in thickness and strength of the cemented material, and likely also high variability in S-wave and P-wave velocity (see discussion in Chapter 4). Further analysis is needed to clearly define effects of cementation and compaction in relationship to P-wave and S-wave velocity.

Unsaturated Soil Mechanics

The relationship between P-wave and S-wave velocity in saturated soils is linear (Castegna et al., 1984). For perfectly elastic and isotropic soil the P-wave velocity is affected by degree of saturation as it approaches the wave velocity of water; whereas the S-wave velocity is strongly influenced by the degree of saturation, as shear waves do not travel through water. Using these concepts, researchers have used the comparison of wave velocity to locate the water table (Bonnet and Meyer, 1988).

More recently, Grelle et al. (2009) compared the results of P-wave and S-wave velocities to identify partially saturated soils above the groundwater table by comparing the changes in P-wave and S-wave to calculate the Water Seismic Index (WSI). In which case a WSI greater than 0.5, identifies a moist soil condition. To determine the WSI requires a detailed grid system of analysis, where the variability in water content is expected with depth (not horizontal across the survey alignment) and the geometry of applied forces and geophone orientation is as specified in their research.

$$WSI = \left(\frac{z\Delta V_p}{V_p}\right) * (1 - (3\frac{z\Delta V_s}{V_s})) \quad (14)$$

Where z is depth (m), V_p is compression wave velocity (m/s), and V_s is shear wave velocity (m/s). Due to the geometry of the P-wave and S-wave measurements for the following research, modification of the WSI as defined from Equation 14 is required. The WSI relationship based on the vertical change in P-wave and S-wave velocity does not account for other factors that may influence the ratio of wave velocity such as the soil stress-state at the time of sampling.

In unsaturated soils, the relationship between P-wave and S-wave velocity is non-linear, with the general trend of increased suction corresponding to increased S-wave velocity being highly dependent of the confining pressure, material type, and

water content (Ortiz, 2004; Heitor, et al. 2013). Research on compacted fills found that small strain shear modulus increases as matric suction increases only at low water contents (Sawangsuriya et al. 2008; Heitor, et al. 2013). Whalley et al. (2013) developed a relationship between the S-wave velocity, net normal stress, matric suction and void ratio, for clayey sand-sandy clay soils, as follows:

$$V_s = A\left(\frac{(2.97-e)^2}{(1+e)}\right)(\sigma_s^r - \psi(X)^{-0.55})^Y \quad (15)$$

where A is the shear velocity when the effective stress is atmospheric pressure, e is the void ratio, X is correlated to saturation, ψ is the matric suction, σ_s is the over burden pressure, and r and Y are factors.

From a micro-level, perspective, Dong and Lu (2016) describes the shear modulus as a function of the stiffness of the soil skeleton and the effect of inter-particle forces (Figure 14). Detailed laboratory investigation found that small strain shear modulus of silty or clayey soil can vary drastically, on an order of magnitude, depending on water content (soil suction) of unsaturated soils. The increased shear modulus is due to soil suction effects, which when viewed from the micro-level perspective may be related to the increase in inter particle contacts and therefore the increase surface area to resist shear forces (Figure 15), as postulated by Dong and Lu. This concept may be relevant to the field behavior identified by Rucker (2008) "when a chemical gel material becomes fractured, fissured, exhibits microcracking, or otherwise loses significant bonding within the material structure, the behavior can approach or revert to a physical gel."

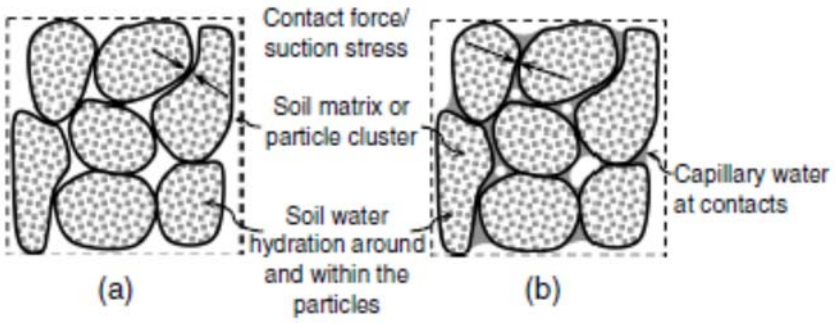

Figure 14. Effect of suction of the soil skeleton and inter particle forces during adsorption (a) and capillary water (b), from Dong and Lu (2016).

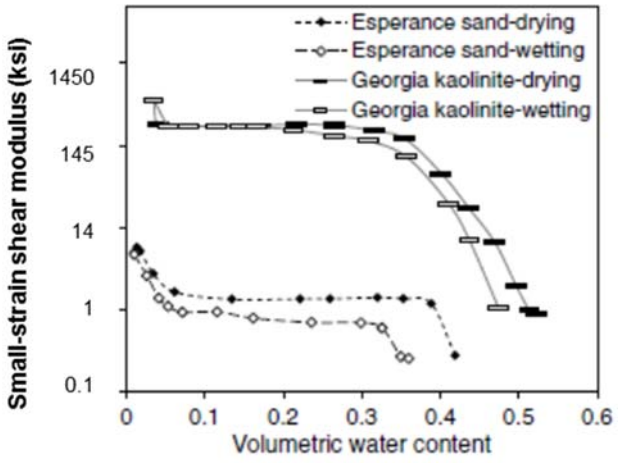

Figure 15. Variation in small-strain shear modulus by water content (Adapted from Dong and Lu 2016).

However, the relationship, as shown in Figure 15, of increased small-strain shear modulus with decreased water content for granular soils (sands) is only true for high confining stress. Research by Heitor et al. (2013) found that for silty sand, the small-strain shear modulus increases with increasing moisture content until a point after which the modulus decreases with increasing water content, under low confining pressure (Figure 16). For their silty sand study, the optimum water content was around 12 percent. A similar pattern is summarized in the literature by Oh and Vanapalli (2014), who propose a complex relationship between the saturated and unsaturated small-strain shear modulus as a function of matric suction, degree of saturation and confining pressure.

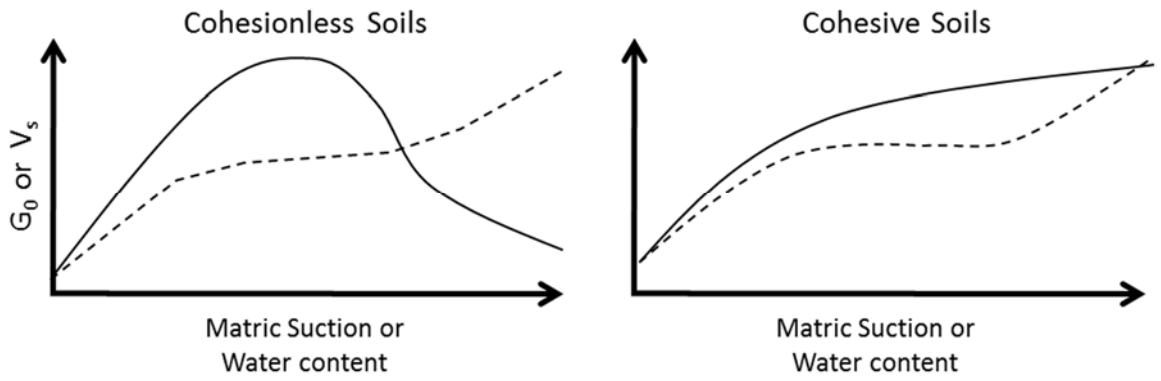

Figure 16. Variation in small-strain shear modulus (or S-wave velocity) by matric suction (or water content) for low confining pressure (solid line) and high confining pressure (dashed line) (Heitor et al. 2013).

The matric suction at the time of sampling, therefore, affects the measurement P-wave and S-wave velocity depending on the material type, confining pressure, and degree of saturation. Chapter 4, discusses the increase of P-wave and S-wave velocity at the flood retention structure sites in the Sonoran Desert during inundation events, which is only apparent for these near surface silty sands. If this variation is fully due to matric suction change, a potential scenario could be envisioned where a soil profile was sampled immediately after a wetting event, results in an estimate of modulus different than during other conditions. Any correlation then, between S-wave velocity and PMT modulus, needs to account for soil suction (or by proxy using water content and grain size) for the given soil type, as the effects of moisture content change on soil strength and stiffness is highly soil-type dependent.

RELATIONSHIP OF PMT WITH S-WAVE VELOCITY

The most common method to relate low strain (dynamic) to high strain (static) modulus relies on the development of a degradation factor (also referred to as a damping coefficient). These factors are used to estimate the intermediate strain modulus required by most engineering calculations. The most widely available factor

for soils was developed for the Federal Highway Administration and assumes an exponential relationship between small and large strain modulus as follows (Sabatini et al., 2002). This degradation factor is limited to non-cemented sands and clays,

$$E_{minimum} = \left(\frac{E_{minimum}}{E_o}\right) E_o \quad (16)$$

$$where, \frac{E_{minimum}}{E_o} = 1 - \left(\frac{q}{q_{ult}}\right)^{0.3} \quad (17)$$

where is $E_{minimum}$ is the large strain modulus, E_o is the small strain modulus, q is the applied working stress, and q_{ult} is the ultimate compressive strength, where q_{ult}/q is equal to the factor of safety.

Others have found a non-linear relationship between the degradation factor and shear strain level (Seed and Idris, 1970; Duncan et al, 2003; Hammam and Eliwa, 2012). Duncan et al. (2003) summarizes the variability in the high to small strain modulus degradation factor as a function of confining pressure, over consolidation ratio, and plasticity index (Figure 17). Similar trends are expected between the small to intermediate strain modulus degradation factor for the Sonoran Desert.

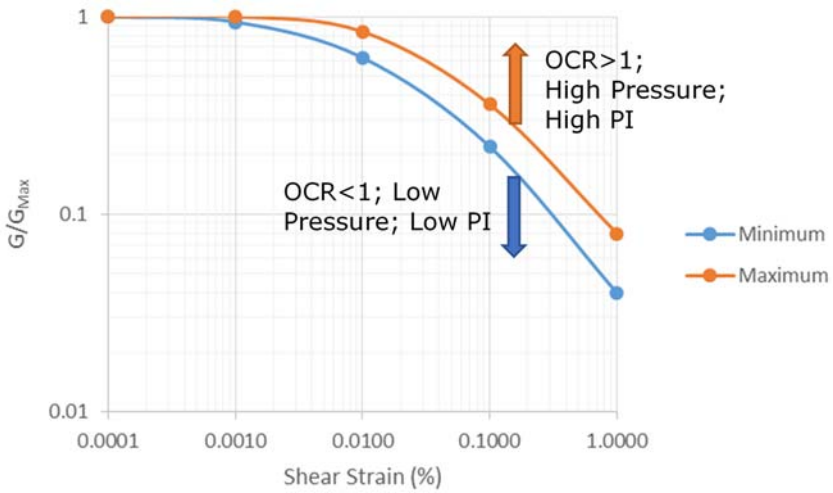

Figure 17. Degradation factor adapted from Duncan et al. 2003

Calculating the small to intermediate strain degradation factor

There are several methods for calculating the degradation factor between small and intermediate strain moduli:

The first method compares unloading and reloading modulus, both derived from PMT with the shear modulus from S-wave velocity. Robertson and Ferreira (1993) used curve fitting to match the unloading selection of PMT results with the low strain shear modulus from seismic refraction testing. Their model assumes that the shear modulus is a function of a hyperbolic shaped stress-strain relationship (Figure 4). To develop the stress-strain relationship, measurement of the strain induced by S-wave velocity is required, which is not possible in field settings.

More recent research conducted in Nevada compared field data from PMT testing with standard penetration tests and ReMi measurement of S-wave velocity to calculate an intermediate to low strain degradation factor. The relationship between the intermediate and low strain modulus was found to be highly variable at depths greater than 17 feet, which may be due to increases in cohesion or water content, or the averaging of deep soils by ReMi measurement (Robbins 2013). Likely these soils at depth are cemented, typical of desert conditions. The intermediate to low strain degradation factor calculated from PMT and ReMi measurements by Robbins (2013) was found to be lower than correlations based on blow count, an intermediate to high strain modulus. This behavior is odd as the blow count derived modulus should be closer to a high strain modulus, and therefore have a much lower modulus than that derived from ReMi S-wave velocity methods. Likewise, the PMT initial modulus was found by Robbins (2013) to be lower than the reload PMT modulus. This pattern is odd as it should have shown the reverse.

Another method uses the degradation factor for rock as a starting point to back calculate the expected relationship in soils, as the relationship between

intermediate and low strain modulus is nearly 1 to 1 (Rucker 2008). Where, rock becomes more fractured and granular it behaves more like granular soils, with lower degradation factor; and as soils cement they become more rock like, with higher degradation factor. Rucker's research indicates the following expositional relationship between high and low strain modulus:

$$E_{high\ strain} = 20.5 * E_{low\ strain}^{0.7} \quad (18)$$

where E is the modulus. This relationship is derived from field data, primarily on rock and cemented samples (Figure 18). There is limited data on the low strain modulus for granular material and calculation of confined modulus from seismic refraction velocity requires accurate measurement of density and specific gravity.

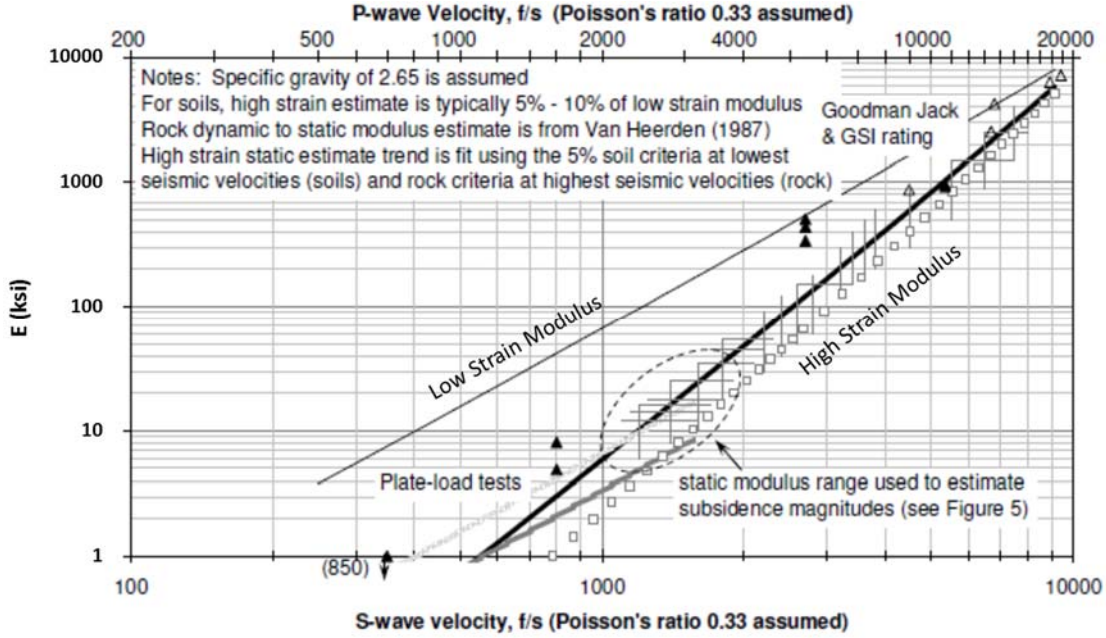

Figure 18. High strain and low strain modulus from rock modulus and select soil testing (adapted from Rucker 2008)

Lastly, the EPRI (1982) full scale foundation tests studies used the intermediate strain (E_{PMT}) moduli to then estimate the low strain and high strain behavior of the soil. During the full-scale foundation testing of the model, the shape of the load-deflection curve was found to be a hyperbolic function, which was linearized, resulting in an intermediate strain stiffness that was 32.5% less than the

low strain modulus for non-rock subsurface materials (see Chapter 6 for additional discussion).

Chapter 5 proposes a new method for developing the low to intermediate strain degradation factor for soils found in the Sonoran Desert in Central Arizona.

CHAPTER 3

CORRELATION BETWEEN MODULUS FROM PMT AND SPT

In central Arizona, a previous analysis was conducted on the correlation between SPT N values and PMT (Kandaris, 1994). The results of this analysis found three different trends by separating the sample into cohesive non-cemented, cohesionless non-cemented, and cohesive cemented groups. The analysis included data from five Salt River Project (SRP) transmission lines including 17 sites (Figure 1) for a total of 59 samples (Figure 7). Since the analysis conducted by Kandaris in 1994 additional PMT tests were conducted across central Arizona for various SRP transmission line projects. A select number of these sites were included in the analysis of shear wave velocity (S-wave velocity) and PMT (Chapter 5). The combined database of SPT and PMT values now includes 149 samples, which also includes a small subset with data on water content, plasticity index (PI), unit weight, and description of cementation. The following analysis updates the pervious correlations with additional PMT and N correlations from reports provided by SRP (SRP 1984, 1996a, 1996b, 2000, 2006, 2010, 2011, 2012a, 2012b, AGRA 1999, GAI 1994). Data from these reports is summarized by Kandaris (1994) with additional data provided in Appendix A. The full reports can be requested from the Salt River Project.

RESULTS

Cemented Soils

The data set for cemented soils was increased from 22 samples to 77 samples. The results indicate a wider scatter in the data for samples than that were described as cemented in Kandaris (1994) (Figure 7). The bore logs did not classify the stage of cementation but did describe the cementation as weakly, moderately, and strongly cemented. These descriptions are subjective, but generally follow a

pattern of increasing cementation with depth and increasing SPT N value. Separating out the data along these classifications, a pattern emerges of generally increasing PMT and N, with increasing cementation, where the samples with the strongest cementation display the least amount of scatter (Figure 19).

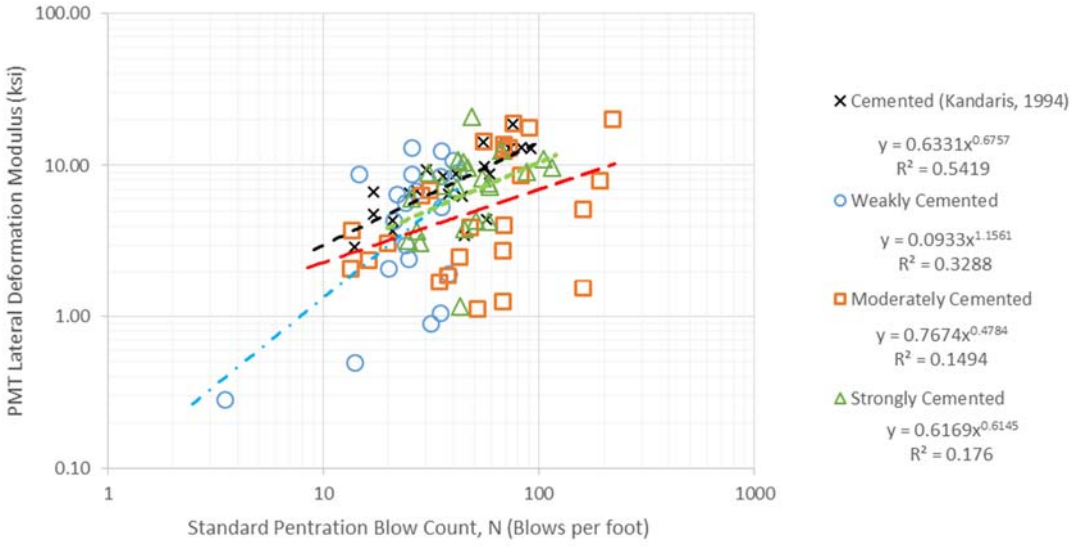

Figure 19. Cemented soils – all soils

For the moderately and weakly cemented materials, two patterns emerge in the data, due to the percentage of clayey material (Figure 20) and sandy material (Figure 21). Gradation and PI values are not available for the majority of the sample. To evaluate the effects of granularity and plasticity, the samples were divided by USCS classifications. Where cemented soils with more non-plastic, sandy material have lower PMT to N values than soils that with more plastic, clayey material. This relationship likely points to the different state properties of the material, that as a soil ages these soils become increasingly cemented (see Duncan and Bursey, 2013).

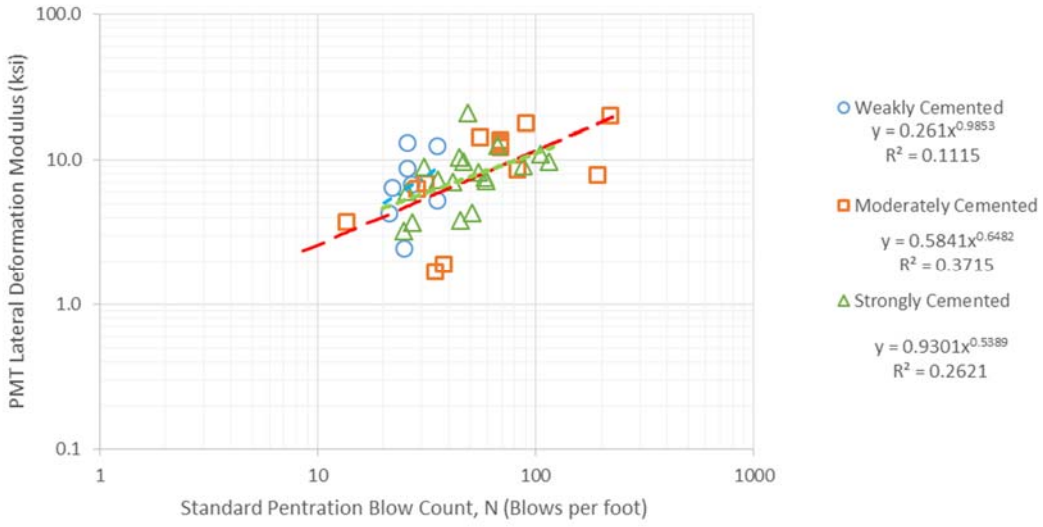

Figure 20. Cemented, plastic and clayey soils

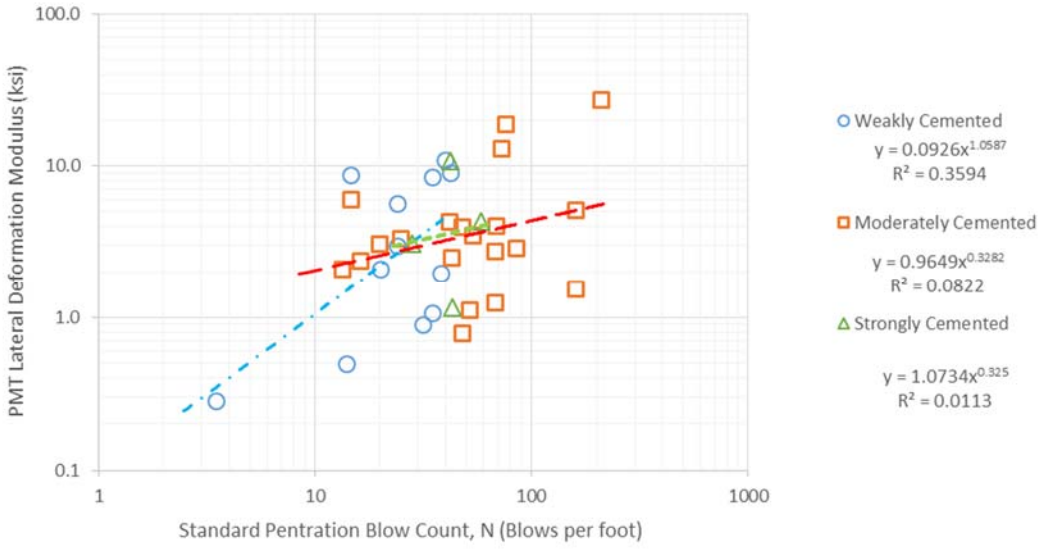

Figure 21. Cemented, non-plastic and sandy soils

Non-cemented Soils

There is a large scatter of data for non-cohesive soils and the trend for cohesive soils is has slightly more scatter than that identified by Kandaris (1994) (Figure 22). This increased scatter may be due to differences in material properties and geologic conditions. To identify trends in the data set the following discussion separates the data by material classification, largely based on USCS classifications from field assessment. Subsets of the data with available PI and water content are evaluated to find possible relationships.

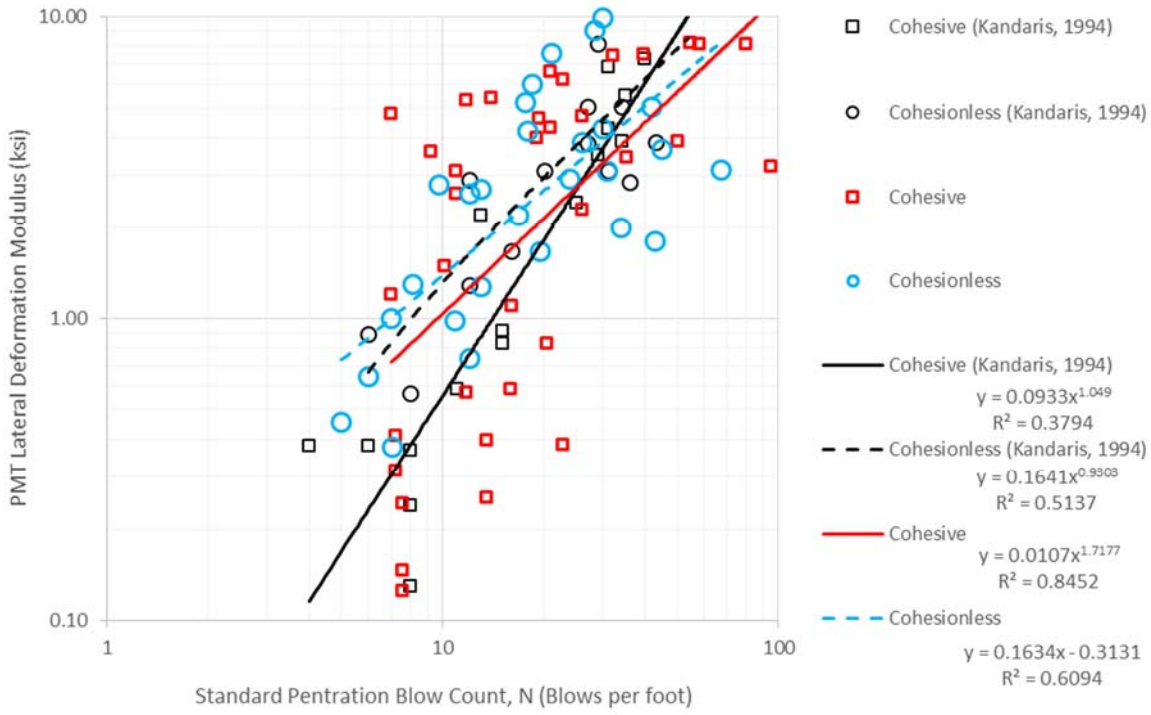

Figure 22. All non-cemented soils

The trend for clayey soils, those with a measurable PI, is for a decreasing PMT to N relationship with increasing sand content (Figure 23). For non-plastic soils, the trend is for decreasing PMT to N relationships with increasing sand and gravel content (Figure 24). These relationships are very weak and only a general trend of increasing grain size with lower PMT to N relationship can be assumed.

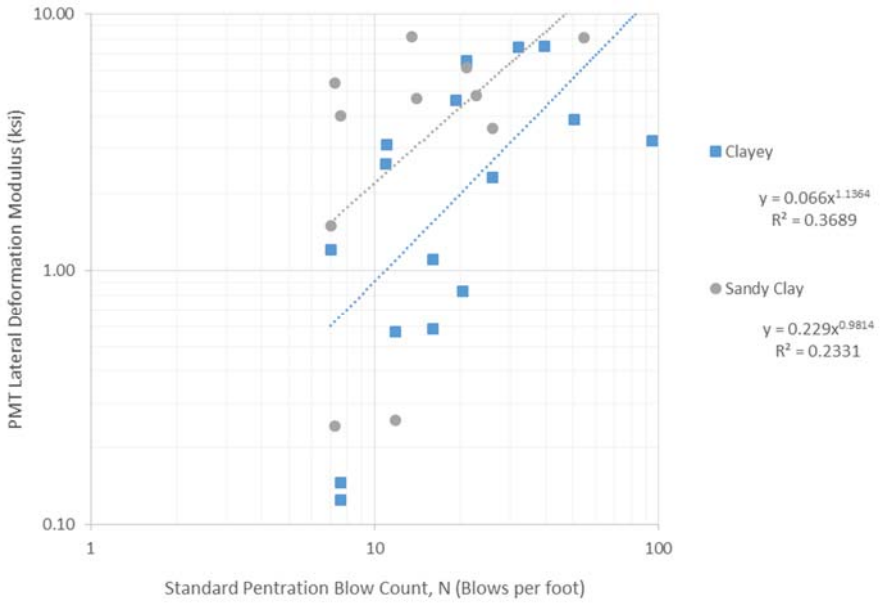

Figure 23. PMT and N for Clayey, Plastic Soils

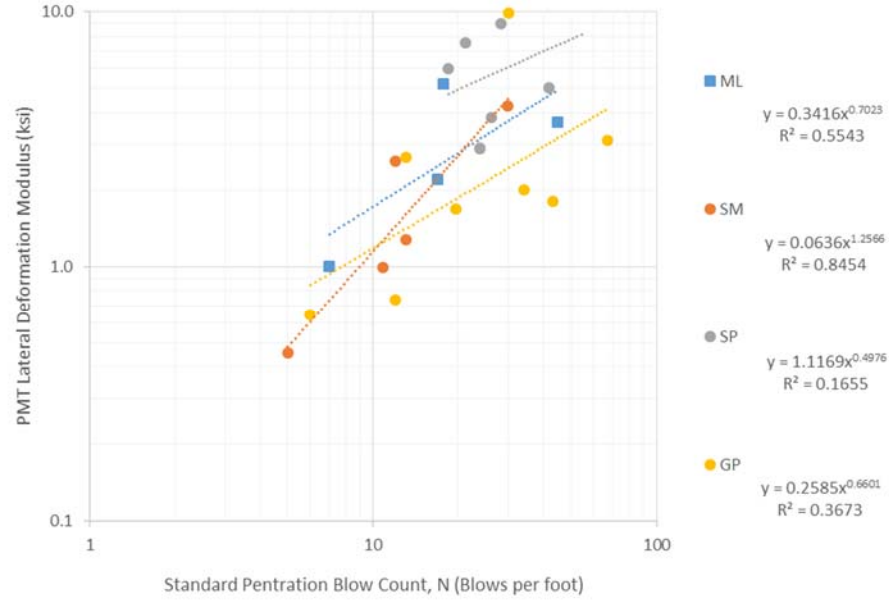

Figure 24. PMT and N for Sandy, Non-plastic soils

Accounting for Load Directionality and Poission's Ratio

As described in Equation 5 to 6, the coefficient of at rest earth pressure can be estimated from Poisson's ratio. The S-wave and P-wave velocity as obtained from ReMi, however, do not provide a direct measurement of Poission's ratio. The S-wave and P-wave velocity may be combined in other ways to evaluate other soil properties, as each wave behaves differently depending on the directionality of the waves. A correlation between with PMT and N factored by the ratio of S-wave to P-wave velocity, provides a slightly better correlation than N alone for the samples (Figure 25), but does not account for all of the scatter in the dataset.

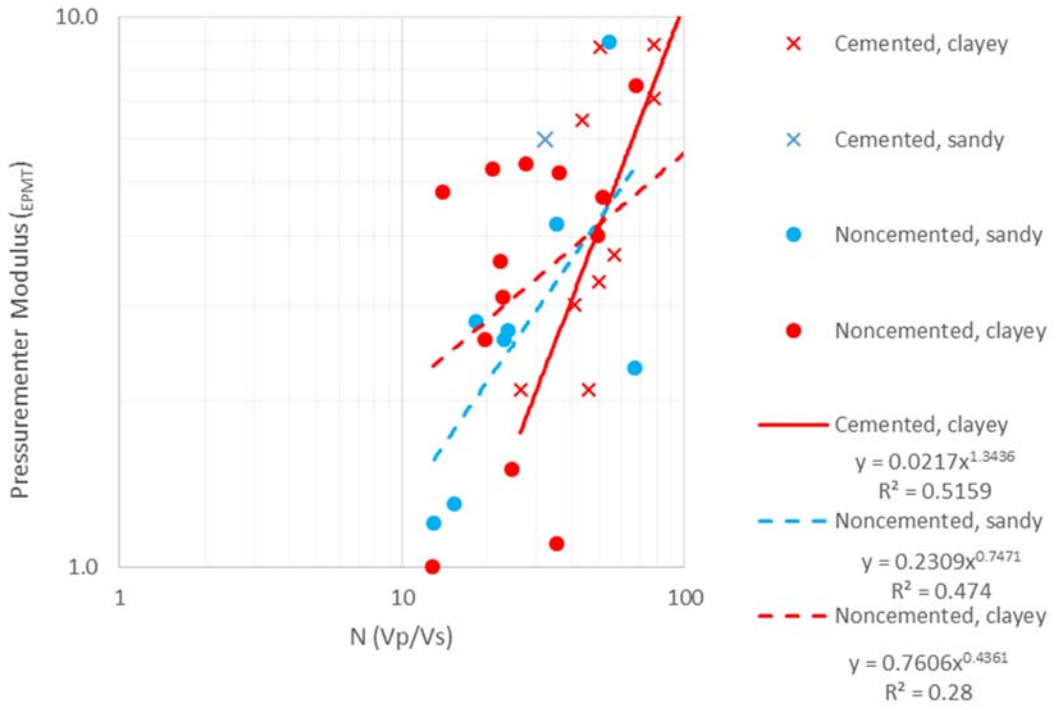

Figure 25. Relationship between PMT and N factored by Vp/Vs

The relationships between PMT and N from the previous analysis by Kandaris (1994) is not improved by the larger dataset. The variation in the stress state that relate to the degree of cementation and the grainsize causes additional scatter in the dataset. Factors of plasticity and water content may also affect the correlations, as

they relate to anisotropy, density, and strength of the soil mass. Use of the lower 90% confidence interval is recommended for the correlations to account for these unknown factors (Kandaris, 1994; Duncan and Bursey, 2013).

Interestingly, normalizing the SPT and PMT dataset by water content greatly improves the correlation for noncemented soils (Figure 26). Whereas normalizing the soils classified as cemented soils by PI improves the correlation (Figure 27). Granted the dataset with PI is very small. These patterns may indicate the different mechanics at play within the soil mass, where, beyond confining stress effects, non-cemented soils are affected by matric suction and cemented soils are affected by both matric suction and the cohesive bounds between particles such as those due to calcium carbonate precipitation. In particular, the Poisson's ratio and coefficient of earth pressure (K_o) that relate the vertical to horizontal stress and strain relationships are affected by water content and PI. As a result, factors of P-wave and S-wave may be useful for accounting for this variability in horizontal and vertical loading.

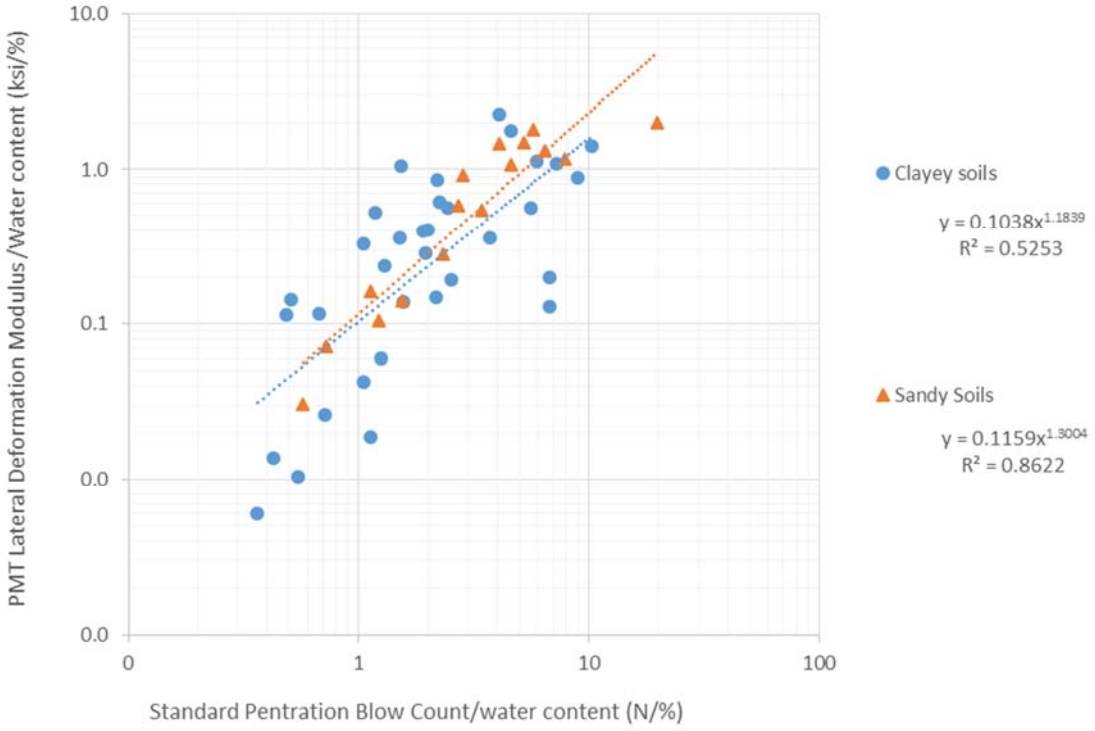

Figure 26. PMT and N normalized by water content

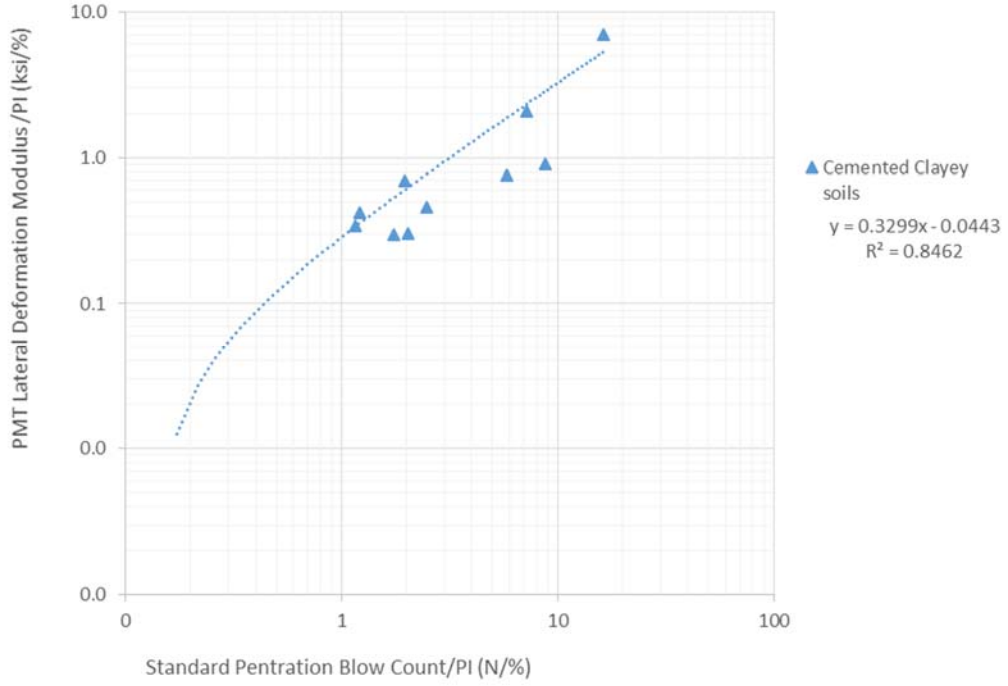

Figure 27. PMT and N normalized by PI

CONCLUSION

The correlations between PMT and SPT are limited by the effects of loading direction and strain level. To account for these effects various correlations based on material type and degree of cementation are evaluated. In general terms, for a given N value, PMT increases with increasing cementation and decreases with increasing grain size. The scatter in the dataset in cemented soils is possibly due to increased fracturing of cemented soils under loading. Likewise, the variability in granular soils is largely related to differences in matric suction, where soils at various stress states (matric suction values) have higher or lower modulus values depending on soil type (Figure 16). Additional analysis is needed to investigate the effect of cementation and matric suction on the PMT and SPT correlation. Correlations between PMT modulus and SPT must account for the effects of loading direction and strain level. Likewise, correlations between PMT modulus and other factors will likely also be influenced by factors of water content, grainsize, material type, and plasticity. The general trends presented here will be further evaluated in the correlation between PMT modulus and S-wave velocity in Chapter 5.

CHAPTER 4

GEOLOGIC VARIABILITY IN GEOPHYSICAL WAVE VELOCITY

There is apprehension in the transmission line industry to use geophysics to identify subsurface conditions. This apprehension in part is due to a disconnect between geophysics and more classical methods of subsurface investigation, which have more well established coefficients of variation and well-defined limitations. Estimation of the subsurface strength through standard penetration test (SPT) is widely used in the industry, and a geotechnical engineer generally understands the limitations of the test, understands the statistical variation expected for a given subsurface condition, and the data can be compared widely with other parameters. The use of geophysics is becoming more necessary, as transmission line structures are increasingly placed in remote areas with limited access for drill rigs and within environmentally sensitive areas that limit subsurface disturbance. The following analysis attempts to clarify what is nominal and what is the expected variability of compression (P-wave velocity) and shear (S-wave velocity) wave velocity measurements within a given geologic and spatial setting.

EXISTING DATA

Geophysical velocity data was provided by Amec Foster Wheeler (now Wood Group) at the Powerline and Vineyard flood retention structures (FRS) located in the southeast of Mesa, AZ (Figure 28). A total of 155 ReMi based S-wave velocity and P-wave velocity surveys were conducted at the FRS structures by Amec Foster Wheeler from January to April, 2015. A total of 20 borings and 14 test pits were also conducted at the FRS sites. Of this large data set, 26 locations had overlapping survey lines that were collected in different seasons and 6 survey lines overlapped with boring locations. The goal of Amec Foster Wheeler's (2015) research was to identify anomalies within a surveyed line, not to compare trends between lines. As

the following analysis is looking at the data differently than the intent of the data collection and analysis, interpretation may be limited and additional analysis required.

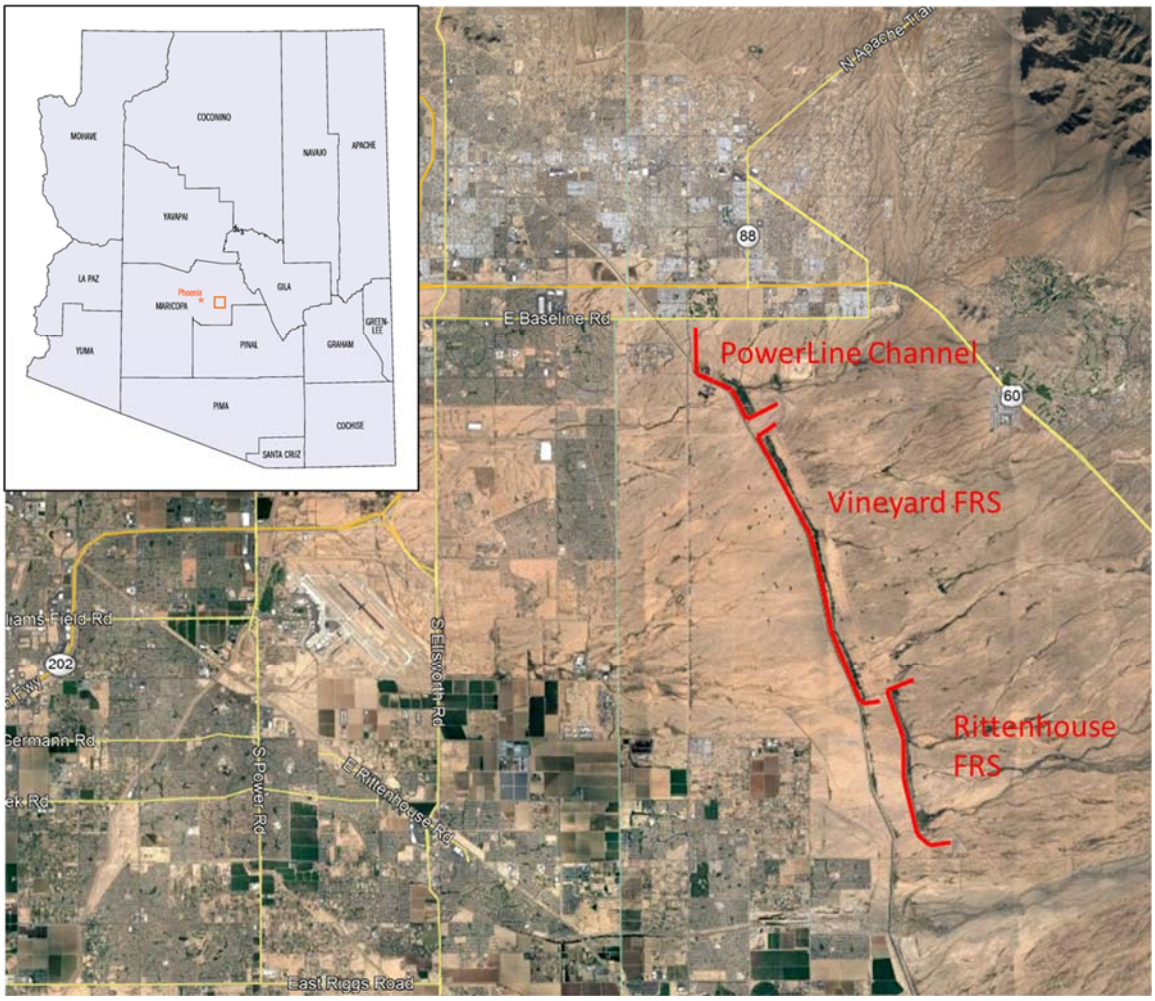

Figure 28. Map of Flood Retention Structures

Data Collection

The additional refraction surveys were performed by Tiana K. Rasmussen, PG of Amec Foster Wheeler with the assistance of Ashley Evans, EIT on December 26, 2016 at the VFRS. A total of six (6) 120-foot long refraction and ReMi surveys were conducted (Table 3). These six additional survey lines were collected to evaluate the

change in S-wave and P-wave velocity over time, as the site goes through seasonal cycles of inundation.

ANALYSIS METHODOLOGY

There has been limited research in identifying site variability, both spatially and temporally, with geophysical velocity profiles. The 143 survey lines at the Vineyard FRS within a similar geologic setting, will be used to evaluate the expected variability in a similar geologic setting. Likewise, there are 7 locations that were repeatedly tested at different times and the evaluation of these sites will be used to address seasonal changes in geophysical velocity measurements.

To compare the velocity profiles at the FRS sites, set depth intervals were used and velocities selected at those depths. The nature of geophysical velocity profiles averages the subsurface profile, with more detail near surface and less detail at depth, as such intervals of 2.5, 5, 10, 15, 20, and 30 feet were selected. The change in elevation across the 14-miles of the Vineyard FRS is only 14 feet or 0.02%. This minimal change in elevation allows for the comparison of velocity measurements at set depths below ground line for each geophysical survey line. As such, the analysis primarily considers the variability in S-wave and P-wave velocity by depth and not elevation across the site.

The overlapping locations for geophysical analysis were located based on GPS positions. Minimal ground elevation occurred between the original data sampling in 2015. However, some parts of the site were regraded prior to the sampling in December 2016. Selection of S-wave and P-wave velocity from the December 2016 data set accounts for this upper ground disturbance, however increased variability in the upper 5 feet is expected due to grading and compaction efforts.

FLOOD RETENTION STRUCTURES

There are two flood retention structures located east of the highway 202 and south of the United States Route 60 in the Phoenix valley region. These two structures divert seasonal rains and retain the 100-year floods from damaging areas to the south. The structures are located within the Mesa-Chandler sub-basin which collects water from the Superstition and Goldfield Mountains located west of the structures. These mountains consist of metamorphic and igneous bedrock. Near the FRS there are thick Holocene age alluvial fan and terrace deposits that are incised by recent channels. Detailed geologic information is summarized in the AMEC (2015a, b, c) reports, the two main geologic descriptions are as follows:

> Holocene Alluvium (Ya)- Grain sizes typically range from sand to cobbles, and the alluvium is permeable. The soils contain cambic, calcic (Stage I or less) and Cox horizons. Age estimates for this unit based on soil development are less than 10,000 years.
>
> Late Pleistocene Alluvium (Ma)- Alluvial sediment sizes range from sand to cobbles; however, surface soils contain significant amounts of pedogenic clay. These soils are variable but most contain moderate argillic and calcic horizons with Stage I to II+ cementation.

The subsurface along the FRS consist of nonplastic to low plastic, well graded silty sand, clayey sand, and sandy clay material. These soils are typically light brown in color near the surface and range from weakly to moderately cemented and tan to white at depth. With occasional noncemented sand and gravel lenses at depth. In the areas of active washes, the soils consist of noncemented sand with gravel, sand with clay and gravel, and sand with silt and gravel to approximately 4 feet below ground surface overlying weak to moderately cemented fine grained material.

Vineyard FRS

A previous analysis conducted by AMEC Foster Wheeler (2015a), included the analysis of 143 survey lines along the length of the Vineyard FRS. Approximately 7 miles of geophysical survey have been conducted along the Vineyard FRS structure (AMEC 2015B). These survey lines were collected in 6 phases, with various overlaps of lines sampled on different days spanning from January to April, 2015 (Table 3). At two locations, both the upstream and downstream side of the FRS was surveyed.

Table 3

Weather data for survey collection dates (FCD 2018)

Survey Phase	Survey Date	Max Temperature (F)	Max Humidity (%)	FRS Impoundment (ft)	7-day Prior Rainfall Total (in)	Date of last rainfall event (rainfall, in)
1	1/30/2015	55	100%	1.45 (VFRS year peak)	1.62	1/30/2015
2	2/13/2015	81	22%	0.0	0.0	1/30/2015
3	2/27/2015	70	42%	0.0	0.04	2/24/2015
4	3/13/2015	88	14%	0.0	0.0	3/2/2015 (0.51)
5	3/27/2015	90	6%	0.0	0.0	
6	4/10/2015	82	7%	0.0	0.0	3/19/2015
New	12/29/2016	77	24%	2.06 (VFRS seasonal peak)	0.39	12/23/2016

Data was collected in 6 phases, each date had slight variation in climate variables at the time of sampling. Importantly the VFRS was inundated during survey phase 1 (1/30/2015) and the during the additional data collection (12/29/2016) (Table 3). Both of these events were peak floods, where there was minor impoundment on 2/27/2015 due to rainfall within the previous seven days, the other survey collection days did not have rain events within a week prior to sampling (Maricopa flood control district). This pattern fits within the seasonal wet and dry

periods for Maricopa County, where the all the data collected only falls within two periods – winter rainy period and the summer dry period (Table 4). The following analysis does not directly address the monsoon season, which caused several significant inundation events in 2015.

Table 4

Seasonal dry and wet periods for Maricopa County

Season Description	Month Range
Winter Rainy	December to March
Dry	April to June
Monsoon	July to September
Tropical	October to November

Considering only values from the Vineyard FRS, there were 566 data points of S-wave velocity measurements and 509 data points for P-wave velocity measurements. There is wide variability in velocity with depth as seen in Figure 29 and Figure 30, with a general trend in increasing velocity with depth. At the time of this analysis the associated borings were not available for comparison. Only general discussion of variation in S-wave and P-wave values is possible.

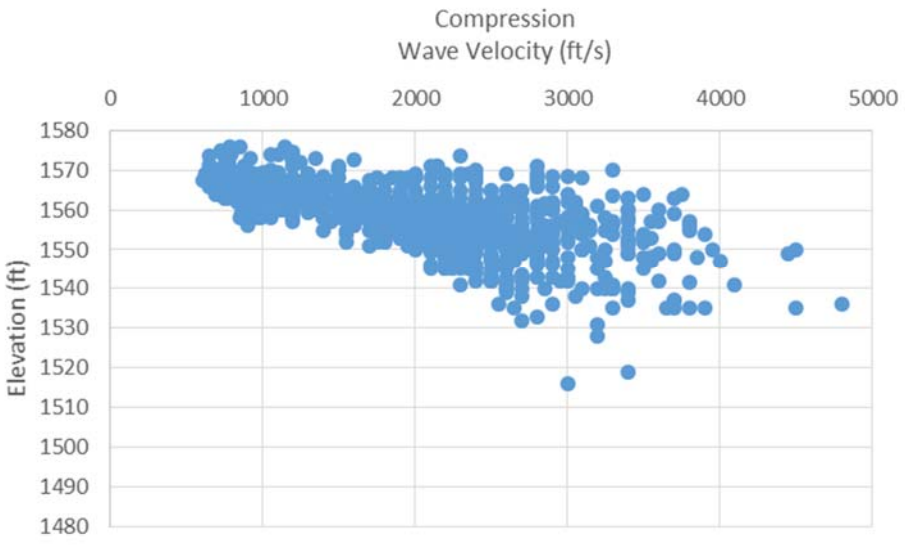

Figure 29. Variation of compression wave velocity across the VFRS

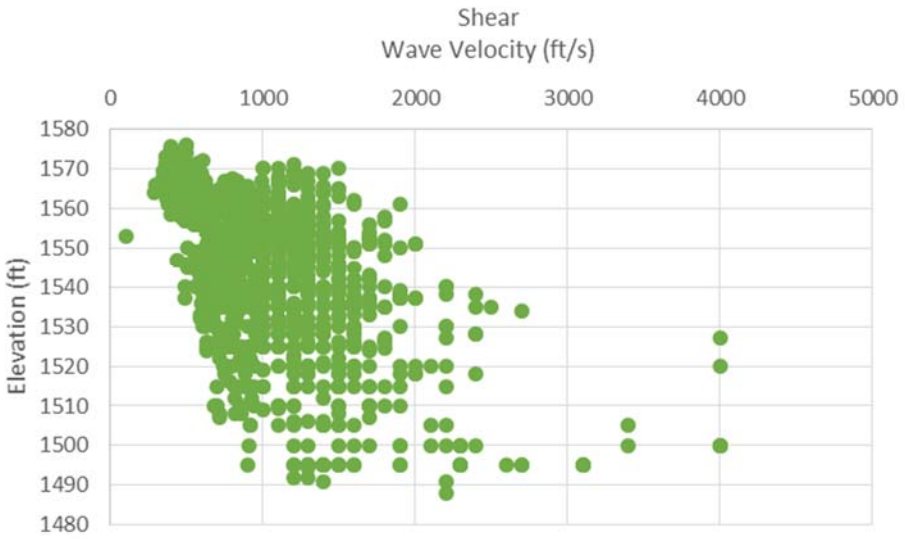

Figure 30. Variation in Shear wave velocity across the VFRS

Powerline Channel

A previous analysis conducted by AMEC Foster Wheeler (2015c), included the analysis of twenty test borings, fourteen test pits, and six refraction surveys. The six refraction surveys were located near the borings and test pits, which allow for comparison of subsurface profiles and geotechnical properties, even though the test borings and trenches were collected in March and the new refraction surveys were collected in January 2015. The results of the borings indicate three separate layers—0-5 feet, 5 -10 feet, and over 15 feet (Figure 31).

Figure 31. Powerline Channel Subsurface properties

SPATIAL VARIABILITY IN GEOPHYSICAL REFRACTION VELOCITY

To identify the influence of geographic variability, results of previous subsurface investigations at the two flood retention structures were compared with additional geophysical analysis at six (6) locations along the structures. Coefficient of variation statistics are used to evaluate the variability for each of the depositional layers identified in the AMEC Foster Wheeler (2015b) report. Typical variation for a defined depositional layer of soil is expected to be less than 30 percent (DiMaggio 2010).

General Site Variation

Table 5 and Table 6 summarize the coefficient of variation by depth for all the survey lines at the VFRS structure, including the multiple dates of sampling. The profile for all 149 survey lines, was broken down into 3 horizons as previously identified by AMEC Foster Wheeler as separate strata (0 to 5 feet, 5 to 15 feet, and 15+ feet). For each depth interval the variation is less than 29% for P-wave velocity and less than 34% for S-wave velocity. Rucker (2018) found that variation in velocity profiles is typically less than 34% across Arizona.

Table 5

Variation in Compression Wave Velocity

Depth (ft)	Mean	Min	St. Dev.	COV	No. of samples	T stat	Variance	Nominal (LEL 5%)
0-5	886	625	214	24%	75	1.29	46339	854
5-15	2076	700	598	29%	184	1.29	359599	2019
15+	2707	1550	521	19%	98	1.29	274175	2639

Table 6

Variation in Shear Wave Velocity

Depth (ft)	Mean	Min	St. Dev.	COV	No. of samples	T stat	Variance	Nominal (LEL 5%)
0-5	454	290	84	18%	124	1.29	7060	444
5-15	932	380	318	34%	224	1.29	101615	905
15+	1021	540	340	33%	198	1.29	116319	990

Variability in the data set could be due to several conditions, the following will be addressed in the discussion:

1. variation in survey collection and interpretation;
2. soil deposition as identified in the geologic maps;
3. degree of saturation during the FRS is inundated; and
4. other factors.

Variation in Data collection

A given set of survey lines was collected each day and each of which may have been collected and interpreted by different individuals. Variation is not expected to be significant between sampling dates or along the length of the FRS, as geologic variation is minimal. The results, however, indicate that certain sampling dates have a different range in variation (as measured with the coefficient of variation) (Table 7). Particularly the samples collected on 1/30/2005 have higher S-wave and P-wave

velocities than the rest of dataset for samples less than 5 feet. All samples show a similar range in values from 5 to 10 feet below ground line and for depths over 15 feet. A similar pattern is seen in the S-wave velocity data. As the largest variation between dates of sampling corresponds to sampling dates (3/13/2015 and 1/30/2015) and these samples were collected at the south end of the alignment where Ma aged material is prevalent (Stationing 300+00 to 400+00). The rest of the alignment is located on Ya aged material (Stationing 75+00 to 300+00). The slight variation in geology (between Ya and Ma) is likely the source of variation in the data.

Table 7

Coefficient of variation of S-wave and P-wave velocities by sampling date

Date	< 5 feet		5 to 15 feet		>15 feet	
	Avg Velocity (ft/s)	COV	Avg Velocity (ft/s)	COV	Avg Velocity (ft/s)	COV
S-wave						
1/30/2015	518	15%	1020	32%	972	30%
2/13/2015	383	13%	843	33%	950	25%
2/27/2015	410	8%	923	27%	1027	34%
3/13/2015	448	14%	1113	34%	1219	30%
3/27/2015	457	21%	821	33%	918	25%
4/10/2015	425	12%	922	35%	954	33%
P-Wave						
1/30/2015	1064	16%	2163	29%	3032	14%
2/13/2015	766	12%	1854	30%	2540	6%
2/27/2015	926	22%	2021	21%	2670	9%
3/13/2015	929	22%	2494	28%	3365	15%
3/27/2015	797	14%	1876	24%	2332	13%
4/10/2015	785	8%	2108	29%	2656	14%

The 1/30/2015 dataset was collected by a different individual than the rest of the surveys, however the data is likely variable as the data collection focused on the active alluvial channels, in older Ma surface geologic deposits, and was collected during a phase of inundation. This data also follows a similar pattern as the data

collected on 3/13/2015, which was collected by the same individuals from both 2/13/2015 to 4/10/2015.

The interpretation of S-wave velocity profiles is non-unique and is largely based on the depth of subsurface horizons as inferred from P-wave velocity profiles and associated borings. Inclination of subsurface layers can be identified in the P-wave velocity profiles but are difficult to identify at depths over 30 feet (outside the limit of P-wave sampling). Considering only the S-wave profile these inclined layers and anomalies appear as thin layers with reversals. These velocity reversals could cause variation in the large dataset (>15 feet). At this level of analysis particular characteristics of the subsurface were not considered and may account for the variation at depth.

Geologic Variation

As boring information was not available for the 149 survey lines at the time of this analysis, identification of specific geologic features relies on the borings conducted at the Powerline Chanel FRS. To evaluate the geologic variation, each survey line is classified based on the surface geologic condition (Huckleberry, 1994). The geology in the area ranges in age of alluvial fills, largely influenced by active channels. The survey lines located in active alluvial channels (Ya) are expected to show the greatest variation near surface material (<5 feet). Where the variation is not expected to change for the deeper, older soil horizons (Ma).

The variation is minimal between the Ma and Ya geologic deposits (Table 8 and Table 9). Except for the P-wave velocity profile of the near surface materials (<5 feet), which shows a low coefficient of variation in the Ma aged soils (Table 9). The older alluvial material is predominately located along the southern end of the alignment from about 300+00 to 400+00 stationing. This would account for the higher velocity readings on the dates of 1/30/2015 and 3/13/2015. The surface

geologic variability does not account for variability entirely, so there are likely other sources of the variation.

Table 8

S-Wave velocity variation between Holocene and Late Pleistocene age alluvium

Holocene Alluvium (Ya)			
Depth (ft)	Mean (ft/s)	Standard Deviation	COV
<5	461	84	18%
5-15'	936	333	36%
15+	1011	348	34%
Late Pleistocene Alluvium (Ma)			
Depth (ft)	Mean (ft/s)	Standard Deviation	COV
<5	423	71	17%
5-15'	885	272	31%
15+	915	282	31%

Table 9

P-Wave velocity variation between Holocene and Late Pleistocene age alluvium

Holocene Alluvium (Ya)			
Depth (ft)	Mean (ft/s)	Standard Deviation	COV
<5	907	193	21%
5-15'	2084	602	29%
15+	2789	506	18%
Late Pleistocene Alluvium (Ma)			
Depth (ft)	Mean (ft/s)	Standard Deviation	COV
<5	764	41	5%
5-15'	2033	588	29%
15+	2253	334	15%

Seasonal Variation

The FRS is designed to retain water. After intense rains, the standing water is often present on the east side, upstream side, of the Vineyard FRS. Intense rains are more frequent during the winter rainy period and monsoon season (Table 4). As the majority of survey lines are located on the east side of the Vineyard FRS, which

retains water, then a reduction in S-wave velocity is expected within the upper 5 feet during these wetter periods, because S-waves do not travel through water. The following graphs compare the nominal S-wave and P-wave velocity to the maximum temperature, maximum humidity, and inundation level within one week of geophysical survey. For the following discussions periods of measurable impoundment (standing water) at the FRS are considered wet and periods without impoundment are considered dry. The actual soil water contents are unknown for these conditions. Based on the literature, an increase in water content is expected to reduce the S-wave velocity for clayey soils (Dong and Lu 2016) or possibly increase the S-wave velocity for sandy soils (Heitor et al. 2013).

The increase in S-wave and P-wave velocity seen in the graph for the upper 5 feet on 1/30/2015 and 12/29/2016 corresponds to inundation events at the Vineyard FRS and is outside one standard variation of the other sampling dates (Figure 32 and Figure 33). The upper 5 feet results on these two dates appear to be influenced by impoundment, where the wetting of the soil during impoundment increases the S-wave and P-wave velocity. In general, an increase in S-wave velocity would imply higher matric suction, but the wetting of the soil from the inundation event should decrease the matric suction. This increase in S-wave velocity upon wetting, in this case, is counter to what is expected for clayey soils (Ortiz, 2004; Dong and Lu, 2016; Sawangsuriya et al. 2008). However, in this study the soils have low plasticity and are granular, and the trend is in line with findings of for silty sands, wherein for initially very dry granular soils a modest increase in soil moisture was found to increase the shear strength and stiffness (Heitor et al. 2013 and Oh and Vanapalli 2014).

Depending on the soil types at the Vineyard FRS two options are possible. On the one hand, for higher confining pressures and cohesive soils a decrease in matric

suction is associated with soil wetting, where a decrease in soil strength and stiffness, and therefore a decrease P-wave and s-wave velocities would be expected. On the other hand, for uncemented granular soils, it is possible that, up to a certain point, an increase in soil moisture actually increases soil stiffness due to the effect of capillary forces tending to pull particles of sand together – particularly at shallow depth where confinement is not a large factor (Figure 16). For example, when building a sandcastle, the addition of water to dry sand increases the strength and stiffness of the sand to a point; but if a large amount of water is added to sand the strength and stiffness will decrease.

Furthermore, it might reasonably be anticipated that wetting of soils having even modest plasticity (PI>10%) would tend to decrease soil stiffness and therefore decrease P-wave and S-wave velocity; whereas, the opposite effect of wetting (not saturation) of soils that are granular and non-cemented would tend to increase P-wave and S-wave velocity. The water within the void space of soils then impacts the seismic velocity measurements and complicates the interpretation of seismic data for determination of S-wave and P-wave of the soil skeleton (soil structure) (Heitor et al. 2013). Further studies on soil moisture effects on seismic velocity measurements and interpretation are clearly warranted. As identified in the SPT and PMT correlations, the PI, water content, and soil type are expected to impact the modulus. Additional analysis is required to evaluate the influence of matric suction with depth and during different seasons and verify the material type for these soils at the Vineyard FRS.

The variability in the average P-wave and S-wave velocity at over 10 feet depth is within the standard variation seen in other periods of time (Figure 32 and Figure 33). At these depths the variation then may be due to differences in alluvial

deposition and cementation across the FRS. Additional field investigation is needed to identify the depth to cementation and the thicknesses of these layers.

Figure 32. Shear wave velocity and seasonal change

Figure 33. Compression wave velocity and seasonal change

Detailed Analysis of Seasonal Changes

The trends identified above are for the entire Vineyard FRS, which may be influenced by geologic variation and other factors, over its 4 mile length. A closer look at individual profiles sampled at different times reveals change that is masked by the geologic variation across the length of the Vineyard FRS. The repeated analysis of a particular survey line is expected to show the influence of the impoundment periods, on both the S-wave and P-wave velocities. The thickness of P-wave and S-wave velocity layers are expected to expand during wetter impoundment periods, where the increased stress state of the soil during impoundment (changes matric suction) increases a given P-wave and S-wave velocity measurement.

During the initial analysis at the Vineyard FRS, one survey line was collected twice. The survey lines L-23 and L-47 were both collected at the same location but were sampled at different times. There was no change in ground line elevation between the surveys and as the line is in the same location the change in seismic wave velocity should be solely the function of the seasonal changes.

Plotting the subsurface profile over each other shows a general thickening of layers and increased velocity of the P-wave velocity zones during periods of wetting (impoundment) (Figure 34). In the upper layer, the P-wave velocity of 630-760 ft/s during the dry period increased to 1200 ft/s during the wet (impoundment) period. Although, increase in P-wave velocity generally suggests increased matric suction, perhaps, for these uncemented granular soils near surface, some increase in stiffness with wetting may occur at the lower range of degree of saturation that likely excited under these field conditions. Further research is needed to verify the water content, degree of saturation, and stress-state of the soil under these wet and dry conditions.

There is also a thickening of the S-wave velocity profile layer and a change in the velocity in this layer (Figure 35). The S-wave velocity changed from a variable

400-1200 ft/s in the upper layer to a consistent 530 ft/s. The thin 1200 ft/s S-wave velocity layer identifiable in the dry period is indicative of a sloped surface or anomaly, which is also seen in the P-wave velocity. One possible interpretation is that the impoundment affects this inclined layer, which may be a desiccation crack, thin layer of cementation, or another geologic feature. When this feature is wet the wave velocity profile is more like the surrounding soil than when it is dry and there is a difference identified in the profile, such as could be related to the variation in matric suction (stress state) to some extent. This observed pattern requires further investigation of actual subsurface conditions to facilitate development of plausible explanations such as those offered above.

The change in S-wave and P-wave velocities between the wet and dry conditions likely indicates a change in the stress state of the subsurface, due to matric suction change, during these periods. The L-47 line was collected on 3/13/2015 (no rain within previous seven days) and L-23 was collected on 1/30/2015 (during a peak inundation period) (FCDMC, 2018a) (Table 3). As seen in Figure 34, when the alignment goes from a wet to dry condition (shift from purple to red), the P-wave velocity layer thickness increases, and the S-wave velocity layer depths also increased. This trend is possibly due to a change in water content between the two conditions and a corresponding change in suction (thickening of P-wave and S-wave velocity), where the additional moisture pulls the granular soil skeleton together.

Interestingly there are reduced S-wave velocity layers that show up in the survey on 1/30/2015, at layers at depths over 40 feet, which are not present on the other sampling date. At 40 feet below ground surface the change in S-wave velocity of over 600 ft/s is unlikely due to surface water inundation and not a function of groundwater, as the groundwater table is over 400 feet below the surface in the

area. These patterns may be due to the interpretation of S-wave velocity from the ReMi Rayleigh wave, as the intent of the original survey project was to identify variation within a profile not between profiles and did not evaluate variation within those depth ranges.

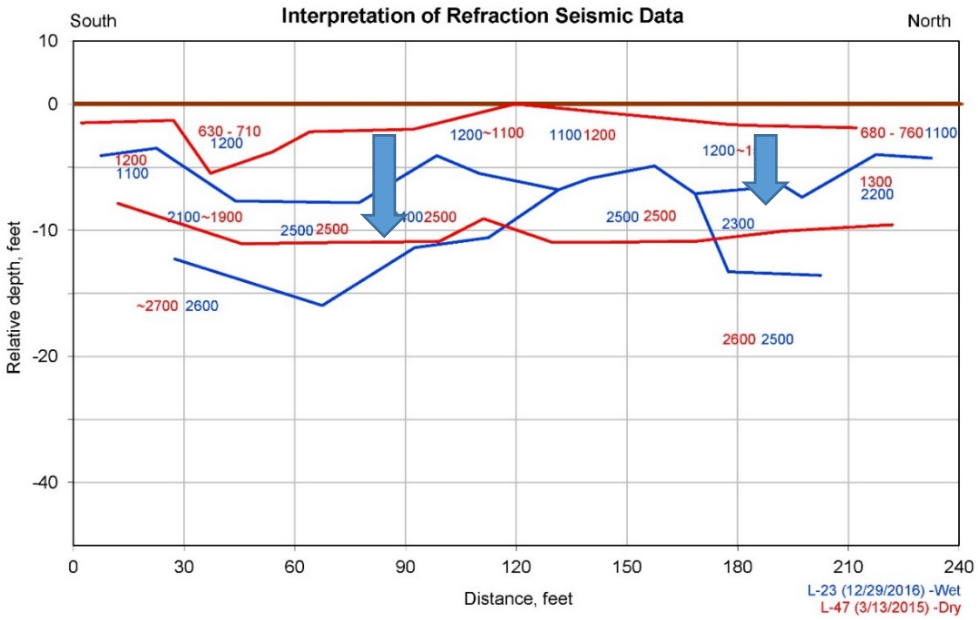

Figure 34. Comparison of compression wave velocity between L-23 (purple) and L-47 (red). (Modified from Amec 2015b)

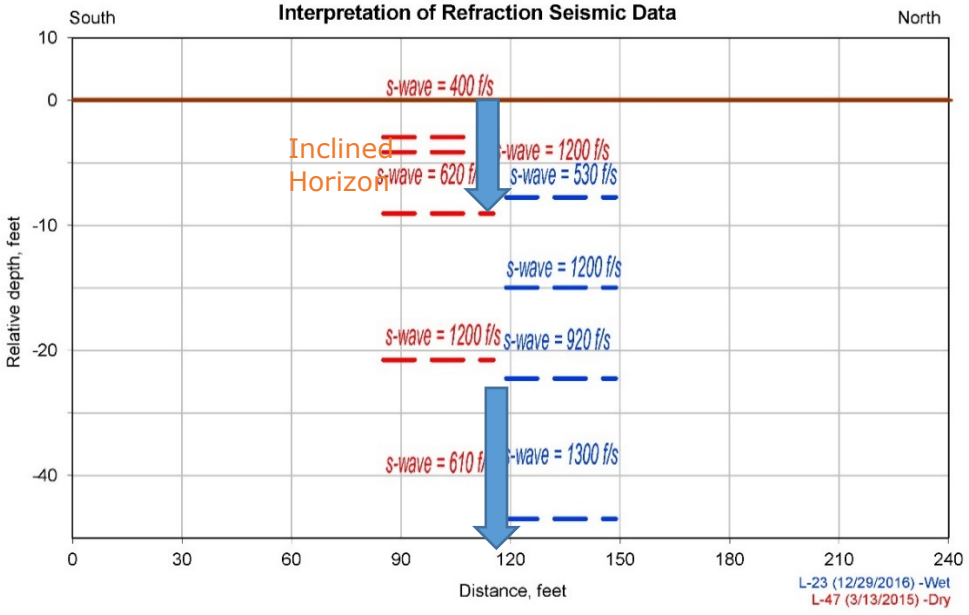

Figure 35. Comparison of shear wave velocity between L-23 (purple) and L-47 (red). (Modified from Amec 2015b)

To evaluate the statistical trend due to inundation, additional survey lines are needed at the Vineyard FRS. For this level of analysis, a total of six additional surveys were collected at the same location as previous surveys, one line crossed two previous survey lines (Table 10). At the time of the additional survey (Lines 1, 3 to 6), water was ponding on the upstream side of the structure. No standing water was present on the downstream side of the Vineyard FRS. Three additional sites are included that were collected on both the upstream and downstream side of the Vineyard FRS as the same stationing (Table 11). The exiting survey lines, L-22, L-23, and PCL-06 were collected in a similar high impoundment time when water was visible on the upstream side of the FRS.

If increased water content has an effect on the S-wave and/or P-wave velocity, (1) the greatest variation in dataset should occur between wet and dry sampling conditions, (2) there should be a high correlation between wet conditions regardless of time collected (multiple dry conditions were not sampled), and (3) there should be a large variation between upstream (wet) and downstream (dry) surveys.

Table 10

Corresponding Survey lines at Vineyard FRS

Survey Line	Date	Condition	Survey Line	Date	Condition
1 (New)	12/29/2016	Wet	L-22 (VFRS)	1/30/2015	Wet
L-23 (VFRS)	1/30/2015	Wet	2 (New)	12/29/2016	Dry
5 (New)	12/29/2016	Wet	L-44 (VFRS)	3/13/2015	Dry
4 (New)	12/29/2016	Wet	L-133 (VFRS)	4/10/2015	Dry
4 (New)	12/29/2016	Wet	L-134 (VFRS)	2/27/2015	Dry
3 (New)	12/29/2016	Wet	L-142 (VFRS)	4/10/2015	Dry
6 (New)	12/29/2016	Wet	PCL-06 (VFRS)	1/30/2015	Wet

Table 11

Upstream and downstream comparisons

Line	Date	Condition	Line	Date	Condition
1 (New)	12/29/2016	Upstream	2 (New)	12/29/2016	Downstream
L-22	1/30/2015	Upstream	L-23	1/30/2015	Downstream
L-24	3/13/2015	Upstream	L-21	1/30/2015	Downstream

Results

There is large variability between the survey lines collected during impoundment (wet conditions) at the FRS (1, 3 to 6, L-23) and those collected in dry conditions with no impoundment (L-22, L-44, L-133, L-134, L-142, PCl-06, 2) (Figure 36). For any given value the change in S-wave and P-wave velocity is on the order of 30% different. However, there is a very strong linear trend between the seismic velocities sampled at different dates of impoundment (wet) conditions (Figure 37). This suggests that the difference in P-wave and S-wave velocities between the two wet sampling periods is very small. This pattern suggests that changes in stress state (likely due to matric suction change) is greatest between wet and dry conditions, than during similarly wet conditions. In which case, for these uncemented granular soils, at low confining pressures, the increased water content during impoundment periods causes seismic velocities to be more similar, likely increasing the soil grain connections and increasing the velocity. Whereas during dry periods the connections between grains are weaker and more variable.

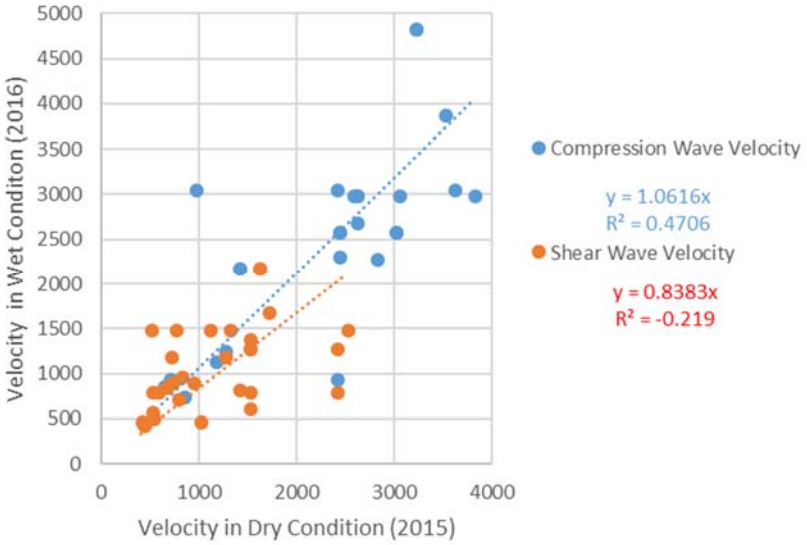

Figure 36. Variation between wet and dry seasons at same survey location

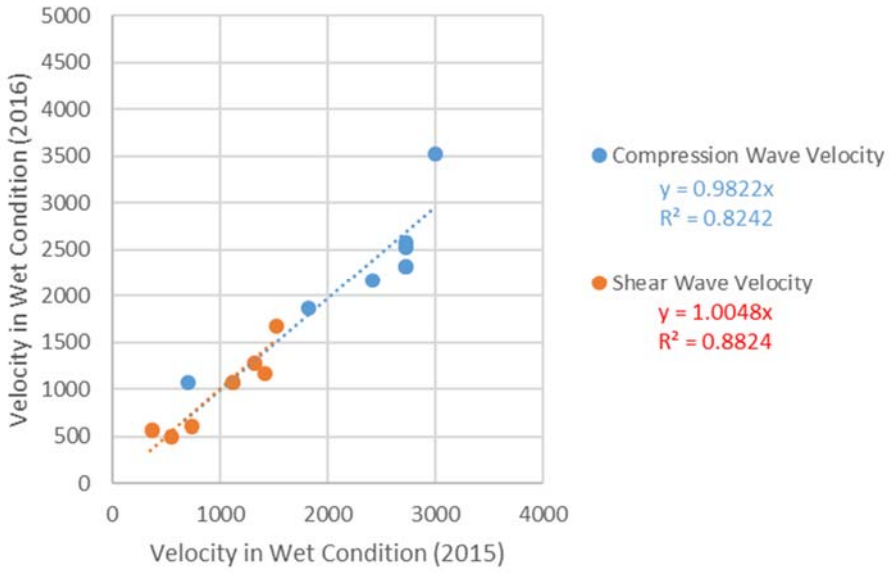

Figure 37. Variation between wet and wet seasons at same survey location

Velocity in Wet Condition

There is also a weak correlation between the velocity profiles upstream (wet) and downstream (dry) of the Vineyard FRS. The difference between upstream and downstream profiles (*Figure 38*), however, is smaller than that seen in the seasonal changes (*Figure 36*). This slight change is variation is likely due to decreased

variation in stress states (smaller change in matric suction) between the upstream and downstream, than seen between the wet and dry season samples.

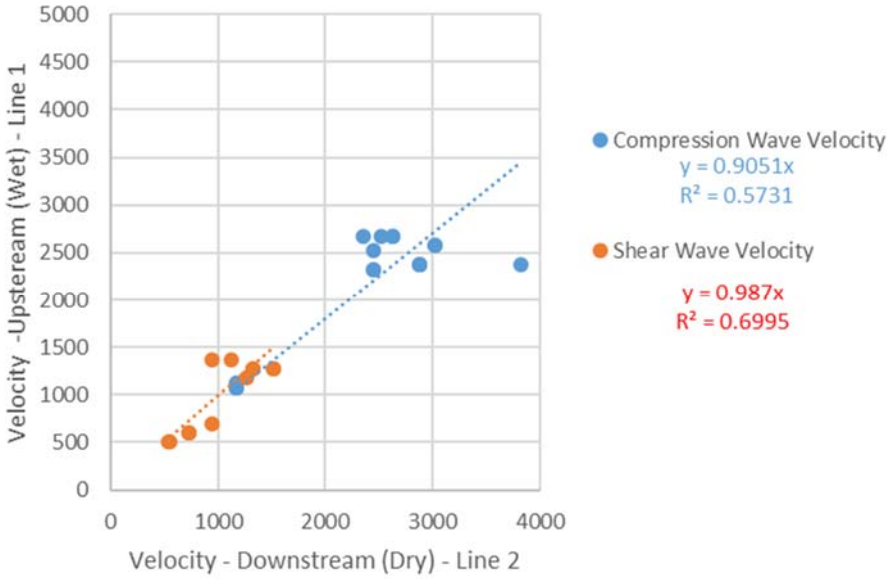

Figure 38. Variation between upstream and downstream of FRS at same survey location

Comparison of S-Wave and P-Wave Velocity with Borings

As direct subsurface sampling was not collected along the 143 survey lines of the Vineyard FRS, the correlation between S-wave and P-wave velocity and subsurface conditions is largely unknown. Comparison between wave velocity and subsurface properties is possible at the Powerline Channel FRS, located on the north end of the Vineyard FRS (Figure 28). At the Powerline Channel FRS, a number of the survey alignments overlap with subsurface sampling, which allows for the analysis of possible changes in velocity due to stress state changes. Previous analysis was conducted by others along the Powerline FRS. For this aspect of the investigation, an additional two survey lines were collected to evaluate the variability between the SPT and survey conditions (Table 12). Atterberg limits, dry unit weight and water content were collected during the original SPT testing.

Table 12

Powerline FRS survey line locations

Survey Line	Date	Bore log No.	Date
PCL-01 (Powerline Channel)	1/30/2015	B15-06 (Powerline Channel)	3/17/2015
PCL-02 (Powerline Channel)	1/30/2015	B15-08 (Powerline Channel)	3/17/2015
PCL-03 (Powerline Channel)	1/30/2015	TP15-03 (Powerline Channel)	3/15/2015
PCL-04 (Powerline Channel)	1/30/2015	TP15-06 (Powerline Channel)	3/17/2015
PCL-05 (Powerline Channel)	1/30/2015	B15-09 (Powerline Channel)	3/18/2015
PCL-05 (Powerline Channel)	1/30/2015	TP15-09A (Powerline Channel)	3/18/2015
PCL-06 (Powerline Channel)	1/30/2015	B15-10A (Powerline Channel)	3/19/2015
PCL-06 (Powerline Channel)	1/30/2015	B15-10A (Powerline Channel)	3/19/2015
Line 6 (New)	12/29/2016	B15-10A (Powerline Channel)	3/19/2015
Line 5 (New)	12/29/2016	B15-12 (Powerline Channel)	3/18/2015
L-46 (Vineyard)	1/30/2015	B15-12 (Powerline Channel)	3/18/2015

Effects of water content on S-wave and P-wave velocities

For the Powerline Channel FRS samples there is a weak trend of increasing S-wave and P-wave velocity with decreasing water content (Figure 39). Where there is a greater change in P-Wave velocity than S-wave velocity between 2 and 6 percent water content. The samples with greater than 6 percent water content were also classified as cemented. This trend may indicate the influence of matric suction, where these water contents are near optimum for the sandy soil and have higher matric suction, than wetter or dryer conditions, and because of the granular nature would be expected to have higher P-wave and S-wave velocities. Such a trend is described by Heitor et al. (2013) (Figure 40) and appears to fit the trend of the field conditions (Figure 39).

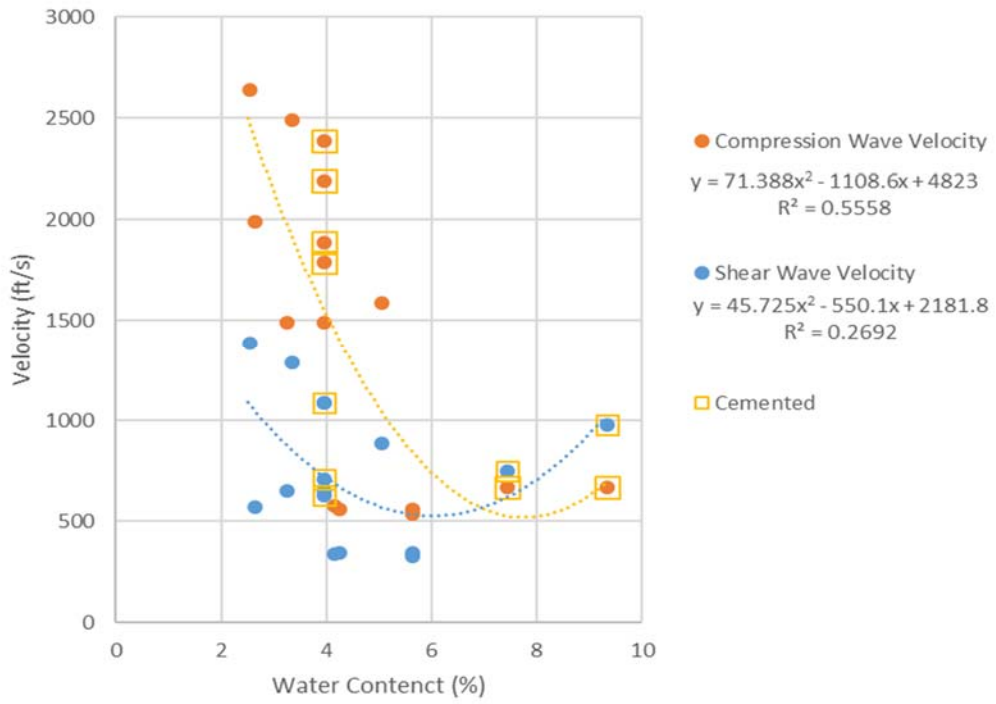

Figure 39. Trend in S-wave and P-wave velocity with water content for the Powerline Channel samples

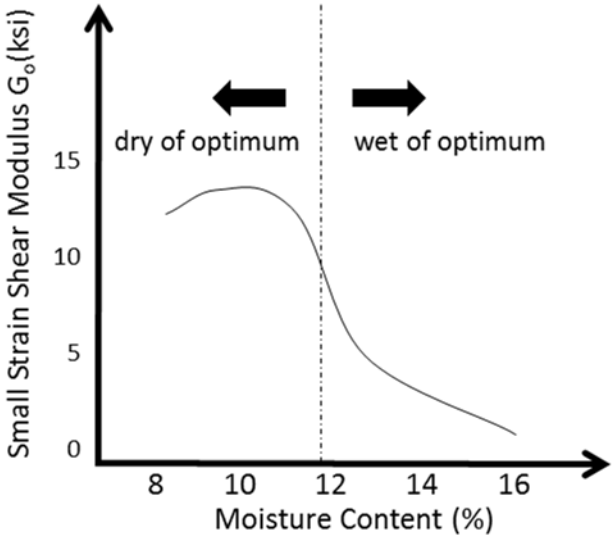

Figure 40. Trend in small strain shear modulus with moisture content for silt sand soils (adapted from Heitor et al. 2013)

Utilizing the relationship between water content and wave velocity, the following relationship is developed that uses the ratio of S-wave to P-wave velocity as an indication of water content (Equation 19). Note that due to the difference in date of survey and date of boring, there may be a change in moisture content, particularly in the upper regions of the soil profile. Therefore, only the samples that were collected in wet conditions (both SPT and geophysical survey) were used in the correlation.

$$\omega(\%) = 2 + 0.64\frac{(7V_s)^2 - V_p^2}{3(V_p^2 + Vs^2)} \quad (19)$$

Where w is the volumetric water content, Vs (ft/s) is the shear wave velocity, and Vp (ft/s) is the compression wave velocity.

The survey dates on 1/30/2015 and 12/29/2016 were both collected during wet conditions and the boring collected on 3/18/2015 and 3/19/2015 were collected in wet conditions (MCFCD, 2018a). This relationship results in a high correlation (R^2=0.9023), compared to the variation seen between wet and dry periods (R^2=-0.0219). This pattern, is supported by the fact that matric suction in unsaturated soils does effect the S-wave and P-wave velocity.

For surveys collected in wet conditions, the water content can be estimated from comparison between S-wave and P-wave velocity. The regression of either S-wave or P-wave velocity to water content is poor (*Figure 41*). However, the proposed relationship in Equation 19 is used to estimate the water content at the time of refraction survey, with a high correlation (R^2=0.84). Additional analysis is needed to increase the sample size to evaluate if this is a measure of water content or suction influences on the soil mass.

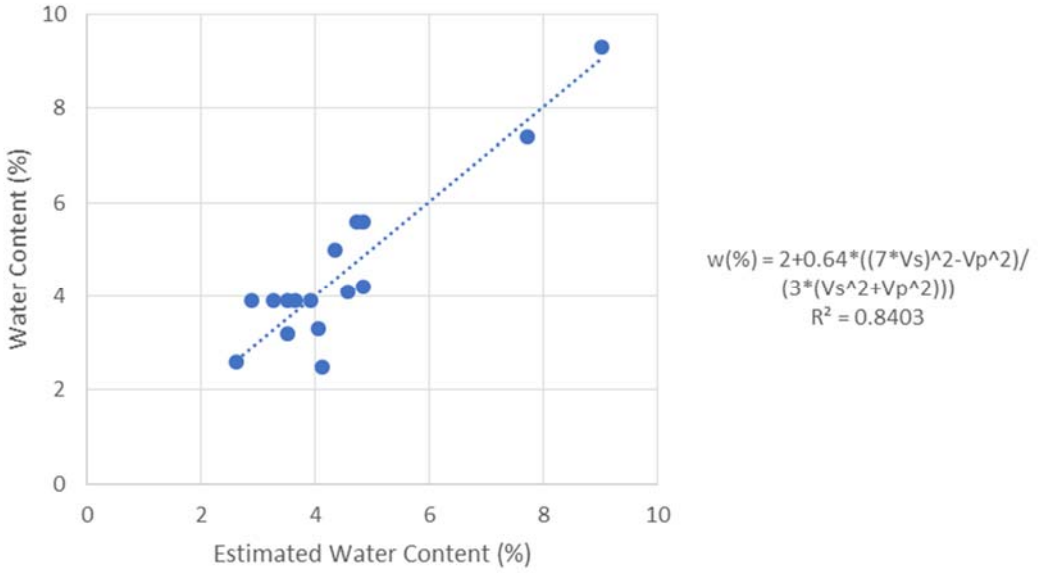

Figure 41. Proposed relationship between water content and velocity for the Powerline Channel samples

DISCUSSION

Few published studies account for the variation in geophysical velocity profiles within a given geologic setting. Results here indicate that for Quaternary alluvial deposits in the Sonoran Desert, the variability within a given geologic horizon is less than 34%. This is comparable to the coefficient of variation in other subsurface testing methods (Kulhawy and Phoon, 2002). Further investigation into the variability, found slight differences between young alluvial deposits (Ya) and older alluvial deposits (Ma) and the influence of stress state on both the S-wave and P-wave velocity, likely due to matric suction.

The S-wave and P-wave velocity profiles show large variation over 15 feet below the ground surface. This variability at depth is within the coefficient of variation of other sampling dates and likely indicate differential cementation at depth along the FRS alignment. Further analysis is required to identify the material at depth.

The largest variability (greater than the samples coefficient of variation) is seen between the dry and wet samples, within the upper 5 feet of the subsurface profile, where there is a general increase in both the S-wave and P-wave velocity when there is impoundment at the flood retention structure. This pattern is not indicative of saturation. In saturated conditions, like the appearance of perched groundwater tables, the P-wave velocity would still be high (>2000 ft/s) and the S-wave velocity would be very low (<1000 ft/s) as shear waves do not travel through water. The S-wave velocity profile developed here is a function of the ReMi dispersion analysis and not a true shear wave. Possibly the ReMi S-wave velocity profile is not capturing the saturated soils, but this seems unlikely for these soils which have a typical water content of less than 10% (Amec, 2015b).

One possible interpretation of the combined increase in S-wave and P-wave velocity relates to the influence of matric suction on these unsaturated soils. Research in the laboratory has shown that small changes in water content in clayey/silty soils can result in large changes in matric suction and therefore soil strength and stiffness, particularly for fine grained soils. On the one hand, for clayey soils high matric suction in turn results in higher S-wave velocity profiles (Dong and Lu, 2016). Laboratory research, by others, found that S-wave velocity increased form a few feet per second to upwards of 2000 ft/s over a 10% change in water content (Dong and Lu, 2016). On the other hand, for silty sandy soils, there is an optimum water content which corresponds to high matric suction and in turns results in higher S-wave velocity profiles at low confining pressures (Heitor et al. 2013). Matric suction as influenced by water content, then likely has an impact on the S-wave velocity measured in the field. The trend identified at the Vineyard FRS, likely relates to the particular grain size, soil type, and degree of saturation. The large degree in variability found in the field in the upper five feet between wet and dry

seasons of sampling, therefore, is likely due to the change in stress state resulting from change in matric suction (Figure 42).

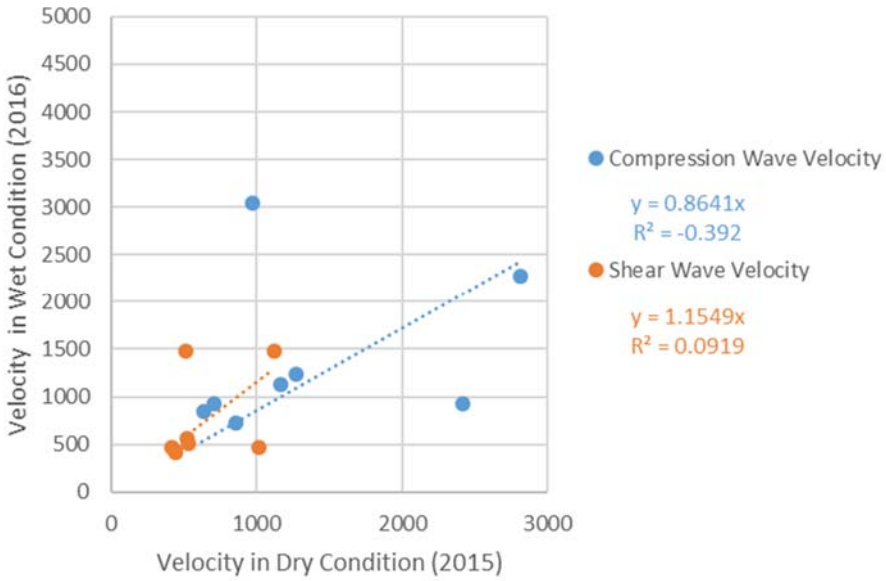

Figure 42. Variation in the upper 5 ft

The overall variability of the given geographic unit at the Vineyard FRS, including across multiple seasons, is less than 34%. Some of this variability is likely due to changes in matric suction and is lost within the noise of natural variability. Due to the naturally high variability of Quaternary alluvial deposits, the seasonal change in S-wave and P-wave velocity related to matric suction, then is likely of limited engineering significance for foundation design. Further testing is needed to evaluate the effect of other wetting events, variation during multiple drying events, and quantify both the water content and matric suction at the time of sampling.

CONCLUSION

The variability in the S-wave and P-wave velocity data from the Vineyard FRS site is less than 34% for a given geologic horizon. The variation is likely due to a combination of geologic age of materials, variations in cementation and the influence of matric suction during wet and dry seasons. Unlike other areas of alluvial deposits

in central Arizona, the flood retention structures have periods of impoundment where water is retained and influences the subsurface properties for prolonged periods. The results presented here suggest that during periods of wetting both the S-wave and P-wave velocity increases, particularly for the upper 5 feet (Figure 29 and Figure 30), which is counter to pervious laboratory based findings for cohesive soils and in-line with findings for silty sandy soils. For the soils near the Vineyard FRS, wetting conditions may increase S-wave velocity by 100-200 feet per second and P-wave velocity 300-400 feet per second in the upper 5-feet (Figure 32 and Figure 33). The deeper soils may also be influenced by the change in water content but are likely influenced more by the variation in non-suction type cementation such as calcium carbonate formation. Further research is needed to increase the sample size, include more periods of wetting and drying, and more direct measurement of subsurface properties.

In engineering terms, geophysical survey lines collected during wet or dry conditions will return different higher S-wave and P-wave velocity values, due to effects of matric suction. The correlations to various engineering parameters then may be overestimated or under estimated when S-wave and P-wave velocity are collected in these conditions. Correlations of soil properties, such as modulus, to S-wave and P-wave velocity should be adjusted to account for the given field moisture conditions during sampling and the expected long-term design condition. More research is needed to identify appropriate adjustments to S-wave and P-wave velocity data to account for soil moisture content changes that may occur over the life of structures to be designed in these arid regions.

CHAPTER 5

CORRELATION BETWEEN PMT AND S-WAVE VELOCITY

The following is an analysis conducted to determine the degradation factor for Sonoran Desert soils, particularly those found within quaternary aged alluvial deposits in the Central Arizona. Quaternary deposits typically have lower moduli compared to older deposits, and these lower moduli soils can control laterally loaded foundation design. To develop the degradation factor, a comparison of 14 sites across the region were evaluated, resulting in a database of 52 samples at varying depth (Table 13). All data used in the analysis is summarized in Appendix A and project reports can be requested from the Salt River Project and Amec Foster Wheeler.

Table 13

Sites used in analysis

Transmission Line Report	PMT No.	Date of PMT Testing	Corresponding Geophysical Survey No.	Date of Geophysical Survey	SRP Report No.
SRP Pinal Central-Abel 500kV (Browning-Dinosaur-Abel)	PM 1	5/28/2009	12	4/18/2017	CE-558
	PM 2	5/27/2009	11	4/7/2017	CE-558
	PM 3	5/27/2009	10	4/7/2017	CE-558
	PM 4	5/28/2009	9	4/7/2017	CE-558
	PM 5	5/14/2009	7	4/7/2017	CE-558
	PM 6	5/14/2009	8	4/7/2017	CE-558
SRP Duke to Pinal Central 500kV	P-202	4/25/2011	13	4/18/2017	CE-593
	P-140	4/25/2011	14	4/18/2017	CE-593
	P-123	4/22/2011	15	4/18/2017	CE-593
	P-73	4/22/2011	20	4/25/2017	CE-593
	P-25a	4/20/2011	19	4/25/2017	CE-593
Pinal West to Duke 500kV	P-88	4/20/2011	17	4/25/2017	CE-592
	P-62	4/19/2011	16	4/25/2017	CE-592
	P-5a	4/19/2011	18	4/25/2017	CE-584

Existing Data

Reports from PMT testing sites were obtained from Salt River Project (SRP) archives and publications (Table 13**,** Figure 1). From the SRP archives, a total of ten

transmission line projects included PMT testing at 29 different sites across central Arizona. Only 14 sites were at known and accessible locations for further geophysical analysis (Table 13) (SRP 2010, 2011, 2012a, 2012b). Additionally, PMT sampling at these 14 sites was conducted in similar dry climatic conditions (see Chapter 4 discussion on seasonal variation). Details on the testing, subsurface conditions, and geology for each site are summarized in the Geology Section and the full reports can be requested from SRP.

Data Collection

Seismic refraction surveys were performed by Tiana K. Rasmussen, PG of Amec Foster Wheeler with the assistance of Ashley Evans, on April 7, 18 and 25, 2017 at the previous sampled PMT locations. A total of fourteen, 120-foot long refraction surveys were conducted (Table 13).

The geophysical survey included both near-surface microtremor (ReMi) surveys to obtain vertical surface wave (s-wave) profiles and seismic refraction surveys to obtain compression wave (p-wave) profiles. The ReMi survey is necessary to identify weaker subsurface layers, evaluate the degree of saturation of the subsurface layers, and calculate the shear modulus. Refraction microtremor (ReMi) surveys use surface wave methods for estimating Rayleigh-wave velocities to depths of 60 feet which enhance traditional seismic refraction surveys and provide a measure of S-wave velocity.

Seismic waves were generated for refraction survey by using a sledge hammer struck perpendicularly to the geophone alignment, at four locations along the alignment, to measure shallow (near surface) compression wave (p-waves) velocity. Wave energy for ReMi analysis was achieved by physically jumping up and down at the end of the geophone array, producing a one-dimensional vertical surface wave (s-wave) profile at each survey line.

Travel-time data for seismic wave traverses were obtained using Geometrics, Inc., Geode 24-Channel signal enhanced seismograph. The geophones are fitted with small metal spikes that were forcibly pushed into the ground to improve coupling. This placement method permits accurate recording of the ground motion caused by seismic waves. Data was recorded along the line to permit calculation of layer inclination or dip along velocity boundaries and S-wave and P-wave velocity were calculated. Final review of the geophysical profiles was conducted by Michael Rucker a registered engineer at Amec Foster Wheeler.

ANALYSIS METHODOLOGY

The methodology outlined in Chapter 6 is used to calculate the degradation factor for the 14 sites with both S-wave velocity and PMT measurements, resulting in a database of 52 samples (all data used is the analysis is presented in Appendix A). Prior to calculation, the PMT values were first corrected to an assumed constant Poisson's value of 0.33, as different geotechnical firms made different assumptions ranging from 0.2 to 0.33 (SRP 2010, 2011, 2012a, 2012b). The assumed constant value of Poisson's ratio is then used to calculate the intermediate strain shear modulus from PMT values. Values of the shear modulus from PMT testing were evaluated based on the shape of the initial loading curve. Reported PMT shear modulus values were adjusted only to insure the calculation of the intermediate modulus. The secant points were selected to stay within the linear-elastic range, as values within the plastic range are more in line with high-strain modulus. This adjustment was only done on two samples (PM-3 at 7 feet, PM-4 at 13 feet).

The corresponding value of S-wave and P-wave velocities were selected for each PMT test. Selection of velocities accounted for the change in ground line, as some samples were collected within agricultural fields that may have altered the ground surface between PMT and S-wave velocity testing times. S-wave velocity

values can be affected by the inclination of subsurface layers. For this analysis low S-wave velocity layers were ignored if the compression wave profile identified sloping subsurface conditions or other anomalies. For the analysis of the 14 sites, only 2 values were adjusted to exclude anomalies (Line 14 at 5.5 feet, Line 19 at 4.5 feet). The nominal P-wave velocity was selected for each subsurface layer to best match the bore log profile and to follow standard practice. All values used in the analysis are reported in Appendix A.

GEOLOGIC SETTING

Regional Geology

The 14 test sites are located along two existing Salt River Project (SRP) transmission lines, Browning-Dinosaur-Able and Duke-Pinal Central lines, which are located to the south of Phoenix, AZ in the Sonoran Desert. The Sonoran Desert Section of the Basin and Range physiographic province is characterized by northwest, north and northeast trending mountains that rise abruptly from broad, elongated, sediment-filled valleys produced by block faulting and folding (Richard et al. 2000). Basins and surrounding mountains of the Sonoran Desert section were formed approximately 13 to 10 million years ago from mid- to late-Tertiary periods (Geological Consultants, 2006). Extensional tectonics resulted in the formation of horsts (mountains) and grabens (valleys) with vertical displacements along high angle normal faults. The basins filled with alluvium from mass wasting of the surrounding mountains as well as from nearby stream and sheet erosion. Coarser-grained alluvial material was deposited at the margins of the basins near mountain fronts, with finer-grained materials trending toward the center of the basins. All of the testing locations are located in basins filled by broad alluvial plains and terraces.

In hydrological terms the sites are located in the Stanfield Basin, East Salt River Valley Basin and Picacho Basin. In these basins, the surface water flows northwestward towards the Gila River and Salt Rivers. Within the Maricopa-Stanfield Sub-basin flow is generally-northwest towards the Gila River. Within the Mesa-Chandler sub basin flow is generally northwestward towards Queen Creek Wash and Salt River. Within the Eloy Sub-Basin flow is generally north ward towards the Gila River.

All of the surface waters within the project area are considered to be ephemeral. All surface waters flow as a sheet on the surface and only flow within small, incised washes during and just after periods of rainfall. Subsidence is a concern for all three sub-basins; however, the ground water table throughout the region is more than 500 feet below groundline and should have minimal effect on the near surface modulus properties.

Surface Geology

Geological Consultants (2006) performed detailed geologic reconnaissance for both the Browning-Dinosaur-Able and the Duke to Pinal Central transmission lines, with the relative geologic units reprinted below:

> Young Alluvial Fan Deposits; < 250ka (Qyaf, Qylf, Qyf, Ql, Qyc) - Younger fan deposits are generally found on lower slope surfaces, along active washes and in the channels of ephemeral streams draining piedmonts, mountain foothill areas and within basin floors. These deposits consist of moderately dense to very dense, poorly sorted, medium to course grained sand and gravel containing some silt and boulders and are slightly damp to moist. Minor caliche development is seen in some areas.
>
> Middle-Age Alluvial Fan Deposits; 250 to 750 ka (Qm, Qml) – These deposits generally
> comprise dissected alluvial fans and terraces with strong soil development primarily associated with middle and upper piedmonts. Soils consist of soft to firm and low plasticity clayey sands and loose to medium dense, non-plastic gravels and sands over very dense/hard and poorly sorted sands, gravels and cobbles and are slightly damp to moist. Local caliche development ranges from Stage II to IV.

Old Alluvial Fan Deposits, 750ka to 2Ma (Qoaf) - Soil development is moderate to strong and consist of dense to very dense, moderately to poorly sorted, medium to coarse grained silty sand with sub-angular to subrounded gravels with random cobbles in varying proportions that are slightly moist to moist. Where clay fines are present in the matrix, caliche development ranges from a Stage II to IV. These deposits vary in thickness from a few feet thick near hills and mountains to a few hundred feet thick in the central basin.

Young Basin Fill, Holocene Flood Plain Deposits (Qbfy, Qy1r, Qy2r, Qysr) – This unit encompasses active channels and low terraces (both connected and spatially separated from main channel and swale networks). Areas more prone to inundation during moderate to large flow events (Qy2r) are generally weakly developed and have clay loam or sandy loam textures with little or no evidence of clay movement or carbonate accumulation. Young basin fill consists of poorly sorted silt and clay interbedded with gravel and sand. The unit ranges from light red-brown to brown, fine- to medium-grained silt, silty sand/clay, clay and clay with gravel.

Intermediate Basin Fill Stage II Middle to Late Pleistocene (Qbf, Qbfo) - Basin fill consists of poorly sorted and poorly graded sand and gravel interbedded with low to high plasticity silt and clay. The sands are fine- to medium-grained and dense. The unit ranges from light red brown, red brown, yellowish red to brown silty sand, clayey sand, silty clay and clay with gravel and is slightly damp to wet. Stage II caliche development is present along with moderate desert pavement and desert varnish when found at the surface. Agricultural development mostly masks basin fill surface features.

Site Conditions

The testing locations are along two different transmission lines but are grouped below based upon their geographic proximity in this report (Table 14). The testing locations have varying depths of unconsolidated Holocene age alluvial terrace deposits that overly cemented and consolidated basin fill deposits. A wide variability in subsurface properties, as seen in the data point scatter in Figure 43, arises from the layered alluvial deposits and variation in cementation at depth.

Table 14

Site Descriptions of PMT Locations

Structures	Location	Transmission Line	Geology	Location	Washes /Levees	Land Development
P62	Maricopa, AZ	SRP Pinal West to Duke	Basin Fill Deposit	West of Haley Hills, northeast of Table Top Mountains, and west of Sacaton Mountains	None	In agricultural field
P88						
5A		SRP Duke to Pinal				Near Duke Substation
25A					East of Santa Rosa Levee	In agricultural field
P73			Young Alluvial Fan			
P123	South of Casa Grande, AZ			Casa Grande Mountains, north of Highway and south of the Sierra Point	East of Santa Crux Wash	In undeveloped land
P140					North side of Casa Grande Canal	Near agricultural field
P202					None	In agricultural field
PM1	South of Coolidge, AZ	SRP Browning-Dinosaur-Able	Basin Fill Deposit	North west of Picacho Mountains and east of the Sacaton Mountains		
PM2					Near McClellan wash	In undeveloped land
PM3					None	In agricultural field
PM4					Near Bogart wash	
PM5	North of San Tan Valley, AZ		Young Alluvial Fan	Northeast of San Tan Mountains and southwest of the Superstition Mountains	West of Rittenhouse FRS	Near FRS
PM6						

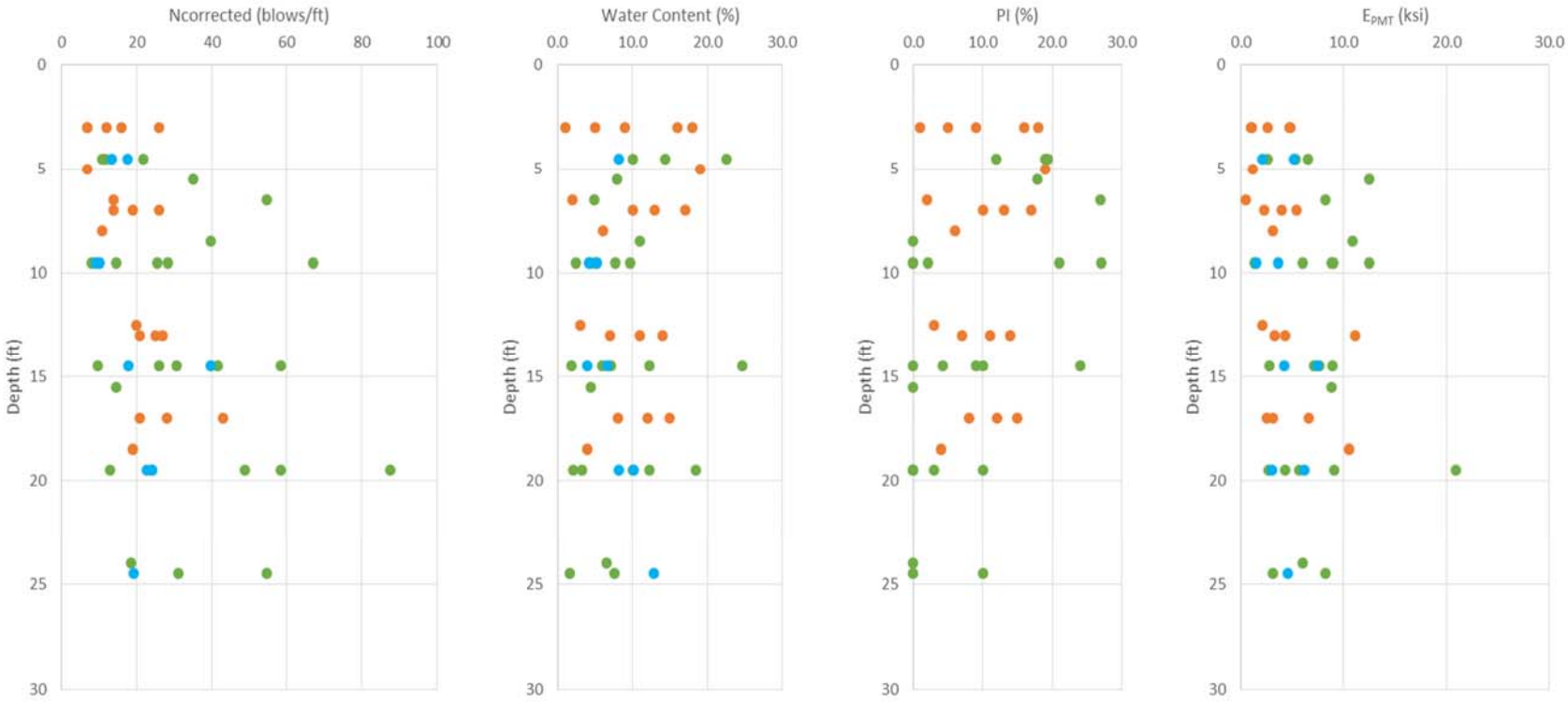

Figure 43. Comparison of subsurface properties at the at the transmission line sites (Orange is Browning-Dinosaur-Able; Green is Duke to Pinal Central, and Blue is at the Duke Substation).

REGIONAL DEGRADATION FACTOR CALCULATION

The goal of this research is to obtain a regional degradation factor between low and intermediate strain moduli to be able to use S-wave velocity as an estimate of PMT modulus for quaternary aged soils in the Sonoran Desert. A poor correlation (R^2 = 0.1665) was obtained from linear regression wherein the S-wave velocity obtained from ReMi survey was related to the constrained elastic modulus from PMT testing. The poor correlation is in line with previous evaluation of desert southwest soils (e.g. Robbins, 2013). This is expected due to the variation in both strain level and direction of forces imparted by PMT and S-wave velocity (Figure 44). A new methodology to relate low to intermediate strain modulus by accounting for the directionality and stress-strain force relationship between PMT and S-wave velocity modulus is proposed. Additional correlations are provided for estimates of density, which allow for an estimate of PMT modulus based solely on the measurement of S-wave and P-wave velocity.

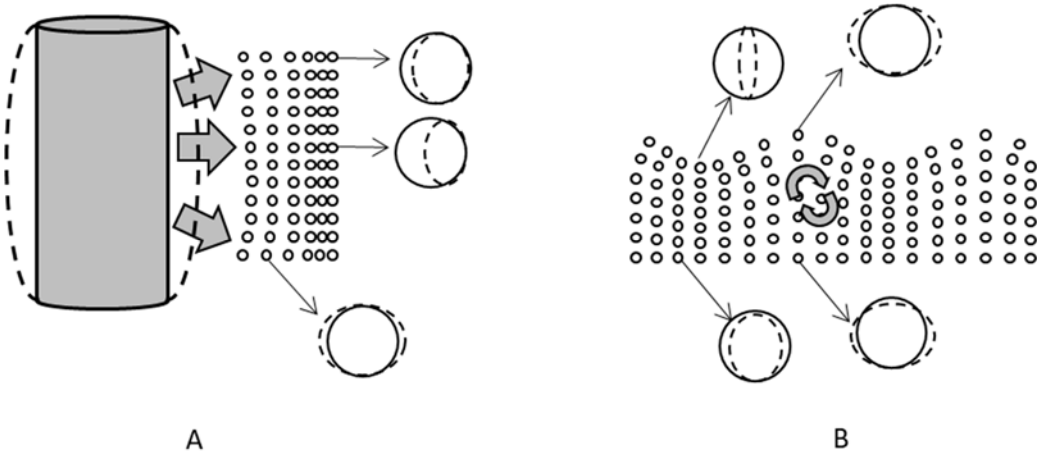

Figure 44. Effect of PMT on soil particle (A) and Remi Rayleigh wave (B) on stationary soil particle (solid line) and alternated particle (dashed line).

Calculating Intermediate-Low Strain Degradation Factor

The degradation factor derived from constrained modulus is the same as that derived from shear modulus (Equation 20). For a particular soil, the intermediate shear modulus from the PMT (G_{PMT}) should have a linear relationship to the low strain modulus from S-wave velocity measurement (G_{Θ}) (Equation 21). Given that the soil measured is the same for both tests, the density derived from the PMT bore log testing can be used to normalize the PMT moduli, creating a calculation of intermediate strain velocity from the PMT testing (Equation 22 and 23). This calculation of velocity from PMT is then comparable to the S-wave velocity obtained from the ReMi survey (Equation 24). These two velocities then are a measure of similar soil fabric changes, but at different strains (Figure 44). The resulting ratio of intermediate to low strain velocities is a degradation factor, which is the same as the degradation factor developed by a direct measure of shear or elastic modulus (Equation 25). The resulting degradation factor, then can be used to calculate intermediate strain moduli from low strain moduli.

$$\frac{E_{PMT}}{E_o} = \frac{G_{PMT}(1+\nu)}{G_o(1+\nu)} \tag{20}$$

$$G_{PMT} = G_o\left(\frac{G_p}{G_o}\right) \tag{21}$$

$$G_o = \left(\frac{\gamma_{total}}{g}\right)V_s^2 \tag{22}$$

$$\frac{G_{PMT}}{\left(\frac{\gamma_{total}}{g}\right)} = V_s^2\left(\frac{G_p}{G_o}\right) \tag{23}$$

$$\left(\frac{G_p}{G_o}\right) = \left(\frac{\sqrt{\frac{G_{PMT}}{\left(\frac{\gamma_{total}}{g}\right)}}}{V_S}\right)^2 = \left(\frac{V_{PMT}^*}{V_S^*}\right)^2 \tag{24}$$

$$E_{PMT} = \left(\frac{G_p}{G_o}\right)E_{o_{SWV}} \tag{25}$$

Using this methodology and normalizing both shear moduli for depth results in a stronger correlation ($R^2 = 0.685$) and the average degradation factor is equal to

0.2969 (Figure 45). This degradation factor is consistent with the MFAD relationship of 0.325 between intermediate and low strain moduli based on full scale foundation testing (EPRI, 1982; EPRI 2001). The lower average degradation factor is likely a specific features of desert (cemented and unsaturated) alluvial soils as the EPRI data was derived largely from non-cemented glacial materials. The EPRI work references Parker and Resse's (1970) relationship of 0.35 between the initial slope of a stress strain curve and the intermediate slope for a uniform fine sand. As the Quaternary aged soils in the Sonoran Desert are interbedded with clays and sands and cemented with depth, then these unsaturated soils with high matric suction and cementation are expected to have higher degradation factor.

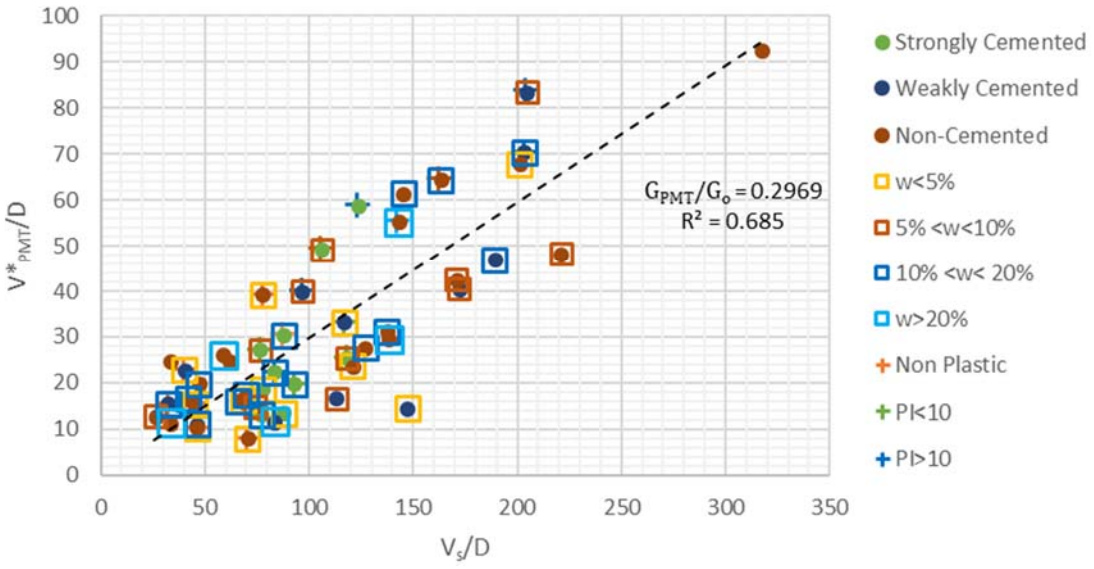

Figure 45. Correlation between high strain to low strain velocity.

DISCUSSION

The ratio of intermediate to low strain moduli is variable based on the material properties of the soil (see scatter of data in Figure 45). This variability is expected because both, the low and intermediate strain moduli are influenced by stress state of the soil mass which is affected by the confining stress, Poisson's ratio, plasticity index, grain size, cementation, water content, and matric suction. As the S-wave velocity data was not collected on the same day as the PMT data, then changes in stress state may have occurred, particularly variations in water content and soil suction (see Chapter 4 for expected seasonal S-wave velocity variability). The following discussion evaluates the effect of these parameters on the correlation between intermediate strain and low strain moduli.

Variations in Density

Although the dry density likely remained the same between the PMT sampling and geophysical survey, there may have been a change in the water content of the soils. This variation is evident when comparing the calculation of degradation factor with either total unit weight or with dry unit weight. Using the total unit weight, including the water content at time of PMT sampling, decreases the variability (R^2=0.6892) compared to considering only the dry unit weight (R^2=0.685) (Figure 46). This variation suggests that there was a change is the stress state between the PMT testing and refraction survey. Both the PMT and refraction surveys were conducted in dry conditions, where there was no measurable rainfall event within a week of sampling. The variability in these dry conditions, then, is likely related to soil suction, which is a stress state variable for unsaturated soils, for which behavior is controlled by net normal stress and matric suction (see Equation 1).

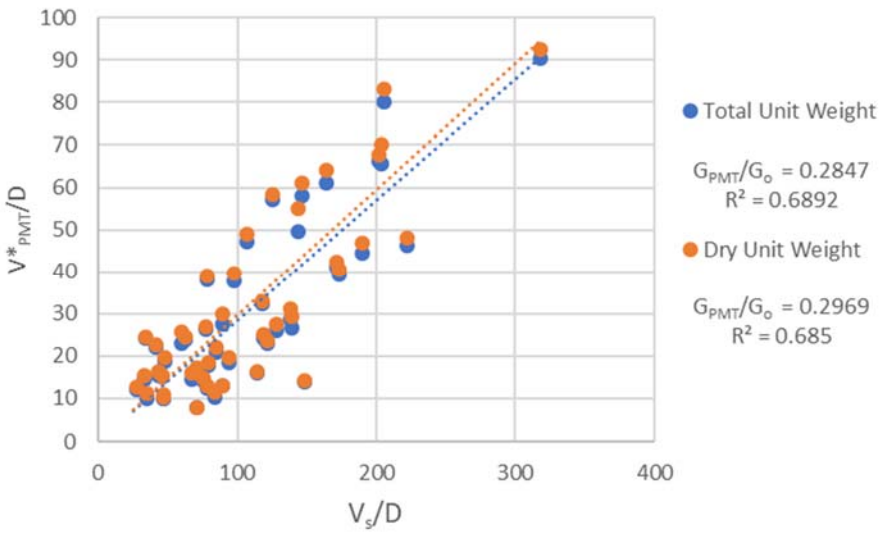

Figure 46. Effect of variation from dry to total unit weight

Correlation with Unit Weight

The correlation between S-wave velocity and dry unit weight fits within previous predictions for the region (Rucker 2008) (Figure 47). New trends for non-cemented and cemented granular materials are proposed (dashed lines) to fit the existing model. However, using only S-wave and P-wave velocity to correlate with dry density, results in large scatter in the dataset.

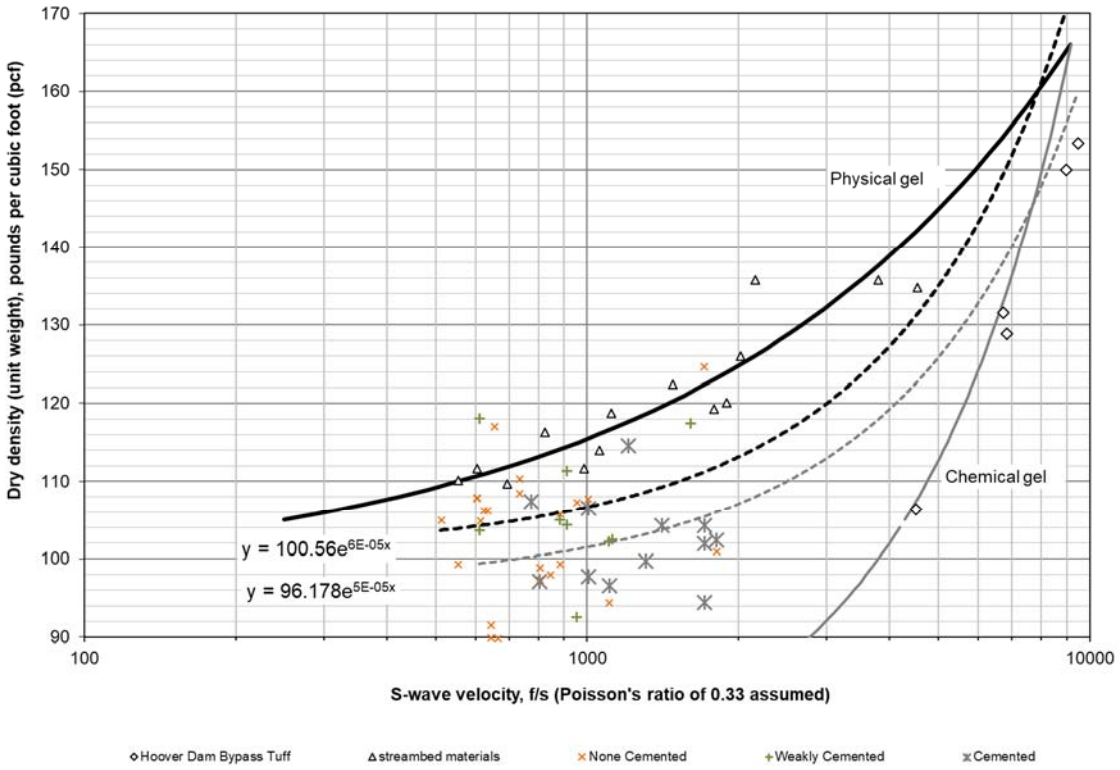

Figure 47. Dry unit weight comparison with Rucker (2008) correlation

Taking a different approach, the previously developed geometric relationships between S-wave and P-wave velocity (based loosely on the relationship of Poisson's ratio) was explored to provide an estimate the of dry unit weight of the soil (see Table 1). The proposed geometric relationship (Equation 26) of the S-wave and P-wave velocity correlates well with soil dry unit weight (Equation 27, R^2=0.9223) (Figure 48). This relationship is based on Equation 11; which in this case, due to the geometry of the ReMi based S-wave velocity is more a measure of the dry unit weight of the soil than variation in strain directionality.

$$\frac{\gamma_{dry}}{d} = \frac{\left(\frac{2*V_p^2 - V_s^2}{2*\left(V_s^2 + V_p^2\right)}\right)}{d} = \frac{(\gamma^*)}{d} \tag{26}$$

$$\gamma_{dry} = 147.26\left(\frac{2*V_p^2 - V_s^2}{2*\left(V_s^2 + V_p^2\right)}\right) \tag{27}$$

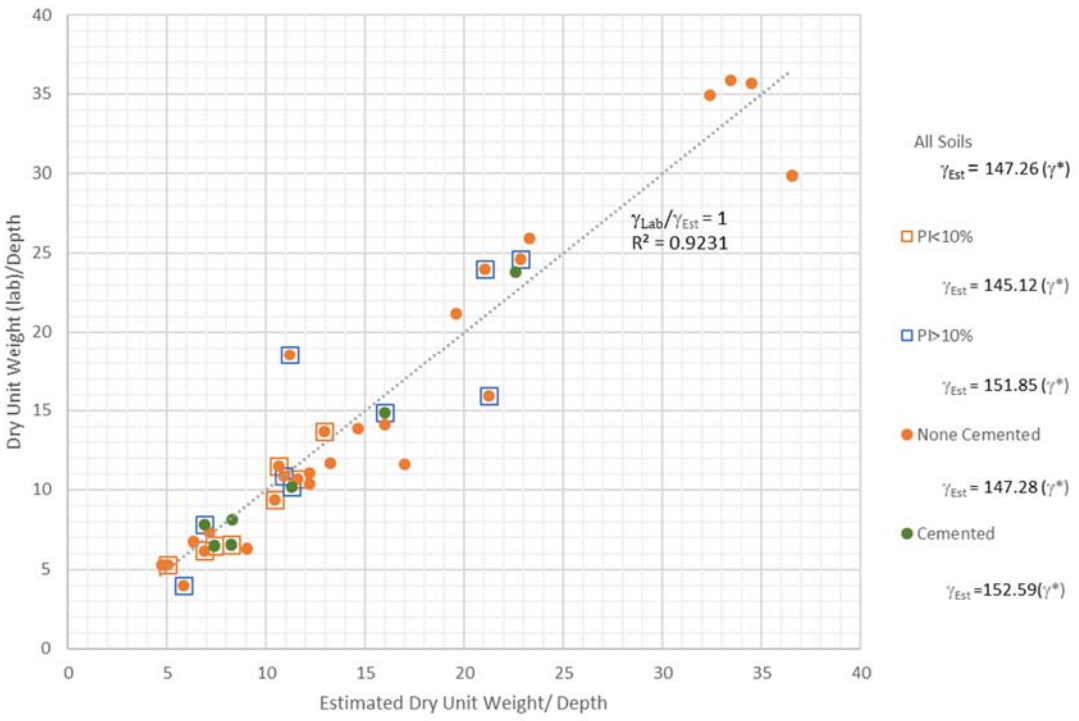

Figure 48. Correlation to dry density

Additionally, the relationship between S-wave velocity, P-wave velocity, and unit weight is slightly different depending on the plasticity index (PI) and degree of cementation, which are functions of matric suction (stress-state) among other particle bonding factors (Table 15). Because relationship between matric suction and soil moisture content is a function of soil type, both cementation and PI (and soil gradation) affect how the waves travel though the media. Although cemented soils and higher PI soils may or may not be denser, the more brittle nature of these soils could result in cracking within the soil structure (including desiccation cracking), which would reduce the S-wave velocity. Soils with higher PI have lower S-wave velocity due to moisture retention characteristics but can have high moduli due to increased strength. Therefore, having information on the level of cementation and PI likely will improve the correlation between S-wave velocity, P-wave velocity, and soil unit weight.

Table 15

Correlation to dry unit weight based on cementation and water content

Condition	Formula	Variation	Equation
Noncemented	γ_{dry} =147.28 ($\gamma*$)	R^2 = 0.9155	(28)
Cemented	γ_{dry} =152.59 ($\gamma*$)	R^2 = 0.9685	(29)
PI>10%	γ_{dry} =151.85 ($\gamma*$)	R^2 = 0.7473	(30)
PI<10%	γ_{dry} =145.12 ($\gamma*$)	R^2 = 0.9014	(31)

Degree of Cementation

Rucker and Ferganson (2008) established a correlation between stage of cementation and wave velocity. Where soils with a P-wave velocity greater than 2000 ft/s and S-wave velocity over 1000 ft/s were found to have visible signs of cementation (Stage I). The recorded PMT bore logs only contained relative information on cementation, not stages (Table 16). The cementation classifications are used to classify the dry strength and relative firmness of subgrade materials.

Table 16

Range of descriptions found in SPR bore logs

Classification	Description
Weakly cemented	Reacts with HCl and some calcium carbonate nodules
Mod. cemented	Reacts strongly with HCl and filaments continuous throughout, nodules are present, sample is white/gray/pink, considerable finger pressure required to break soil
Strongly cemented	Reacts strongly to HCl, filaments continuous and almost indistinguishable, sample is white, will not crumble or break with firm pressure, refusal blowcounts

The general trend in the bore logs, consisted of increased cementation with depth within a given bore log. The reported visual observation of cementation did not correlate well with S-wave and P-wave velocity, except that most soils identified as moderately to strongly cemented had a S-wave velocity over 1000 ft/s (2000 ft/s P-

wave velocity). There were, however, soils described as noncemented that had higher S-wave velocities.

Note that the trend in degradation factor for cemented soils is significantly different from the non-cemented and weakly cemented soils (Figure 49). The trend starts at a higher velocity, this feature is supported by Rucker and Fergason's (2006) correlations where cementation was found to correspond to shear wave velocities over 2000 feet per second. Also, the trend for cemented soils is steeper which indicates that the degradation factor for cemented soils approaches one, which is more in line with rock materials following Rucker (2008). A larger database of cemented soils with PMT and S-wave velocity is needed to evaluate this trend, although this is unlikely due to the issues of conducting PMT samples in highly cemented soils.

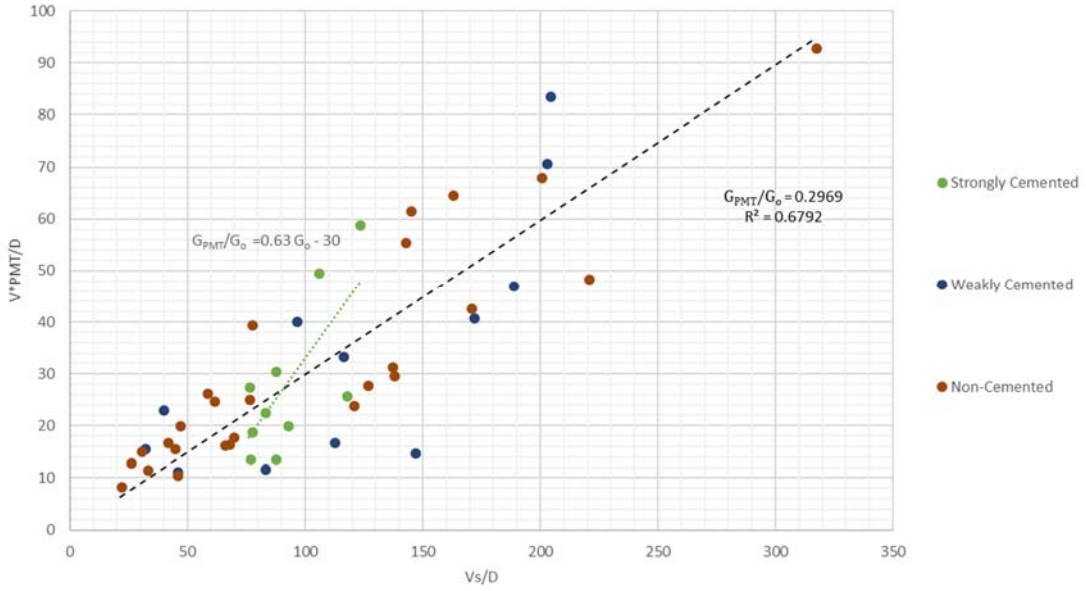

Figure 49. Variation in trend for moderately to strongly cemented soils

Water Content

In unsaturated soils, the soil water characteristic curve illustrates the relationship between the water content and matric suction, where decreasing water content while drying relates to increased matric suction, and therefore increases shear strength and stiffness. All soils reported had a water content between 3 and 25%, with the higher water contents associated with the clayey soils and lower water contents associated with cemented soils. The variation in water content between samples during PMT testing only has a slight effect on the correlation (Figure 50). Evaluation of the WSI (e.g. Grelle et al., 2009) and other geometric relationships between S-wave and P-wave velocity were not viable. This may be because the geometry of S-wave velocity from ReMi and P-wave velocity may be more a factor of the soil type, including soil skeleton structure, than measurement of water content alone. The effect of water content change on soil suction, and therefore, shear strength and stiffness, is highly soil-type dependent. Another factor, likely of less importance, is the long length of time between PMT and ReMi testing (See Chapter 4 for further discussion on seasonal variability).

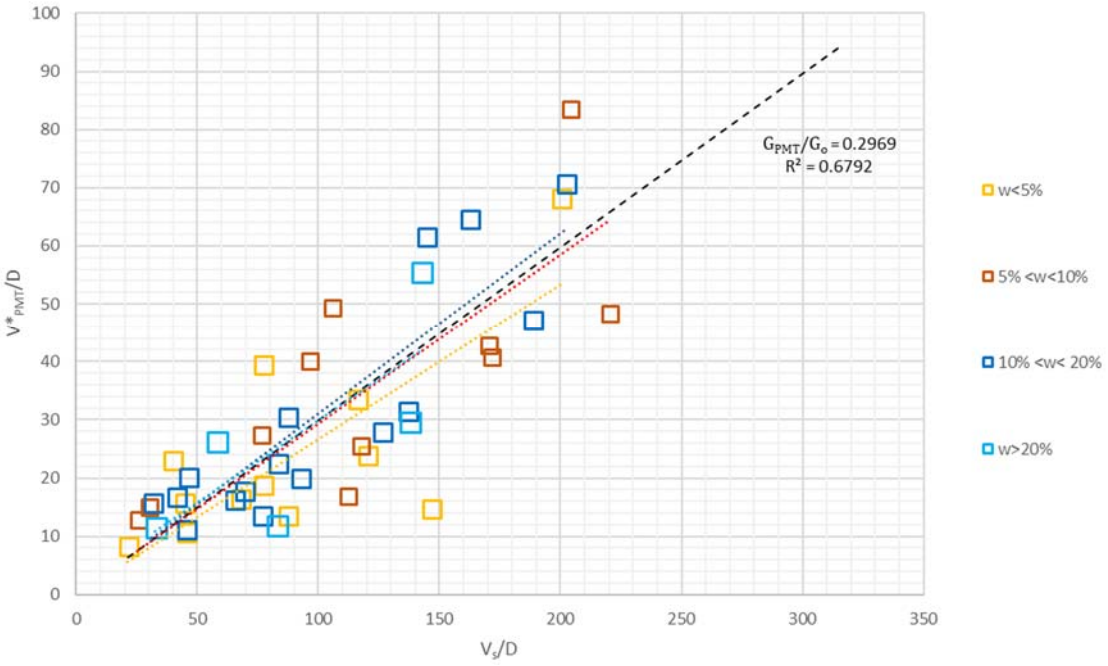

Figure 50. Effect of water content on correlation

Chapter 4 provides a detailed discussion on the effects of seasonal changes in water content, with the greatest effect seen within the upper 5-feet of the soil profile. The 14 selected PMT and S-wave velocity samples were collected in similar seasons and neither sites had received measurable rain within a week before sampling. Some sites, however, are located in or near active agricultural fields. The frequent watering of the soil in agricultural fields would be expected to increase the degradation factor due to possible increased suction and cementation. The number of samples is small but there is a slight increase in the degradation factor of the sites located near agricultural fields, however the trend is within the coefficient of variation of both samples (Figure 51). Further analysis is needed to evaluate the effects of agricultural watering on modulus.

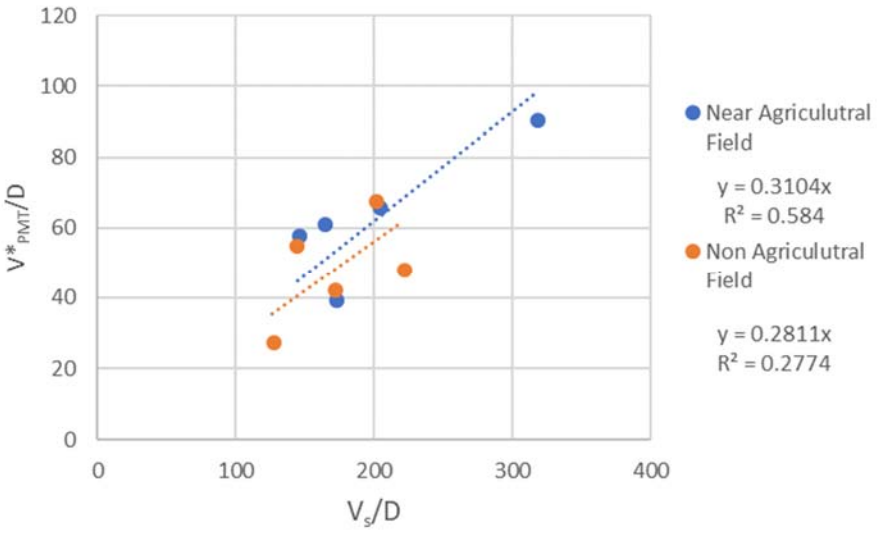

Figure 51. Variation in upper 5 feet between agricultural fields and undeveloped lands

Plasticity Index

Clayey soils can sustain high matric suctions, in part due to a small in particle size, whereas sandy soils tend to desaturate at very low values of matric suction. To evaluate the effect that matric suction may have on the non-cemented soil samples, the correlation to plasticity index is evaluated as an estimate of clay content. Other factors related to soils grainsize could not be evaluated due to a lack of grainsize data in the dataset. The resulting dataset with recorded plasticity set only included 23 samples. Note that samples with PI greater than 10% caused a significant shift in the correlation, where these samples have a higher degradation factor. The non- and weakly-cemented samples with less than 10% plasticity also have a higher trend than that of the sample average trend (Figure 53). Considering only the noncemented, sandy soils (removing samples that have PI>10% and have moderate to strong cementation) improved the correlation between intermediate and low strain modulus (R^2 = 0.7374).

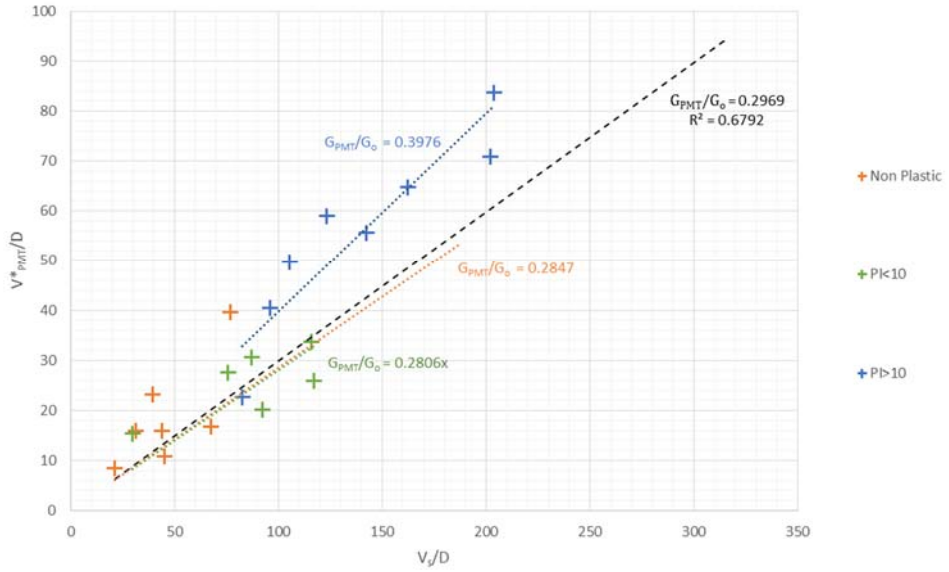

Figure 52. Effect of PI on degradation factor

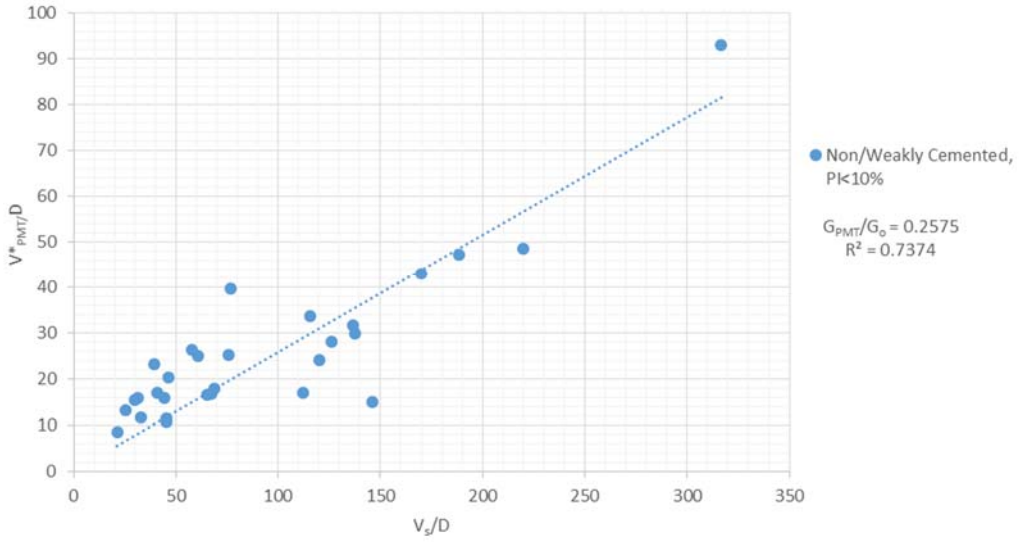

Figure 53. Non to weakly cemented and low PI degradation factor

Correlation of P-Wave and S-Wave with SPT

The standard penetration test (SPT) is commonly used as an index for correlation to numerous geotechnical engineering parameters. When considering geophysical velocity survives, the correlations to SPT are typically used for site

classification in terms of seismic hazard. These correlations take the form of Equation 32 and depend on the geologic age of the material and grain size (Hussien and Karray, 2016). For which,

$$V_s = aN^b \quad (32)$$

where N is the corrected blow count, a and b are factors, and Vs is the S-wave velocity. Likewise, previous correlations to modulus that used blow count data found a significant correlation between geologic age of deposition (Wair et al. 2002).

For the Sonoran Desert, the linear regression between SPT N values and S-wave or P-wave velocity is poor, with less than a 0.4 R-squared value for S-wave velocity (Figure 54) and 0.5 R-square value for P-wave velocity (Figure 55). The lack of strong correlation is likely due to the fact the data does not account relative density or grainsize as has been identified in other research (see Hussien and Karray, 2016). As relative density increases the N value should increase for a given S-wave velocity and as the grain size diameter increases the S-wave velocity should increase for a given N value.

As the dataset does not include grainsize data, only the relative trend based on USCS from visual description can be evaluated. In general N increases with S-wave and P-wave velocity, where clayey soils have a lower velocity for a given N than sandy soils. Cemented clayey soils tend to have a higher velocity to N relationship, which is likely a function of the small particle size and increased density that results in higher strength and wave velocity. Whereas non-cemented soils display a wide scatter in S-wave velocity but not in P-wave velocity, likely due to the effect of degree of saturation and influence of matric suction, which allows for a higher strength but at a slower velocity.

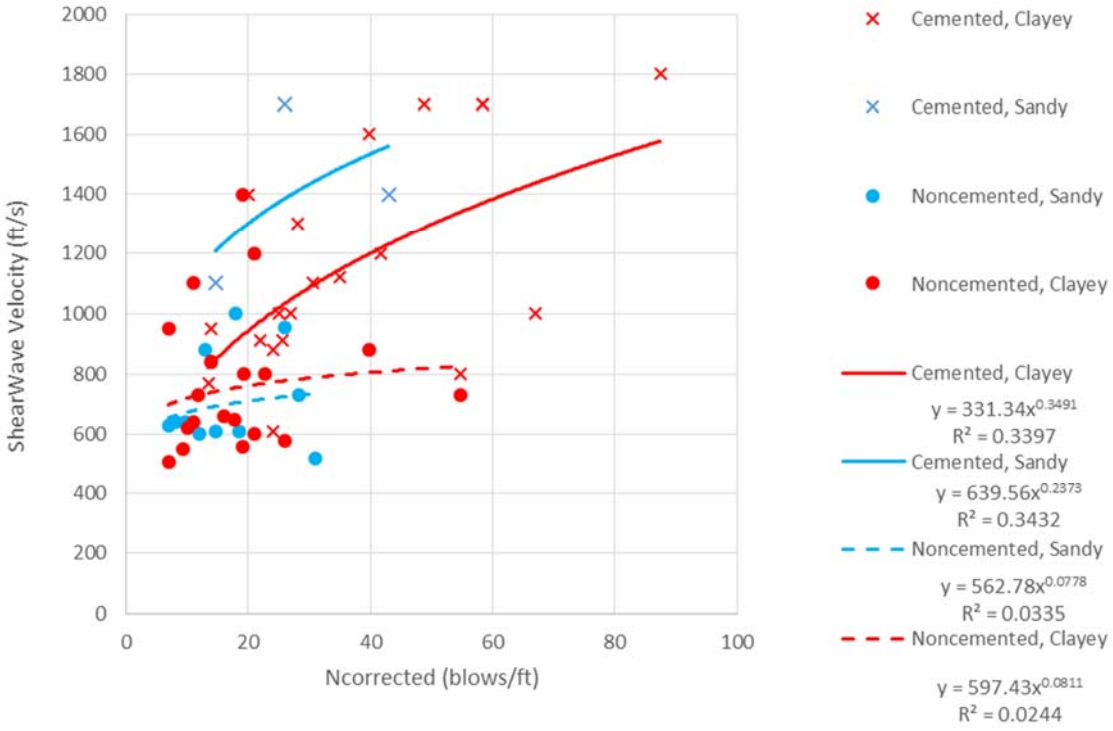

Figure 54. Relationship between SPT and Vs

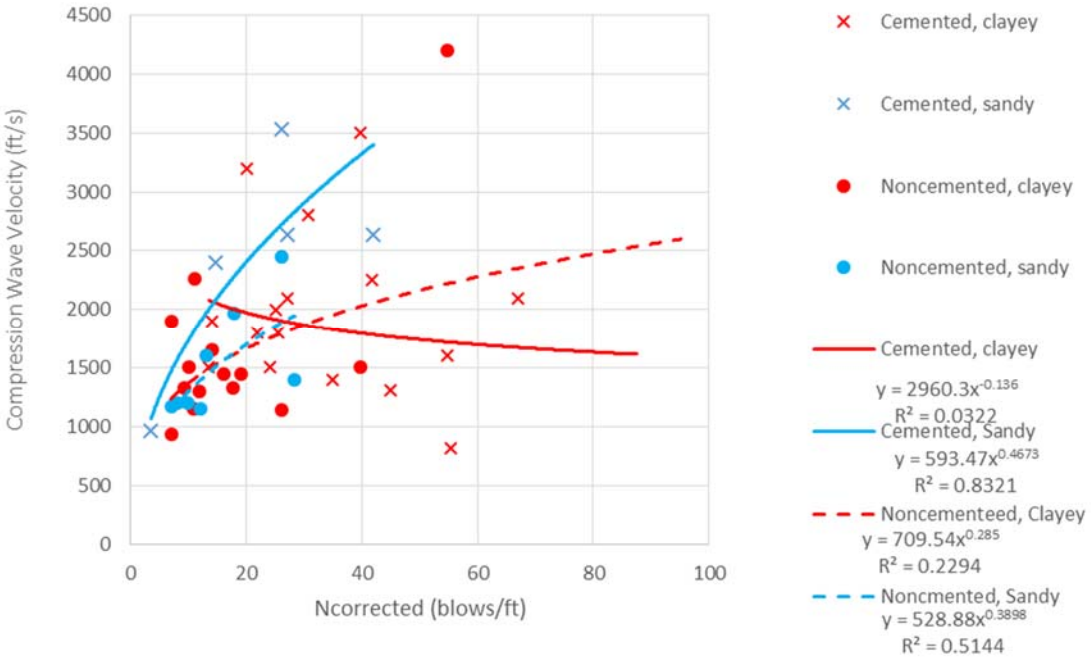

Figure 55. Relationship between SPT and P-Wave Velocity

The values of alpha and beta in Equation 32 for the samples are in line with pervious testing of sandy and clayey soils as summarized by Hussien and Karray (2016). However, the regression between either S-wave or P-wave velocity with N are highly variable (Figure 54, Figure 55). Additional testing is needed to establish the effect of cementation and matric suction on the correlation of N to S-wave and P-wave velocity directly. The variability in the data set is likely due to stress-state changes as the unsaturated soils are affected by variable moisture conditions. Additional causes of the variability may include the difference in scale and direction of the forces between PMT and ReMi. Based on the available data, the correlation to PMT modulus by first correlating wave velocity with N is not recommended for the Sonoran Desert region.

Calculating High to Low Strain Degradation Factor

When the PMT test is conducted, the shear stress-volumetric strain plots can provide information on both the plastic and elastic portions; and therefore, the modulus at high strain and intermediate strain, respectively. Using curve fitting the shear modulus (G) at the different relative volumetric strains (γ) can be plotted. The volumetric strain from PMT testing is known and the small strain modulus is assumed at a very small strain (10^{-6} to 10^{-3}%). The resulting curves can be used to estimate the relationship between high, intermediate, and low strain moduli (e.g. Duncan et al. 2003). A similar approach has been conducted by others for rock using rock quality values (Deere et al., 1967).

The results of this analysis were comparable with Rucker's (2008) relationship between high and low strain velocity based largely on rock properties (Figure 56). Clearly there is a large degree of scatter in the high strain soils data. In general, the cemented and high PI soils trend above 1000 ft/s S-wave velocity. With non-cemented, non-plastic soils at lower velocities.

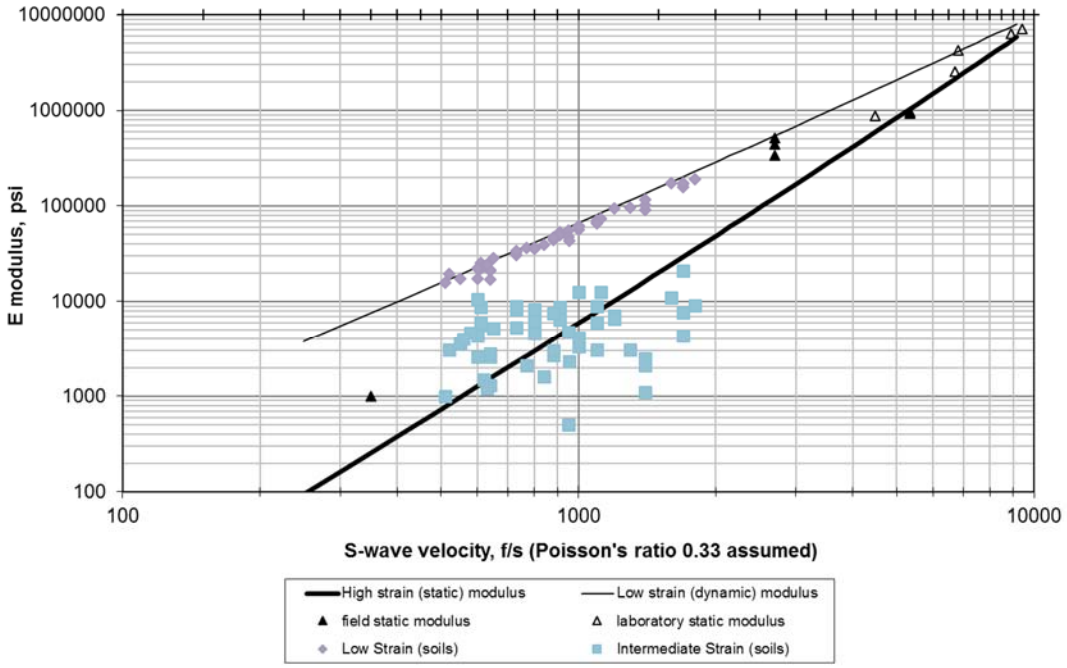

Figure 56. Comparison with Rucker (2008) results

Only a small subset of the data had sufficient information to evaluate the relationship between high, intermediate and low strain modulus — six locations from the Browning-Dinosaur-Able transmission line (Figure 57). These results show the general shape of the function is a Weibull equation as has been previously identified. More data is needed at the high strain modulus to evaluate the curve fit. However, there is an approximately 30% relationship between intermediate and low strain, and an approximately 10% relationship between high and intermediate strain. Additional data is needed to evaluate the shape of the shear stress to volumetric strain curve for desert southwest soils.

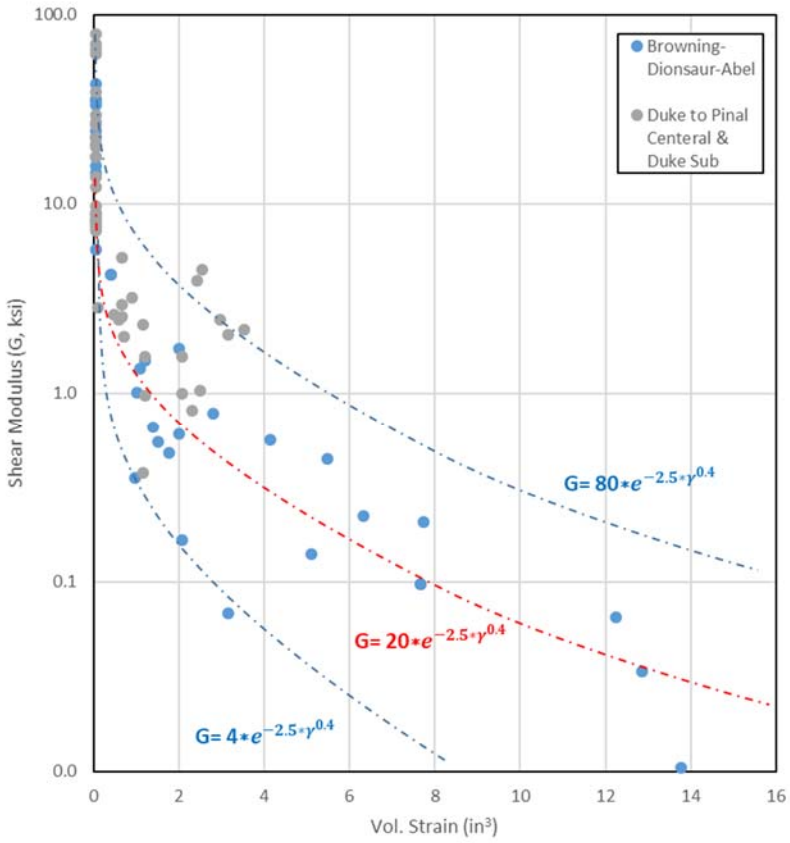

Figure 57. Comparison of high, intermediate, and low strain modulus for PM1-PM6 of the Browning-Dinosaur-Able transmission line (red line is average trend, blue line is minimum and maximum trend)

CORRELATION BETWEEN PMT AND S-WAVE VELOCITY

Combining Degradation Factors

The following chart provides relationship of the average degradation factor for non-cemented soils, >10% PI soils, and cemented soils (Figure 58). Where the degradation factor becomes steeper for increasingly finer grained, more plastic, and higher density soils (or in other words, increasing matric suction). Note that the trend for strongly cemented soils is shifted. These degradation factors can be used in Equation 36, for estimating the PMT modulus from s-wave velocity when density and Poisson's ratio are known.

$$E_{PMT} = 2(1+v) * (\frac{G_{PMT}}{G_o}) * V_s^2 * (\frac{\gamma_{total}}{g}) \quad (33)$$

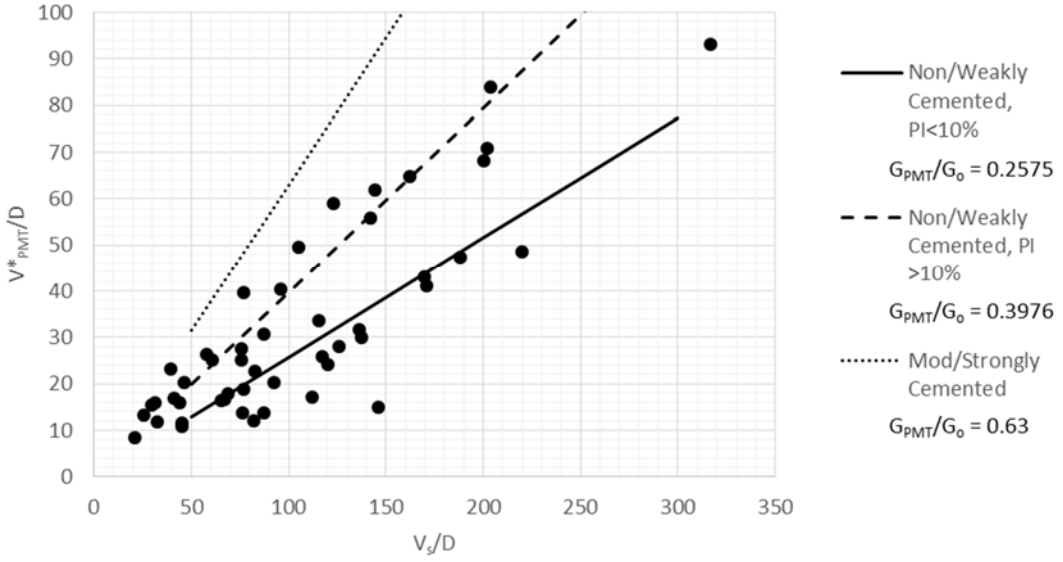

Figure 58. Average degradation factors based on soil conditions

$$\frac{G_{PMT}}{G_o} = 0.2575, non - weakly\ cemented\ soils \quad (34)$$

$$\frac{G_{PMT}}{G_o} = 0.3976, high\ plasticity\ soils \quad (35)$$

$$\frac{G_{PMT}}{G_o} = 0.63, moderate\ to\ strongly\ cemented\ soils \quad (36)$$

Combining Equations for Estimating PMT Modulus

If information on the subsurface properties are is unknown, such as when only geophysical survey is available, then the correlation between PMT modulus and S-wave velocity needs to account for density and Poisson's ratio (following Equation 36).

As the ReMi measurement is not a direct measure of S-wave velocity, the correlations to dry unit weight (Equation 27) and water content (Equation 19) each likely include effects for soil anisotropy, matric suction and cementation. As such the coefficients to the individual equations can be combined as follows into equation:

$$E_{PMT}(ksi) = A * \left(\frac{G_{PMT}}{G_o}\right) * V_s^2 * \left(\frac{\gamma_{dry}*(1+w)}{g}\right) \quad (37)$$

Where V_s the s-wave velocity is in ft/s, γ_{dry} is the dry unit weight is in lbs/ft^3, w is the water content is in percent, and g is gravity assumed as 32.2 ft/s^2. For the Sonoran Desert samples, adding in the correlations for unit weight and water content, and correcting for units results in the following equation:

$$E_{Estimated}(ksi) = 138.2 * \left(\frac{G_{PMT}}{G_o}\right) * V_s^2 * \frac{\left(\frac{2*V_p^2 - V_s^2}{2*(V_s^2+V_p^2)}\right)*\left(1+\frac{(7V_s{}^2)-V_p^2}{3(V_p^2+Vs^2)}/100\right)}{32.2*1000*12^2} \quad (38)$$

Which can be further simplified to the following, where velocity is measured in feet/second:

$$E_{Estimated}(ksi) = 3 * 10^{-5} * \left(\frac{G_{PMT}}{G_o}\right) * V_s^2 * \left(\frac{2.26*V_s^2+1.28*V_p^2}{5*(V_s^2+V_p^2)}\right) \quad (39)$$

This relationship is based only on the S-wave (derived from ReMi), P-wave velocity, and degradation factor as developed here for the Sonoran Desert. Comparison of the estimated PMT modulus correlate well with the actual measured PMT modulus (Figure 59). For engineering design purposes, the 90% confidence interval is recommended to account for variability.

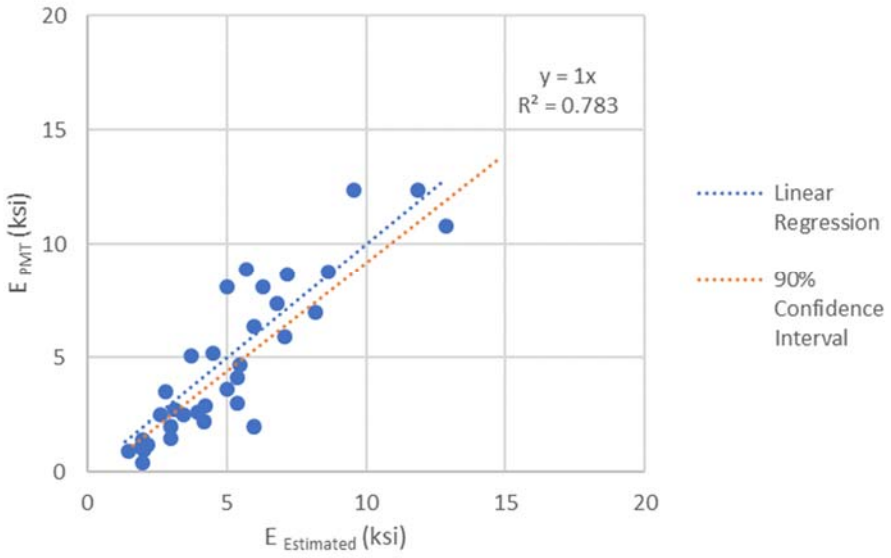

Figure 59. Comparison of PMT modulus to estimate modulus (Equation 39)

CHAPTER 6

EFFECT OF CORRELATION ON FOUNDATION DESIGN

LATERALLY LOADED FOUNDATIONS

The function of a transmission line foundation is to transfer applied steady-state and transient loads into the surrounding subsurface with limited structure movement (Kandaris et al., 2017). Loads are conveyed to the subsurface at the ground line interface, where either a separate foundation system is installed and connected to the structure (Figure 60A), a member is embedded with a secondary reinforcement (Figure 60B), or the above grade structure is directly embedded and backfilled (Figure 60C). Regardless of the foundation type, the primary load on the foundation is lateral (shear and/or moment) for all three structure types (Figure 61). The ability to resist lateral reactions, therefore, controls the design of transmission line structures.

A single mono-pole structure acts as a cantilever with a pivot point about two-thirds depth below grade, causing large reactions just below grade and at the base of the structure. For the foundation, the applied lateral shear load and overturning moment reaction is transferred to the foundation at ground line and the foundation then applies lateral pressure to the subsurface. The focus of design is to properly dimension foundations, so they induce lateral soil pressures to counter large reactions while keeping foundation lateral movement within prescribed deflection and rotation ranges. The behavior of laterally loaded foundations is dependent on the relative stiffness of the foundation and the soil, which relates to embedment depth, foundation diameter, modulus of foundation, and modulus of the subsurface material (Kandaris et al., 2017).

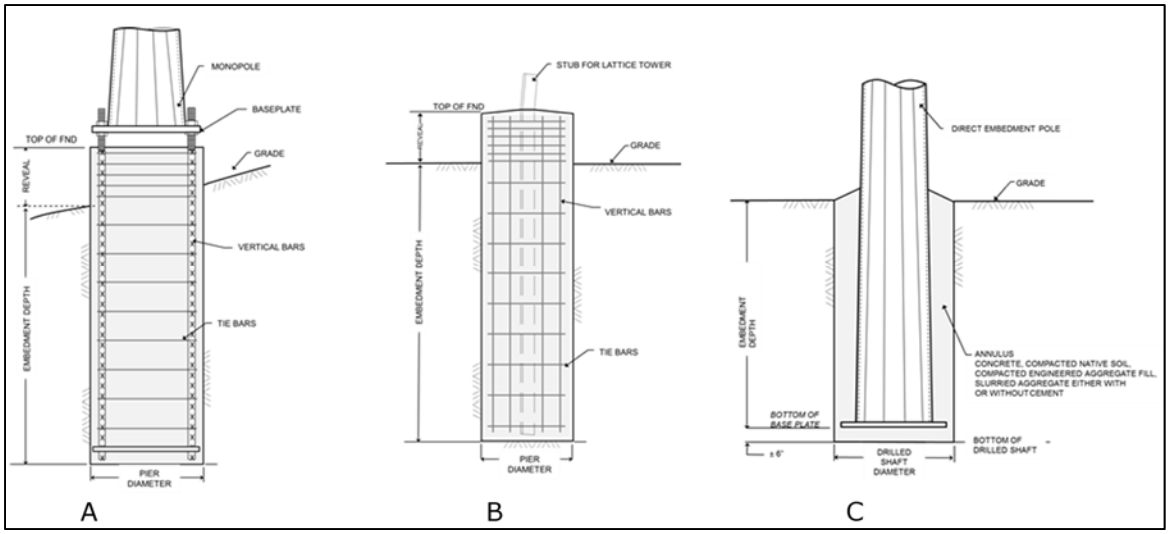

Figure 60. Drilled shafts for monopoles (A), lattice towers (B) and direct embedment foundations (C)

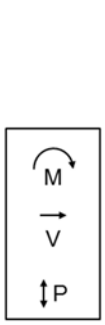

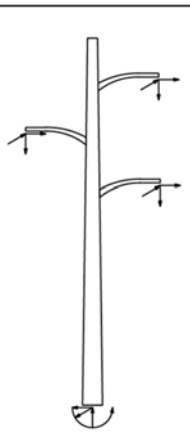

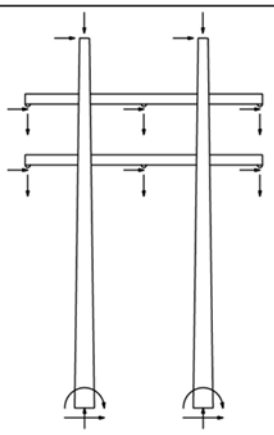

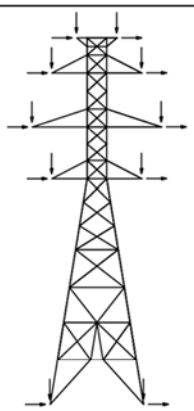

	Monopole	H-Frame	Latticed Tower
Moment (M)	High	Moderate – High*	None
Shear (V)	Moderate	Low – Moderate*	Moderate
Axial (P)	Low	High – Moderate*	High

* Depends on Rigidity of H-Frame

Figure 61. Typical transmission line structures and types of loading reactions

Short Rigid Shaft Foundations

A number of researchers have observed the need for different deformation analysis methods for short, intermediate and long shafts (under free head conditions) and have developed classifications based on shaft properties (Broms, 1964; Vallabhan and Alikhanlou, 1982; Ashour and Norris, 2000) (Figure 62). A short pier exhibits a near linear lateral deflection profile with a single inflection point or a center of rotation within approximately the lower one-third of the foundation depth. Bending stiffness of the foundations remains constant along the full length of the pier and has a significant influence on soil deformation. Alternately, a long, slender pier will show more than one inflection point along the pier length with a point of fixity at depth. The rigidity of the foundation dictates the behavior of the foundation and the applicability of either the short-rigid or long-flexible model (e.g. Broms, 1964). The primary mechanistic model for evaluating the embedment depth of foundations for the transmission line industry is based on the short, rigid shaft behavior (EPRI, 1982).

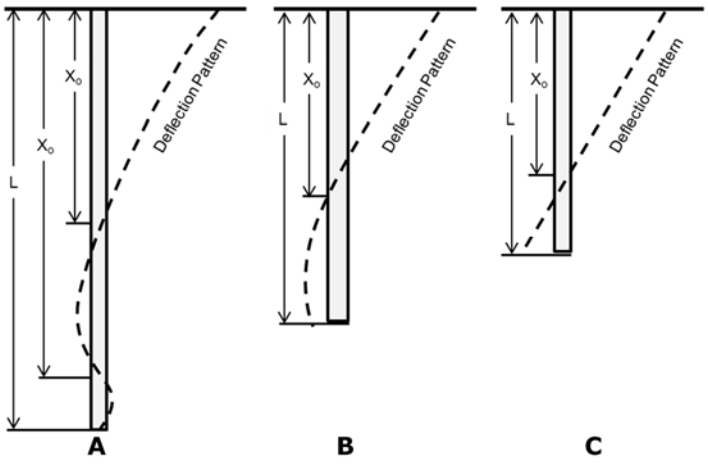

Figure 62. Laterally loaded pile / pier behavior for long (A), intermediate (B) and short shafts (C)

FOUNDATION DESIGN MODELS

Drilled foundations (including reinforced concrete drilled shafts and direct embedded poles) support lateral loads through a combination of lateral resistance of the subsurface, side shear and end bearing. Foundation design models must reflect a complex soil-structure interaction where movement mobilizes soil strength, transferring load in a non-uniform manner (Grigsby, 2012). Numerous analysis models for predicting the soil-structure interaction of laterally loaded drilled shaft foundations have been developed. In general, these models relate the load-deflection and/or load-resistance relationship (foundation capacity) of piers with primarily lateral load applied at or near ground line. There are three categories of foundation models— equilibrium methods, p-y analyses and continuum approaches.

Equilibrium methods calculate a state of static equilibrium assuming ultimate lateral capacity based on the passive resistance of soil along the vertical pier face (Hansen, 1961; Czerniak, 1957; Broms, 1964, 1965). The models attempt to predict lateral soil resistance along the foundation as a function of pier deflection. It is necessary that conditions of both static equilibrium and compatibility of deformation be achieved simultaneously for all parts of the system. These theories assume uniform mobilization of strength from top to bottom of the pier.

However, the load-deflection and load-rotation relationship for a laterally loaded drilled shaft foundation are highly non-linear. In which case, equilibrium methods tend to under-predict capacity and provide only limited evaluations of movement (Brown et al., 2010; EPRI, 2012). Non-linear methods can include limits to lateral soil pressure resistance in relation to movement, commonly referred to as a "p-y" analysis (Reese and Matlock, 1956; Davisson and Prakash, 1963; Reese and Allen, 1977; Poulos and Davis, 1980; EPRI 1982). The "p-y" analysis involves the idealization of soil resistance as a series of relationships between local lateral

pressure of the foundation diameter (p) and local lateral deflection (y) at various locations along the shaft embedment, as a function of stress and foundaiton diameter. The shaft itself is modeled as an elastic beam supported by non-linear springs whose characteristics are represented by the p-y curves. Bending of the shaft under lateral loading can be carried out by either finite difference or finite element analyses and the relationship between lateral loading and deflection can be obtained. Laterally loaded pile/pier commercially available computer programs have been developed to simplify the computation of complex interaction between the foundation and subsurface conditions. Each program makes assumptions of both the mechanistic model and the design methodology. Regardless of the computer model used in design, the model must fit within the larger design methodology and meet the expected behavior of the system. The Moment Foundation Analysis and Design (MFAD) model, is the predominate model used in the transmission line industry because it assumes a rigid shaft (IEEE, 2001).

Alternative approaches uses mathematical models to estimate the limit states based on direct measurement of the stress-strain relationship of the subsurface (Prasad et al., 1996; Budhu and Davies, 1987). The Prasad and Chari (1999) model was developed to more accurately model the pressure distribution of cohesionless soils (Equation 40).

$$H_u = 0.24(10^{1.3*tan(\phi+0.3)}) * \gamma x B(2.7x - D) \quad (40)$$

Where H_u ultimate lateral capacity, ϕ is the friction angle, γ is the unit weight, and x is the depth to the center of rotation of the foundation, B is the diameter of the foundation, and D is the total depth of the foundation. This method does not account for variability in subsurface materials and is based on scaled foundation tests. Alternatively, the method proposed by Budhu and Davies (1987) evaluates cohesionless soils, where the behavior of the foundation is a function of friction angle

and a parameter of soil stiffness, a function of modulus, with depth. Tests were conducted on uniform sands. These models are not widely used within the electric utility industry. As such, the following discussion focuses on improvements to the "p-y" foundation models for rigid piers, primarily the MFAD model.

Comparison of MFAD and LPILE for rigid shaft foundations

The MFAD program was designed for short, rigid shaft foundations. A newly developed model in the LPILE program titled elastic section (non-yielding) was also developed for the analysis of rigid shaft foundations.

The main difference between the MFAD and LPILE (non-yielding) foundation models revolves around the assumption of shaft rigidity. Differences of assumed elasticity within the LPILE and MFAD models for both the entire foundation and on the incremental strain level impact foundation design results. The LPILE program uses stiffness (k_{py}) based on secant subgrade modulus while MFAD uses stiffness (k_h) based on the deformation modulus but also includes the influence of additional springs. The deformation modulus is a result of the pressuremeter testing, whereas the secant subgrade modulus is derived from laboratory testing or from material classifications. The moduli used in MFAD and LPILE (non-yielding mode) have a direct relationship to each other but represent slight differences in stress history.

The LPILE (non-yielding) model assumes that lateral loading is resisted solely by a lateral p-y relationship of each subsurface layer (modeled as a non-linear lateral spring) (Isenhower et al. 2016). The original LPILE model is based on the assumption that the pile is a long, flexible pile foundation with multiple inflexion points and a point of fixity at the base of the foundation (Figure 63A). The newest version of the software does include an option for an elastic, non-yielding pier solution which allows for the kick-out of the foundation base and a point of rotation along the shaft and for shaft bending (Figure 63B).

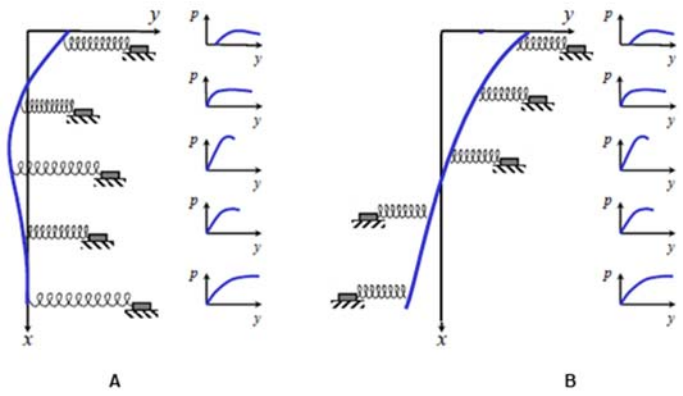

Figure 63. (A) LPILE long pier foundation; (B) LPILE elastic section (non-yielding) foundation, adapted from LPILE 2016 User's Guide

In LPILE, the reaction of the foundation is based as the secant modulus of the soil-response curve and is a function of user input k_{py} values (Figure 63A) (LPILE, 2016) (Equation 41).

$$E_s = k_{py} * x \tag{41}$$

Where E_s is the secant modulus (ksi), k_{py} is a stiffness term (ksi/ft) and x is depth (ft). However, in MFAD the stiffness of a given soil layer is a tangent modulus which is based on PMT modulus (Table 17). The MFAD model assumes that lateral loading is primarily restricted by the lateral spring, but also includes the influence of the vertical side-shear, base moment and base shear springs (Figure 64).

Table 17

Equations of stiffness for MFAD model as a function of pressuremeter modulus (E_p), depth (D) and diameter (B)

Stiffness	Description	Equation
k_h	Lateral Spring	$= \frac{E_{pmt}}{B} * 5.7 \left(\frac{D}{B}\right)^{-0.40}$
k_θ	Vertical side shear moment spring	$= E_{pmt} * B * 0.55$
k_b	Base shear spring	$= \left(\frac{E_{pmt}}{B}\right) * 2.1 * \left(\frac{D}{B}\right)^{-0.15}$
$k_{\theta b}$	Base moment spring	$= \left(E_{pmt} * B\right) * 0.24 * \left(\frac{D}{B}\right)^{0.40}$

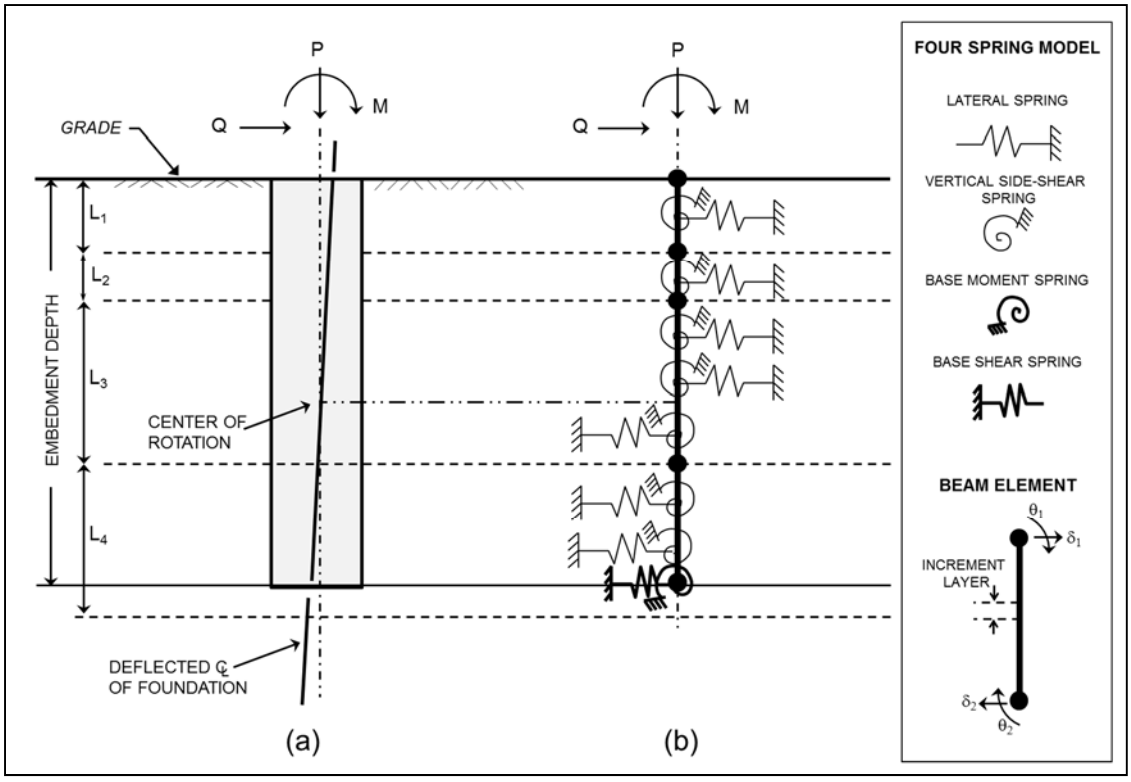

Figure 64. MFAD Model of combined lateral and side-shear springs

In MFAD, the stiffness terms (k_h,k_θ, k_b,$k_{\theta b}$) are a function of the deformation modulus (Table 17). The load-deflection curve is modeled as a piece-wise function that piecewise-linearly mimics the nonlinear stress-strain relationships of each subsurface layer (Figure 64b). The MFAD model assumes that the design capacity of the foundation as a whole is within the elastic range of motion, although the springs of a given layer may vary in behavior as shown in the piece-wise linear lateral spring model**.** MFAD results, therefore, have great non-linearity as loads are increased. The behavior of the entire foundation is verified by analysis of the foundation load-deflection plot (equivalent to a free head push over analysis), as follows:

$$p = 0.6 * p_{ult}\left(\frac{2k_h y}{P_{ult}}\right)^{0.5} \quad (42)$$

where p is the lateral pressure (ksi), p_{ult} is the ultimate lateral pressure as derived from Hansen's equation (ksi), k_h is a lateral subgrade modulus spring which is a function of PMT(ksi/in), and y is the lateral deflection (in).

MFAD assumes the pier element rotates in a rigid manner, with no flexure of the foundation. The assumption of rigid pier rotation (MFAD) versus some elastic pier bending (LPILE, non yielding mode) will result in greater top of pier movement for LPILE than for MFAD. This would be expected to result in deeper pile embedment for piers designed with the LPILE (non-yielding) model, as more rigid subgrade strata would be required to account for greater bending of the shaft than in the MFAD program. The MFAD program is the predominate commercially available program for transmission line foundation design. As such, the measurement of modulus from PMT is critical to the calculation of foundation performance and design, regardless of the model used in analysis.

COMPARISON OF RESULTS

A comparison of the foundation performance (degree of rotation) using the MFAD program was conducted for the 14 samples using the modulus from PMT test and the modulus form the S-wave velocity correlation. Each of the PMT tests was conducted at a location of a future transmission line structure, as such foundation design was performed for each site and the foundations were constructed. Results of the MFAD runs are provided in Appendix B.

Results of the comparison indicate there is minimal change in performance (R^2=0.84) (Table 18, Figure 65). At low modulus estimates the degree of rotation is overestimated when compared to the modulus from PMT measurement. At high modulus estimates the degree of rotation is underestimated when compared to the modulus from PMT measurement.

Table 18

Comparison of Foundation Performance with PMT and Estimated Modulus

PMT #	Str #	Groundline Rotation (degrees)	
		E PMT	E Est
P-123	P-123	0.20	0.20
P-140	P-140	0.12	0.16
P-202	P-202	0.11	0.14
P-25a	P-25a	0.18	0.21
P-5a	P-5a	0.51	0.43
P-62	P-62	0.25	0.24
P-73	P-73	0.26	0.24
P-88	P-88	0.17	0.24
PM 2	37	0.30	0.26
PM 3	73	0.37	0.48
PM 4	90	0.35	0.29
PM 5	89	0.28	0.23
PM 6	84	0.64	0.53

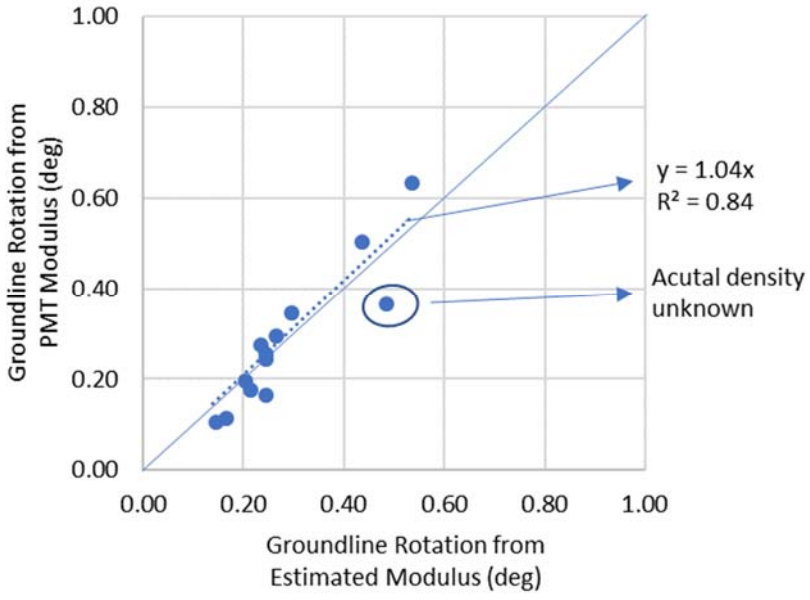

Figure 65. Correlation between foundation performance using PMT modulus and estimated modulus from S-wave velocity

Results for Structure 14 (PM-1) were not included as the foundation design was not reported in the SRP documents. The variation from the trend line for Structure 73 (PM-3) is because a good estimate of degradation factor could not be made, as the dry unit weight and water content were not provided for this sample. In this case the degradation factor was likely underestimated.

Overall, the estimated modulus does not have a significant effect on the design of the foundation when compared to direct measurement of the PMT modulus. Typical variation was less than a tenth of a degree (Table 18). The correlation did not take into account the reductions in modulus for various design conditions but relied on the parameters form the PMT testing conducted at the structure location. The typical design process includes reduction in properties for the expected nominal condition and possible reduction in properties over the life of the foundation structure. These reductions would be applied equally to either estimated modulus from S-wave velocity or from PMT testing and would further reduce the rotation of the structure.

The design of foundations from S-wave velocity correlations appears to be feasible when PMT data is not available for foundations located in the Sonoran Desert of central Arizona. Further testing to increase sample size and comparison with other geologic settings in Arizona is recommended.

CHAPTER 7

CONCLUSIONS

The goal of this study was to evaluate the relationship between small strain and intermediate strain modulus for quaternary alluvial deposits in the Sonoran desert as a means to use S-wave velocity to estimate the PMT modulus. Soils in the Sonoran Desert have unique characteristics, where there is strong cementation (Stage III to IV), with depth and the upper unconsolidated soils can have high strength from matric suction-type cementation of fine grained materials as well as at least some crystalline-type cementation. These characteristic properties of the unsaturated soils in the Sonoran desert result in particular stress-strain relationships that do not conform to standard deformation modulus correlations (e.g. EPRI 1982). Where on the one hand, the cemented soils can vary in modulus due to the type of cementation and the density of the material, from very dense rock like material with a high modulus to a very porous granular material with low modulus. On the other hand, loose granular interbedded alluvial materials can have higher deformation modulus than expected depending on the influence of matric suction.

CORRELATION VARIATION

The majority of the soils within the range of short, rigid shaft foundations (upper 30 feet) are Quaternary in age for the Sonoran Desert. Soil ageing of these sediments result in induration with depth, where cementation begins from chemical precipitation of small particles (Stage 1) and gradually transforms the entire soil mass into a solid (Stage 4). As cementation is strongly correlated to depth, a considerable amount of variation in the dataset was resolved by normalizing with depth. The soils described as "moderately to strongly cemented soils" (likely State II cementation or greater) have an average over 1280 feet per second but the PMT modulus ranges from 2.5 to 21 ksi. This wide range in moduli is likely due to other

factors that affect the soil mass. For this data sample, the correlation between intermediate and low strain modulus of cemented soils did not trend like the other soil groups. As the sample size is small for cemented soils, additional study is required to identify the effects of cementation on S-wave velocity. Degree of cementation is difficult to identify without the use of test-pits to identify geologic horizons. Additionally, measurement of PMT modulus in highly cemented soils is limited by the required pressures of the standard device. In this way, measurement of modulus of highly cemented soils requires the use of geophysical measurement.

S-wave velocity derived from ReMi survey is the inverse of the frequency, and a sinusoidal curve fitting approach is used to determine the S-wave velocity at various depths. As a result, velocity reversals at depth may be a product of the curve fitting near surface and may not reflect the velocity of the actual in situ subsurface conditions. Understanding of the geologic conditions and P-wave velocity profiles is needed for evaluation. The identification of different layers then could cause a shift in interpretation of S-wave velocity profile at depth. One option to account for this possible variation is to constrain the profile by bore log information, as was done for this correlation. Alternatively, measurement of surface moisture content could be used to constrain the S-wave profiles.

For the development of PMT correlation, the effects of seasonal changes in moisture contents were largely ignored, as the PMT and S-wave velcoity were collected in the same dry season although with several years between testing. There were no rain events within a week of either the PMT or S-wave velocity testing. Seasonal changes, however, in the upper 5 feet or less may impact the interpretation of S-wave velocity at depth (Chapter 4). Results from the flood retention structure located on the east valley of Phoenix, found that moisture changes where full inundation occurred can result in changes in both the P-wave

velocity (~200 ft/s) and S-wave velocity (~100 ft/s) within the upper 5 feet. A change of wave velocity at this scale, could account for the variation seen in unit weights and could result in the interpretation of a separate layer.

Another factor that may influence S-wave velocity and PMT correlation is the variability in sampling scales. PMT tests look at an isolated layer about two feet long, whereas S-wave and P-wave velocity measurements include the soil mass as a whole. For geophysical velocity measurements there is more detail in the upper material, due to the proximity of multiple geophones. At depth the velocity patterns are averaged out over more soil mass. This averaging is a particular function of survey line length, where with longer survey lines produce deeper profiles but the variability between thin horizons at depth is lost. This variability in scale may have resulted in some the variability seen at depth in the correlation, particularly if thin interbedded alluvial layers are present and were measured by PMT. In this case, the sites located in alluvial fans would be expected to have more interbedded layers. Based on the general geologic locations (Table 7), the sites located on young alluvial fans had a slighter greater scatter in the data (R^2=0.6723) than those located on basin fill material (R^2= 0.7412) but did not produce a significantly different trend. Likely the variation between a single point and the soil mass has a minimal effect on the resulting modulus, but additional research is needed, such as through the use of downhole geophysics techniques.

EFFECTS ON FOUNDATION DESIGN

A comparison of the foundation performance (degree of rotation) using the MFAD program was conducted for the samples using the modulus from PMT test and the estimated modulus form the S-wave velocity (Chapter 6). Each of the PMT tests was conducted at a location of a future transmission line structure, as such foundation design was performed for each site. Results of the comparison indicate

there is minimal change in predicted performance from PMT and the proposed correlation (Table 19). This variation is likely further reduced by the typical reduction factors applied during foundation design. Therefore, the design of foundations from S-wave velocity correlations is feasible when PMT data is not available for foundations located in the Sonoran Desert in central Arizona.

However, users are cautioned that the correlations developed here are for the specific use of S-wave velocity as obtained from ReMi. Also, the correlations with both S-wave and P-wave velocities require a similar geometric relationship in waves as sampled here (see description in Chapter 4). Importantly, the direct calculation of Poisson's ratio could not be evaluated with the given S-wave and P-wave velocities. As such, the simplified correlation between PMT modulus and S-wave velocity indirectly accounts for the Poisson's ratio (Equation 39). Additional research is needed to identify the range of Poisson's ratio for the Sonoran Desert samples and refine the correlation.

The user is also cautioned that the moisture conditions at the time of either geophysical survey or PMT testing may affect the estimation of modulus. The results of Chapter 4 suggest that during wet conditions, the unsaturated sandy soils in the Sonoran Desert can have a higher modulus than if they were sampled during constantly dry conditions for the upper 5-feet of the soil profile. While, clayey soils would have lower modulus when tested under wet conditions. Consideration should be taken about the testing conditions and how they compare with the desired long-term design condition for the structure. The current standard practice is to reduce the modulus for the upper 3-feet of the soil profile to account for ground disturbance over the life of a transmission line structure. In unsaturated soils in the Sonoran Desert the reduction of the upper soil profile, from already reduced properties (such as those taken during dry conditions for sandy soils) may be overly conservative.

Granted designing foundation for long term conditions where suction is required may be an unconservative assumption if saturation occurs (particularly in clayey soils).

The MFAD foundation design program requires the input of deformation modulus as obtained from PMT. The rest of the p-y curve is then determined based on an assumption of a degradation factor developed from full scale foundation tests (Figure 66b). For granular, low PI soils the MFAD based degradation factor is appropriate (approximately 30%). However, for high PI and cemented soils (likely also soils with high suction), the MFAD coefficient underestimates the stress-strain behavior (Equation 39). Existing foundation designs for these conditions using the MFAD soil mode are conservative, as they do not fully account for the higher modulus of cemented and unsaturated soils at low strains.

Furthermore, the MFAD model assumes the high strain modulus for soils to be constant over high strains (Figure 66b). This is a conservative assumption, which forces the foundation design to be within the elastic range of motion. For the soils tested in this analysis, which had appropriate PMT data, the high strain modulus continued to increase with strain rate (Figure 57). At high strains, these soils had minimum moduli at approximately 5 to 10 percent of the intermediate strain moduli. This relationship is more in line with the rock model in the MFAD program, where strength is grained even in the plastic range of motion (Figure 66a). Existing foundation designs using MFAD, then, in cemented and unsaturated soil conditions are also likely conservative as they do not account for the increasing modulus at high strains.

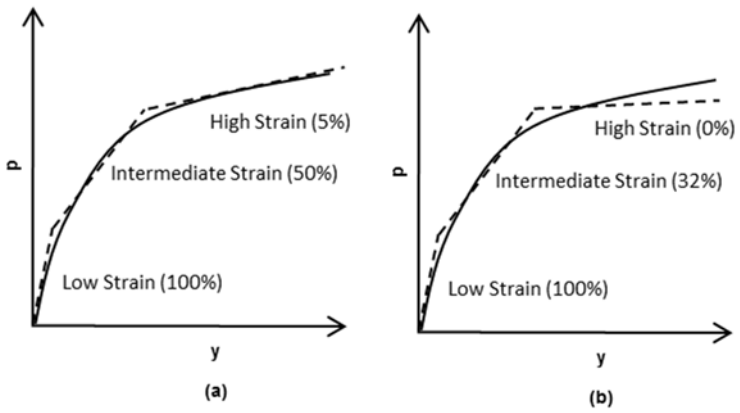

Figure 66. Comparison of MFAD rock model (a) and soil model (b), solid line is actual p-y relationship, dashed line is approximated.

Likewise, the analysis of the entire soil mass from geophysical survey may be more appropriate for estimating the behavior of the entire foundation. The results of MFAD foundation analysis include a moment-deflection curve for the entire foundation, which by definition is a Weibull curve. By knowing the capacity of the foundation and the low strain moduli the rest of the curve can be determined for the average subsurface properties, compared to fitting multiple estimates of modulus from PMT along the length of the foundation. Further research is needed to evaluate the use of low strain modulus from S-wave velocity with the results of full scale foundation testing (Ong et al. 2007).

In MFAD by using the degradation factor between low and intermediate strain modulus, foundation design could be conducted by inputting the low strain modulus from S-wave velocity measurements instead of the intermediate strain modulus form PMT. This may be appropriate for foundation designs within the working load range of design, which for transmission line structures is near the low strain portion of the load-deflection curve. For foundations within the elastic range of motion, estimates of intermediate strain moduli from low strain moduli would require detailed regional analysis, as presented here for the Sonoran Desert samples.

Conclusion

Lateral deformation modulus is a critical property used in the design of laterally loaded foundations. As transmission line structures have strict performance controls, the behavior of the foundation can have an impact on the entire system. The research presented here evaluates the relationship between low strain and high strain shear modulus for Sonoran Desert Quaternary aged soils and provides several degradation factors for unsaturated and cemented soil conditions, with the intent to allow engineers to estimate modulus from S-wave velocity measures when direct measurement by PMT is not possible. These modulus estimates can be improved with accurate measurement of density and plasticity along with S-wave and P-wave velocity.

RECOMMENDATIONS & FUTURE RESEARCH

- The correlations for geotechnical parameters from correlation of both P-wave and S-wave velocities is highly dependent on the geophysical survey setup. Use of the proposed correlations and comparison to other studies requires similar survey line set up, particularly the orientation of the applied forces to the geophone alignment. The degradation factor between low and intermediate strain modulus is based on measurement of S-wave velocity form ReMi survey. Other methods of S-wave measurement (such as MASW survey) should produce similar results but additional research is needed to evaluate the relationship.
- Field quantification of cementation is needed. Currently the classification of cementation is primarily descriptive and there is no clear standard for engineering analysis. The United States Department of Agriculture (USDA) provides guidance only on the material type of cementing agent (Schoeneberger, 2012). Classification is particularly important for identifying

the separation between cemented materials and highly compacted fine-grained materials. A simple field identification could include a measure of aggregate dispersion (ATSM D6572), field dry strength test (or rupture resistance, per Schoeneberger, 2012), and visual description to provide a full explanation of the behavior of the cemented material. Further correlation of cemented material is needed to verify the trends presented here, particularly the transition of unsaturated soils into both compacted and cemented materials.

- For unsaturated soils, seasonal changes in water content can influence both the S-wave and P-wave velocity at shallow depths, as drying and wetting events result in changes in matric suction. Engineers should be cautious of either PMT or geophysical surveys conducted in non-representative dry or moist conditions of the desired design conditions. Depending on soil type, over- or under-prediction of the deformation modulus can occur for different moisture conditions for unsaturated soils. Only two conditions of sandy soils were evaluated here, a wet condition identified by impoundment of water at the flood retention structures (in which the soils were wetted and there was an increase in matric suction) and "dry/natural" conditions identified by no impoundment and lack of rainfall at the flood retention structures (in which the soils had a decrease in matric suction) (Chapter 4). Data from additional periods of moist and dry conditions and different soils are needed. Quantification of the water content, as an indicator of soil matric suction, is also needed. A possible future research project may include a reoccurring geophysical survey at the exact same location to account for effects of matric suction on both S-wave and P-wave velocity. Such a study should include both granular non-cemented soils and soil with varying plasticity (PI).

- Downhole geophysics may provide a more direct comparison with downhole PMT testing (e.g. Hammam and Eliwa, 2012). Surface geophysical methods like the ReMi survey conducted here, result in averaging of larger soil masses with depth. The correlations presented here should be evaluated by downhole methods to evaluate the influence of thin soil horizons at depth and their influence on PMT modulus values.
- The correlation between SPT blow counts and PMT modulus is highly dependent on the coefficient of lateral earth pressure which is difficult to determine, because of the difference in loading direction and strain rates between the two tests. Correlations between SPT and PMT can be improved with measurement of water content, plasticity index, grainsize, and ratio of S-wave and P-wave velocity.
- An accurate measurement of density is needed to calculate the small strain shear modulus from S-wave velocity. If possible, direct subsurface sampling of density, water content, and grain size will improve the estimation of PMT modulus from S-wave velocity. The correlations presented here for dry density and water content are based on limited data and highly dependent on the set up of the geophysical survey. Use of the lower exclusion limit (90% confidence interval) is recommended for correlations without direct subsurface sampling.
- Geophysical survey was conducted largely in the deserts south of Phoenix, Arizona. The correlations presented here are likely applicable to other unsaturated conditions in Quaternary aged alluvial deposits throughout the Sonoran Desert. However, additional research is needed to evaluate these correlations in other unsaturated geologic settings.
- The performance of laterally loaded short rigid shaft foundations, such as transmission line structures, is highly dependent on the PMT modulus. Other

models of foundation rotation under lateral load could be developed to use S-wave and P-wave velocity measures directly.

- The MFAD method of classification of subgrade as either soil or rock does was not calibrated for unsaturated soils or cemented soils. Refinement of the MFAD p-y curves is needed to account for these particular soil conditions. In lieu of model refinement, the MFAD rock model can be used to more appropriately reflect unsaturated soil with plasticity index over 10% and moderate to highly cemented soils, as identified here for the Sonoran Desert samples.

REFERENCES

AGRA (1999). Pressuremeter Testing Supplemental Geotechnical Investigation RS18 Transmission System Gileter & Mesa, Arizona. Job No. 9-117-001114.

Amec (2015A). Preliminary Geotechnical Investigation Report Powerline Channel Powerline, Vineyard Road and Rittenhouse Flood Retarding Structures. Project No. 17-2014-4062

Amec (2015B). Seismic Refraction and ReMi Evaluation Vineyard Road Flood Retarding Structure Auxiliary Spillways Powerline, Vineyard Road and Rittenhouse Flood Retarding Structure. Project No. 17-2014-4062

Anderson, J. B., Townsend, F. C., and Grajales, B. (2003). Case history evaluation of laterally loaded piles. Journal of Geotechnical and Geoenvironmental Engineering, *129*(3), 187-196.

Ashour, M., and Norris, G. (2000). Modeling lateral soil-pile response based on soil-pile interaction. Journal of Geotechnical and Geoenvironmental Engineering, *126*(5), 420-428.

ASTM D4719-07 (2016), Standard Test Methods for Prebored Pressuremeter Testing in Soils, ASTM International, West Conshohocken, PA.

ASTM D5777-00 (2011), Standard Guide for Using the Seismic Refraction Method for Subsurface Investigation, ASTM International, West Conshohocken, PA.

ASTM D6572-13e2 (2013), Standard Test Methods for Determining Dispersive Characteristics of Clayey Soils by the Crumb Test, ASTM International, West Conshohocken, PA.

Bellana, N. (2009). Shear Wave Velocity as Function of SPT Penetration Resistance and Vertical Effective Stress at California Bridge Sites. M.S. Thesis, University of California, Los Angeles

Biarez J., Gambin M., Gomes-Correia A., Flavigny E., Branque D. (1998) Using pressuremeter to obtain parameters to elastic-plastic models for sands. In Roberton & Mayne (Ed.), *Geotechnical Site Characterization*, Balkerna, Rotterdam.

Bonnet, G., and Meyer, M. (1988). Seismic refraction tests above water table. Journal of Geotechnical Engineering, *114*(10), 1183-1189.

Bowland, A. G., Cass, P. G., & DiGioia Jr, A. M. (2015). Recommendations for Steel Pole and Drilled Shaft Deflection Criteria Based on a Parametric Study of a

138kV Double Circuit Transmission Line. In *Electrical Transmission and Substation Structures*, 127-142.

Briaud, J. L., Pacal, A. J., and Shively, A. W. (1984). Power Line Foundation Design Using the Pressuremeter, *International Conference on Case Histories in Geotechnical Engineering*, *40*.

Briaud, J.L. (1992). *The Pressuremeter*. Rotterdam, Netherlands: A.A. Balkema.

Briaud, J.L. (2001). Introduction to soil Moduli. Geotechnical News, June, BiTech Publishers Ltd, Richmond, B.C. Canada.

Briaud, J.L., Smith, T. D., & Meyer, B. J. (1982). Design of Laterally Loaded Piles using the Pressuremeter Test Result. Paper presented at the Symposium on the Pressuremeter and Its Marine Applications, Paris, France.

Briaud, J.L. (1984). Coefficient of Variation of In Situ Tests in Sand. Paper presented at the Probabilistic Characterization of Soil Properties: Bridge Between Theory and Practice.

Briaud, J. L. (2013). Ménard Lecture: The pressuremeter Test: Expanding its use. In *Proceedings of the 18th International Conference on Soil Mechanics and Geotechnical Engineering, Paris, France* (pp. 107-126).Broms, B. B. (1964). Lateral resistance of piles in cohesionless soils. *J. Soil Mech. and Found. Div.*, *90*(3), 123–158.

Brutsaert, W., and Luthin, J. N. (1964). The velocity of sound in soils near the surface as a function of the moisture content. *Journal of Geophysical Research*, *69*(4), 643-652.

Budhu, M., and Davies, T. G. (1987). Nonlinear analysis of laterally loaded piles in cohesionless soils. *Canadian Geotechnical Journal*, *24*(2), 289-296.

Callanan, J. F., and Kulhawy, F. H. (1985). Evaluation of procedures for predicting foundation uplift movements. Report No. EPRI-EL-4107. Cornell Univ., Ithaca, NY

CEATI. (2017). Guide for transmission line foundation with least impact to environment. Transmission Overhead Line Design & Extreme Event Mitigation (TODEM) Interest Group. CEATI Report No. T153700-33107

D' Appolonia, D. J., D' Appolonia, E., and Brisette, R.F. (1970). Discussion of "Settlement of Spread Footings in Sands", *J. Soil Mechanics and Foundation Engineering Division*, ASCE, *96*(SM2), 754-761.

Dahl, K. R. (2011). Evaluation of seismic behavior of intermediate and fine-grained soils (3499425). Available from ProQuest Dissertations & Theses Global.

Davisson, M.T., and Prakash, S. (1963). A Review of Soil-Pole Behavior. *Stresses in Soils in Layered Systems*, HRR 39, 25-48.

DiGioia Gray (2013). Foundation Investigation and Design Report: Palo Verde to Delaney 500kV Transmission Line. DiGioia Gray and Associates Report Number 2013-924.

DiGioia Gray (2015). Foundation Design Report: Mazatzal 345kV Substation Intertie Lattice Tower Foundation Design. DiGioia Gray and Associates. Report Number 2015-926. Dated 12/17/2015.

Dikmen, Ü. (2009). Statistical correlations of shear wave velocity and penetration resistance for soils. Journal of Geophysics and Engineering, *6*(1), 61.

DiMaggio, J. (2010). Partial Implementation of LRFD for Geotechnical Engineering Features: subsurface explorations and soil and rock testing. Presentation presented April 15, 2010.

Duncan, J. M., and Chang, C. Y. (1970). Nonlinear analysis of stress and strain in soils. *Journal of Soil Mechanics & Foundations Div*.

Duncan, J.M. and Bursey, A. (2013). Soil modulus correlations. In *Foundation Engineering in the Face of Uncertainty: Honoring Fred H. Kulhawy*, 321-336.

Durkee, D., Rucker, M., Smith, D., & Ackerman, A. (2006). Role of Practical Geophysics in In-Situ Characterization for Underground Construction in Phoenix, Arizona. Geotechnical Special Publication, *147*(1), 577.

EPRI (1982a). EL-2197: Laterally Loaded Drilled Pier Research, Volume 1: Design Methodology, Project 1280-1, Final Report. *Electric Power Research Institute*, Palo Alto, CA.

EPRI (1982b). EL-2197: Laterally Loaded Drilled Pier Research, Volume 2: Research Documentation, Electric Power Research Institute, Palo Alto, CA, Project 1280-1, Final Report, *Electric Power Research Institute*, Palo Alto, CA.

EPRI (1990). EL-6800: Manual on Estimating Soil Properties for Foundation Design. *Electric Power Research Institute*, Palo Alto, CA.

EPRI (2012). TR-1024138. Transmission Structure Foundation Design Guide. *Electric Power Research Institute*, Palo Alto, CA.

Fawaz, A., Hagechedhade, F., and Farah, E. (2014). A study of pressuremeter modulus and its comparison to the elastic modulus of soil. *Study of Civil Engineering and Architecture*, *3*, 7-15.

Fredlund, D.G. (2006. Unsaturated Soil Mechanics in Engineering Practice. *Journal of Geotechnical and Geoenvironmental Engineering*, *132*(3), 286–321.

Flood Control District of Maricopa County (FCDMA) (2018a). Vineyard Road FRS- ID #6688. Last accessed on 6/15/2018. http://alert.fcd.maricopa.gov/alert/Flow/6688.htm

Flood Control District of Maricopa County (FCDMA) (2018b). Powerline FRS- ID #6683. Last accessed on 6/15/2018. http://alert.fcd.maricopa.gov/alert/Flow/6683.htm

Flood Control District of Maricopa County (FCDMA) (2018c). Rittenhouse FRS- ID #6683. Last accessed on 6/15/2018. http://alert.fcd.maricopa.gov/alert/Flow/6703.htm

GAI (1994). Pressuremeter Tests: Santan-Kempton 230 kV/69 kV T/L. Project No. 93-152-10.

Gambin, M. P., and J. Rousseau. (1988). The Menard Pressuremeter: Interpretation and Application of Pressuremeter Test Results to Foundation Design. *ISSMFE Technical Committee on Pressuremeter and Dilatometer Testing*, General Memorandum, Sols Soils, *26*, 50.

Geological Consultants (2006) "Geologic Investigation and Reconnaissance Survey, Proposed 500kV Transmission Line, Pinal West to Dinosaur, Maricopa and Pinal Counties, Arizona," GCI Project No. 2006-2101, December 21.

George, K. P. (2004). Prediction of resilient modulus from soil index properties.

Goh, K. H., K. Jeyatharan, and D. Wen. (2012). Understanding the Stiffness of Soils in Singapore from Pressuremeter Testing. *Geotechnical Engineering Journal of the SEAGS & AGSSEA*, *43*(4), 21–29.

Gomes, C.A., Antão, A., and Gambin, M. (2004). Using non-linear constitutive law to compare Menard PMT and PLT E-moduli. In Proceedings of the 2nd international conference on site characterization, Porto, Portugal, 927-933.

Grelle, G., and Guadagno, F. M. (2009). Seismic refraction methodology for groundwater level determination: "Water seismic index". *Journal of Applied Geophysics*, *68*(3), 301-320.

Grigsby, L. L., 2012. The electric power engineering handbook (3 ed.): CRC Press.

Hammam, A. H., and Eliwa, M. (2013). Comparison between results of dynamic & static moduli of soil determined by different methods. Housing and Building National Research Center, *9*, 144-149.

Hansen, W. D. (1961). The ultimate resistance of rigid piles against transversal forces. Bull., No. 12, Danish Geotechnical Institute, *Geoteknisk Institut, Copenhagen*, Denmark.

Hardin, B. O. (1978) "The nature of stress-strain behavior for soils." Proc., Geotechnical Division Special Conf. on Earthquake Engineering and Soil Dynamics, ASCE, Pasdena, Calif., 1, 3–39.

Heitor, A., Indraratna, B., and Rujikiatkamjorn, C. (2013). Laboratory study of small-strain behavior of a compacted silty sand. *Canadian Geotechnical Journal*, 50(2), 179-188.

Huckleberry, G. (1994) Surficial geology of the Apache Junction area, Northern Pinal and Eastern Maricopa Counties, Arizona. Arizona Geological Survey. Open-File Report 94-10

Hunt, R. E. (1984). Geotechnical Engineering Investigation Manual. New York: McGraw-Hill Book Company.

Hussien, M.N. and Karray, M. (2016). Shear wave velocity as a geotechnical parameter: an overview. *Canadian Geotechnical Journal.* 53, 252-272.

IEEE (2001). IEEE guide for transmission structure foundation design and testing. IEEE Std 691-2001, Piscataway, NJ.

Isik, N. S., Doyuran, V., & Ulusay, R. (2008). Assessment of deformation modulus of weak rock masses from pressuremeter tests and seismic surveys. *Bulletin of Engineering Geology and the Environment*, 67(3), 293-304.

Isenhower, W.M., Wang, S-T., Gonzalo Vasquez, L., (2016). Technical Manual for LPile 2016. Ensoft, Inc.

Jardine, R. J., Symes, M. J., & Burland, J. B. (1984). The measurement of soil stiffness in the triaxial apparatus. *Géotechnique*, *34*(3), 323-340.

Karray, M., and Lefebvre, G. (2008). Significance and evaluation of Poisson's ratio in Rayleigh wave testing. Canadian Geotechnical Journal, 45(5), 624-635.

Karray, M., Hussien, M. N., Chekired, M., & Ethier, Y. (2016). Small strain stiffness and stiffness degradation curve of sensitive Champlain clay. In *69th Canadian Geotechnical International Conference, Vancouver, Canada*. Kalaga, S. and Yenumula, P. (2017) *Design of Electrical Transmission Lines: Structures and Foundations*, *1*, CRC Press.

Kandaris, P. (1994). Pressuremeter Testing for Electric Power Transmission Line Structure Foundations in Desert Southwest Soils. *ASCE: Unsaturated Soils*.

Kandaris, P. M., DiGioia, Jr, A. M., & Heim, Z. J. (2012). Evaluation of Performance Criteria for Short Laterally Loaded Drilled Shafts. In *GeoCongress 2012: State of the Art and Practice in Geotechnical Engineering*, 165-174.

Kandaris, P.M., Davidow, S., and Evans, A. (2017). Framework for risk-based electric system deep foundation design. *Deep Foundation Institute 42nd Conference*. New Orleans, October 24, 2017.

Kandaris, P.M., Gadok, J.S., Russo, N.T. (2017). Probabilistic subsurface characterization for transmission line foundation design. *Deep Foundation Institute 42nd Conference*. New Orleans, October 24, 2017.

Kulhawy, F.H., Duncan, J.M. and Seed, H.B., (1969) Finite Element Analyses of StReeses and Movements in Embankments During Construction., *U.S. Army Waterways Experiment Station.* Contract Report 569-8, Vicksburg, Mississippi.

Kulhawy, F. H., & Mayne, P. W. (1990). Manual on estimating soil properties for foundation design (No. EPRI-EL-6800). *Electric Power Research Inst.,* Palo Alto, CA (USA); Cornell Univ., Ithaca, NY (USA). Geotechnical Engineering Group.

Kulhawy, F. H., and Phoon, K. K. (2002). Observations on geotechnical reliability-based design development in North America. *Foundation Design Codes and Soil Investigation in View of International Harmonization and Performance Based Design*, Proceedings of IWS Kamakura, 31-48.

Louie, J. N. (2001). Faster, Better: Shear-Wave Velocity to 100 Meters Depth From Refraction Microtremor Arrays. *Bulletin of the Seismological Society of America*, *91*(2), 347-364.

Massarasch, K.R. (2014) Deformation properties of fine-grained soils from seismic tests. *Keynote lecture, International Conference on Site Characterization, ISC'2*, 19-22 Spt. 2004. Porto Rico.

Matlock, H., and Reese, L.C. (1960). Generalized Solutions for Laterally Loaded Piles. Journal Soil Mechanics and Foundation Engineering, ASCE, *86*(SM5), 63-91.

Mayne, P. W., and Brown, D. A. (2003). Site characterization of Piedmont residuum of North America. *Characterization and engineering properties of natural soils*, *2*, 1323-1339.

Menard, L. (1975). The Menard Pressuremeter: Interpretation and Application of Pressuremeter Test Results to Foundation Design, General Memorandum, Sols-Soils, No. 26.

Miller, G. A., and Muraleetharan, K. K. (2000). Interpretation of pressuremeter tests in unsaturated soil. In *Advances in Unsaturated Geotechnics*, 40-53.

Montoya, B. M., & DeJong, J. T. (2015). Stress-strain behavior of sands cemented by microbially induced calcite precipitation. *Journal of Geotechnical and Geoenvironmental Engineering*, 141(6), 04015019.

Oh, W. T., and Vanapalli, S. K. (2014). Semi-empirical model for estimating the small-strain shear modulus of unsaturated non-plastic sandy soils. Geotechnical and Geological Engineering, 32(2), 259-271.

Ohya, S., Imai, T., and Matsubara, M. (1982). Relationships Between N Value by SPT and LLT Pressuremeter Results. *Proceedings, 2nd European Symposium on Penetration Testing*, Amsterdam, *1*, 125-130.

Ong, C. K., Chen, S. E., Galloway, C., Munden, C., and Mize, D. (2007). Innovative Application of Geophysical Techniques for Design of Direct-Embedded Pole Structures. In Electrical Transmission Line and Substation Structures: Structural Reliability in a Changing World (pp. 207-214).

Parker, F., Jr., and Reese, L. C. (1970) Experimental and Analytical Studies of Behavior of Single Piles in Sand Under Lateral and Axial Loading, Research Report 117-2, Center for Highway Research, The University of Texas at Austin, TX.

Pereira, J-M., Dubujet, P., Wong, H. (2003) Numerical modeling of unsaturated soils in pressuremeter test. *16th ASCE Engineering Mechanics Conference*. July 16-18, 2003, University of Washington, Seattle.

Poulos, H.G., and Davis, E.H. (1974). *Elastic Solutions for Soil and Rock Mechanics*, John Wiley and Sons, New York.

Prasad, Y.V.S.N and Chari, A.H. (1999). Lateral capacity of model rigid piles in cohesionless soil. Soils and foundations. Jap*anese Geotechnical Society*, *39*(2), 21-29, April 1999.

Reese, L. C., and O'Neill, M. W. (1999). Drilled shafts: Construction, procedures and design methods. Publication FHWA-IF-99-025, *Federal Highway Administration*, Washington, DC.

Reese, L.C., and Matlock, H. (1956). Nondimensional Solutions for Laterally Loaded Piles with Soil Modulus Assumed Proportional to Depth. *Proc, 8th Texas Conf. Soil Mechanics and Foundation Engineering*, ASCE, SP 29.

Richart, F. E., Hall, J. R. J., & Woods, R. D. (1970). *Vibration of Soils and Foundations*. Englewood Cliffs, New Jersey: Prentice Hall.

Robbins, D. (2013) Initial elastic modulus degradation using pressuremeter and standard penetration test results at two sites. UNLV Dissertation paper 1878.

Robertson, P., and Ferreira, R. (1993). Seismic and pressuremeter testing to determine soil modulus. Paper presented at the Predictive Soils Mechanics. *Proceedings of the Worth Memorial Symposium*, 27-29 JULY 1992, St. Catherine's College, Oxford.

Rojas-Gonzalez, L.F., DiGioia, A.M., Kandaris, P.M., and Kondziolka, R.E. (1992) Rock socketed drilled shaft and directly embedded pole tests. *IEEE Transaction on Power Delivery*, *7*(2), April, 1992.

Rucker, M. L. (1998). Seismic Velocity in cohesionless granular material deposits. In R. Mayne (Ed.), *Geotechnical Site Characterization*.

Rucker, M. L. (2003). Applying the refraction microtremor (ReMi) shear wave technique to geotechnical engineering. Paper presented at the *Third International Conference on the Application of Geophysical Methodologies to Transportation Facilities and Infrastructure*, Orlando, Florida.

Rucker, M. L. (2008). Estimating In-Situ Geo-Material Mass Density, Modulus and Minimum Uniaxial Compressive Strength from Field Seismic Velocity Measurements. Amec Foster Wheeler.

Rucker, M. L. (2000) Percolation Theory Approach to Quantify Geo-Material Density-Modulus Relationships. Paper presented at the 9th *ASCE Specialty Conference on Probabilistic Mechanics and Structural Reliability*.

Rucker, M. L., and Fergason, K. C. (2006). Characterizing unsaturated cemented soil profiles for strength, excavatability and erodibility using surface seismic methods. *4th International Conference on Unsaturated Soils*, Carefree, AZ, April 2-6, 2006.

Rucker, M. L., and Frechette, D. (2015). Preliminary Geotechnical Investigation Report: Powerline Channel, Powerline, Vineyard Road and Rittenhouse Flood Retarding Structures. Retrieved from Phoenix, AZ:

Rucker, M. L., and Frechette, D. (2015). Seismic Data Report: Powerline, Vineyard Road and Rittenhouse Flood Retarding Structures. Retrieved from

Rucker, M. L., and Frechette, D. N. (2015). Seismic Refraction and ReMi Evaluation: Vineyard Road Flood Retarding Structure Auxiliary Spillways Powerline, Vineyard Road and Rittenhouse Flood Retarding Structure. Retrieved from Phoenix, AZ.

Sabatini, P.J. Bachus, R.C, Mayme, P.W., Schneider, J.A., and Zettler, T.E. (2002) Geotechnical engineering circular No.5: Evaluation of Soil and Rock Properties. US Department of Transportation. FHWA-IF-02-034

Sawangsuriya, A., Edil, T. B., & Bosscher, P. J. (2008). Modulus− suction− moisture relationship for compacted soils. *Canadian Geotechnical Journal*, *45*(7), 973-983.

Salt River Project (SRP) (1984). Mead-Phoenix 500kV DC Project: Transmission Line and Coverter Stations. Project No. 84-217. Report No. MP-533.

SRP (1996a). Schrader 230kV Electric System Optimization of Transmission Line Foundations Geotechnical Study-Final Report. File No. NM-587, Report No. CE-382.

SRP (1996b). Schrader Transmission Project 230kV Transmission Lines and Substation Geotechnical Investigation. File No. NM-587/553. Report No. CE-367.

SRP (2000). Geotechnical Investigation: RS18 500/230/69kV Transmission System. Santan Receiving Station to Browning Substation. File No. NG-125. Report No. CE-405.

SRP (2006). Geotechnical Investigation Report: Browning-Dinosaur 230/500kV T/L, Browning-Silverking 500kV T/L. File No. NG-623. Report No. CE-492

SRP (2010). Browning-Dinosaur-Abel 500/230kV Transmission Line, Pinal Central-Abel 500/230kV Transmission Line: Final Geotechnical Investigation Report. Report No. CE-558, File No. NG-629 and NG-630.

SRP (2011). SRP Duke 500/230kV Substation: Geotechnical Engineering Report-Final. File No. AV-05040, Report No. CE-584.

SRP (2012a). Duke to Pinal Central 500kV Transmission Line: Final Geotechnical Investigation Report. Report No. CE-593, File No. AV-5051, 5056.

SRP (2012b). Pinal West to Duke 500kV Transmission Line – Final Report: Geotechnical Investigation Report. Report No. CE-592, File No. AV-5031.

Schmerttmann, J.H. (1970). Static Cone to Compute Static Settlement Over Sand. *Journal of Soil Mechanics and Foundation Engineering*. ASCE, *96*(SM3), 1011-1043.

Schoeneberger, P. J. (2012). Field book for describing and sampling soils. Government Printing Office.

Shirato, Masshiro; Nakatani, Schoichi; Matui, Jenji; Nakaura, Takashi. (2009) Geotechnical criterion for serviceability limit state of horizontally-loaded deep foundations. Conference Paper. https://www.pwri.go.jp/eng/activity/pdf/reports/shirato.0610.23.pdf

Seed, H.B., Wong, R.T., Idriss, I.M., and Tokimatsu, K., (1984) *Moduli and Damping Factors for Dynamic Analyses of Cohesionless Soils*. College of Engineering, University of California, Berkeley, EER C 84/14, September 1984.

Thornburgh, H. R. (1930). Wave-front diagrams in seismic interpretation. *American Association of Petroleum Geologists*, *14*(2), 185-200.

Turesson, A. (2007). A comparison of methods for the analysis of compressional, shear, and surface wave seismic data, and determination of the shear modulus. *Journal of Applied geophysics*, *61*(2), 83-91.

Uhlemann, S., Hagedorn, S., Dashwood, B., Maurer, H., Gunn, D., Dijkstra, T., and Chambers, J. (2016). Landslide characterization using P-and S-wave seismic refraction tomography—The importance of elastic moduli. *Journal of Applied Geophysics*, 134, 64-76.

Vallabhan, C. V. G., and Alikhanlou, F. (1982). Short rigid piers in clays. *Journal of Geotechnical Engineering*, *108*(10), 1255–1272

van Paassen, L. A., Ghose, R., van der Linden, T. J., van der Star, W. R., & van Loosdrecht, M. C. (2010). Quantifying biomediated ground improvement by ureolysis: large-scale biogrout experiment. *Journal of Geotechnical and Geoenvironmental Engineering*, 136(12), 1721-1728.

Vucetic, M., and Dobry, R. (1991). Effect of soil plasticity on cyclic response. *Journal of Geotechnical* Engineering, *117*(1), 89-107.

Wair, B.R, DeJong, J.T., Shantz, T. (2012). Guidelines for Estimation of Shear Wave Velocity Profiles. PEER Report 2012/08. Pacific Earthquake Engineering Research Center, Headquarters at the University of California.

Whalley, W. R. et al (2012). The velocity of shear waves in unsaturated soil. *Soil and Tillage research*, Elsevier, *125*, 30 - 27.

APPENDIX A

DATABASE OF SUBSURFACE PROPERTIES

Appendix A Table 1 Summary of geophysical velocity data

Project	Name	Depth (ft)	Geophysical Survey Line	Vp (ft/s)	Vs (ft/s)
Duke Substation (SRP CE-584)	PM-3(5A)	4.5	18	1150	640
Duke Substation (SRP CE-584)	PM-3(5A)	9.5	18	1200	640
Duke Substation (SRP CE-584)	PM-3(5A)	14.5	18	1200	640
Duke Substation (SRP CE-584)	PM-3(5A)	19.5	18	1600	880
DUE-PCL (SRP CE-593)	PM-6(P123)	6.5	15	1600	800
DUE-PCL (SRP CE-593)	PM-6(P123)	9.5	15	2100	1000
DUE-PCL (SRP CE-593)	PM-6(P123)	14.5	15	#N/A	1700
DUE-PCL (SRP CE-593)	PM-6(P123)	19.5	15	#N/A	1700
DUE-PCL (SRP CE-593)	PM-6(P123)	24.5	15	#N/A	520
DUE-PCL (SRP CE-593)	PM-7(P140)	5.5	14	1400	1120
DUE-PCL (SRP CE-593)	PM-7(P140)	8.5	14	3500	1600
DUE-PCL (SRP CE-593)	PM-7(P140)	15.5	14	#N/A	610
DUE-PCL (SRP CE-593)	PM-7(P140)	19.5	14	#N/A	610
DUE-PCL (SRP CE-593)	PM-7(P140)	24.0	14	#N/A	610
DUE-PCL (SRP CE-593)	PM-8(P202)	4.5	13	1300	730
DUE-PCL (SRP CE-593)	PM-8(P202)	9.5	13	1400	730
DUE-PCL (SRP CE-593)	PM-8(P202)	19.5	13	#N/A	1700
DUE-PCL (SRP CE-593)	PM-4(P25A)	4.5	19	1800	910
DUE-PCL (SRP CE-593)	PM-4(P25A)	9.5	19	1800	910
DUE-PCL (SRP CE-593)	PM-4(P25A)	14.5	19	2250	1200
DUE-PCL (SRP CE-593)	PM-4(P25A)	19.5	19	#N/A	1800
DUE-PCL (SRP CE-593)	PM-4(P25A)	24.5	19	4200	730
DUE-PCL (SRP CE-593)	PM-5(P73)	9.5	20	2400	1100
DUE-PCL (SRP CE-593)	PM-5(P73)	14.5	20	2800	1100
PW-DUE (SRP CE-592)	PM-1(P62)	4.5	16	1500	770
PW-DUE (SRP CE-592)	PM-1(P62)	9.5	16	1500	620
PW-DUE (SRP CE-592)	PM-1(P62)	14.5	16	1967	1000
PW-DUE (SRP CE-592)	PM-1(P62)	19.5	16	#N/A	800
PW-DUE (SRP CE-592)	PM-1(P62)	24.5	16	#N/A	800
PW-DUE (SRP CE-592)	PM-2(P88)	4.5	17	1325	650
PW-DUE (SRP CE-592)	PM-2(P88)	9.5	17	1325	550
PW-DUE (SRP CE-592)	PM-2(P88)	14.5	17	1500	880
PW-DUE (SRP CE-592)	PM-2(P88)	19.5	17	1500	880
BRN-DINO-ABEL (SRP CE-558)	PM-1 (BDA8)	3.0	12	1900	950
BRN-DINO-ABEL (SRP CE-558)	PM-1 (BDA8)	6.5	12	1900	950
BRN-DINO-ABEL (SRP CE-558)	PM-1 (BDA8)	12.5	12	3200	1400
BRN-DINO-ABEL (SRP CE-558)	PM-1 (BDA8)	18.5	12	#N/A	1400
BRN-DINO-ABEL (SRP CE-558)	PM-2 (PCA1)	3.0	11	1450	660
BRN-DINO-ABEL (SRP CE-558)	PM-2 (PCA1)	8.0	11	2267	1100
BRN-DINO-ABEL (SRP CE-558)	PM-2 (PCA1)	13.0	11	#N/A	600
BRN-DINO-ABEL (SRP CE-558)	PM-2 (PCA1)	17.0	11	#N/A	1400
BRN-DINO-ABEL (SRP CE-558)	PM-3 (PCA-4)	3.0	10	1143	580
BRN-DINO-ABEL (SRP CE-558)	PM-3 (PCA-4)	7.0	10	1650	840
BRN-DINO-ABEL (SRP CE-558)	PM-3 (PCA-4)	13.0	10	2000	1000
BRN-DINO-ABEL (SRP CE-558)	PM-3 (PCA-4)	17.0	10	#N/A	1200
BRN-DINO-ABEL (SRP CE-558)	PM-4 (PCA7)	7.0	9	1450	560
BRN-DINO-ABEL (SRP CE-558)	PM-4 (PCA7)	13.0	9	2100	1000
BRN-DINO-ABEL (SRP CE-558)	PM-4 (PCA7)	17.0	9	#N/A	1300
BRN-DINO-ABEL (SRP CE-558)	PM-5 (PCA9)	3.0	7	1150	600
BRN-DINO-ABEL (SRP CE-558)	PM-5 (PCA9)	7.0	7	2450	955
BRN-DINO-ABEL (SRP CE-558)	PM-6 (PCA8)	3.0	8	938	510
BRN-DINO-ABEL (SRP CE-558)	PM-6 (PCA8)	5.0	8	1167	630

Appendix A Table 2 Summary of PMT data

Project	Name	Depth	PMT Date	PMT Company	E_{PMT} (ksi)	2(1+v)	G_{PMT} (ksi)
Duke Substation (SRP CE-584)	PM-3(5A)	4.5	4/19/2011	AMEC 17-2011-4017	2.6	2.66	1.0
Duke Substation (SRP CE-584)	PM-3(5A)	9.5	4/19/2011		1.3	2.66	0.5
Duke Substation (SRP CE-584)	PM-3(5A)	14.5	4/19/2011		2.8	2.66	1.1
Duke Substation (SRP CE-584)	PM-3(5A)	19.5	4/19/2011		2.7	2.66	1.0
DUE-PCL (SRP CE-593)	PM-6(P123)	6.5	4/22/2011		8.2	2.66	3.1
DUE-PCL (SRP CE-593)	PM-6(P123)	9.5	4/22/2011		12.5	2.66	4.7
DUE-PCL (SRP CE-593)	PM-6(P123)	14.5	4/22/2011		7.6	2.66	2.9
DUE-PCL (SRP CE-593)	PM-6(P123)	19.5	4/22/2011		4.3	2.66	1.6
DUE-PCL (SRP CE-593)	PM-6(P123)	24.5	4/22/2011		3.1	2.66	1.2
DUE-PCL (SRP CE-593)	PM-7(P140)	5.5	4/25/2011		12.5	2.66	4.7
DUE-PCL (SRP CE-593)	PM-7(P140)	8.5	4/25/2011		10.9	2.66	4.1
DUE-PCL (SRP CE-593)	PM-7(P140)	15.5	4/25/2011		8.8	2.66	3.3
DUE-PCL (SRP CE-593)	PM-7(P140)	19.5	4/25/2011		5.7	2.66	2.1
DUE-PCL (SRP CE-593)	PM-7(P140)	24.0	4/25/2011		6.0	2.66	2.3
DUE-PCL (SRP CE-593)	PM-8(P202)	4.5	4/25/2011		5.3	2.66	2.0
DUE-PCL (SRP CE-593)	PM-8(P202)	9.5	4/25/2011		9.0	2.66	3.4
DUE-PCL (SRP CE-593)	PM-8(P202)	19.5	4/25/2011		20.9	2.66	7.9
DUE-PCL (SRP CE-593)	PM-4(P25A)	4.5	4/20/2011		6.5	2.66	2.4
DUE-PCL (SRP CE-593)	PM-4(P25A)	9.5	4/20/2011		8.8	2.66	3.3
DUE-PCL (SRP CE-593)	PM-4(P25A)	14.5	4/20/2011		7.1	2.66	2.7
DUE-PCL (SRP CE-593)	PM-4(P25A)	19.5	4/20/2011		9.1	2.66	3.4
DUE-PCL (SRP CE-593)	PM-4(P25A)	24.5	4/20/2011		8.2	2.66	3.1
DUE-PCL (SRP CE-593)	PM-5(P73)	9.5	4/22/2011		6.0	2.66	2.3
DUE-PCL (SRP CE-593)	PM-5(P73)	14.5	4/22/2011		8.9	2.66	3.3
PW-DUE (SRP CE-592)	PM-1(P62)	4.5	4/19/2011		2.1	2.66	0.8
PW-DUE (SRP CE-592)	PM-1(P62)	9.5	4/19/2011		1.5	2.66	0.6
PW-DUE (SRP CE-592)	PM-1(P62)	14.5	4/19/2011		4.2	2.66	1.6
PW-DUE (SRP CE-592)	PM-1(P62)	19.5	4/19/2011		6.2	2.66	2.3
PW-DUE (SRP CE-592)	PM-1(P62)	24.5	4/19/2011		4.6	2.66	1.7
PW-DUE (SRP CE-592)	PM-2(P88)	4.5	4/20/2011		5.2	2.66	2.0
PW-DUE (SRP CE-592)	PM-2(P88)	9.5	4/20/2011		3.6	2.66	1.4
PW-DUE (SRP CE-592)	PM-2(P88)	14.5	4/20/2011		7.5	2.66	2.8
PW-DUE (SRP CE-592)	PM-2(P88)	19.5	4/20/2011		3.0	2.66	1.1
BRN-DINO-ABEL (SRP CE-558)	PM-1	3.0	5/28/2009	AMEC 09-117-01022	4.8	2.66	1.8
BRN-DINO-ABEL (SRP CE-558)	PM-1	6.5	5/28/2009		0.5	2.66	0.2
BRN-DINO-ABEL (SRP CE-558)	PM-1	12.5	5/28/2009		2.1	2.66	0.8
BRN-DINO-ABEL (SRP CE-558)	PM-1	18.5	5/28/2009		10.5	2.66	3.9
BRN-DINO-ABEL (SRP CE-558)	PM-2	3.0	5/27/2009		1.1	2.66	0.4
BRN-DINO-ABEL (SRP CE-558)	PM-2	8.0	5/27/2009		3.1	2.66	1.2
BRN-DINO-ABEL (SRP CE-558)	PM-2	13.0	5/27/2009		4.3	2.66	1.6
BRN-DINO-ABEL (SRP CE-558)	PM-2	17.0	5/27/2009		2.5	2.66	0.9
BRN-DINO-ABEL (SRP CE-558)	PM-3	3.0	5/27/2009		4.7	2.66	1.8
BRN-DINO-ABEL (SRP CE-558)	PM-3	7.0	5/27/2009		1.6	2.66	0.6
BRN-DINO-ABEL (SRP CE-558)	PM-3	13.0	5/27/2009		3.3	2.66	1.2
BRN-DINO-ABEL (SRP CE-558)	PM-3	17.0	5/27/2009		6.6	2.66	2.5
BRN-DINO-ABEL (SRP CE-558)	PM-4	7.0	5/28/2009		4.0	2.66	1.5
BRN-DINO-ABEL (SRP CE-558)	PM-4	13.0	5/28/2009		3.7	2.66	1.4
BRN-DINO-ABEL (SRP CE-558)	PM-4	17.0	5/28/2009		3.1	2.66	1.2
BRN-DINO-ABEL (SRP CE-558)	PM-5	3.0	5/14/2009		2.6	2.66	1.0
BRN-DINO-ABEL (SRP CE-558)	PM-5	7.0	5/14/2009		2.3	2.66	0.9
BRN-DINO-ABEL (SRP CE-558)	PM-6	3.0	5/14/2009		1.0	2.66	0.4
BRN-DINO-ABEL (SRP CE-558)	PM-6	5.0	5/14/2009		1.2	2.66	0.5

Appendix A Table 3 Summary of SPT data

Project	Name	Depth (ft)	Blows Corrected	Blows Uncorr.	Blow Type	Vp (ft/s)
Duke Substation (SRP CE-584)	PM-3(5A)	4.5	11	13	U	#N/A
Duke Substation (SRP CE-584)	PM-3(5A)	9.5	8	15	U	#N/A
Duke Substation (SRP CE-584)	PM-3(5A)	14.5	10	18	U	#N/A
Duke Substation (SRP CE-584)	PM-3(5A)	19.5	13	24	U	#N/A
DUE-PCL (SRP CE-593)	PM-6(P123)	6.5	55	75	U	#N/A
DUE-PCL (SRP CE-593)	PM-6(P123)	9.5	67	109	U	#N/A
DUE-PCL (SRP CE-593)	PM-6(P123)	14.5	58	122	U	#N/A
DUE-PCL (SRP CE-593)	PM-6(P123)	19.5	58	80	U	#N/A
DUE-PCL (SRP CE-593)	PM-6(P123)	24.5	31	57	U	#N/A
DUE-PCL (SRP CE-593)	PM-7(P140)	5.5	35	48	U	1233
DUE-PCL (SRP CE-593)	PM-7(P140)	8.5	40	55	U	1233
DUE-PCL (SRP CE-593)	PM-7(P140)	15.5	15	27	U	3705
DUE-PCL (SRP CE-593)	PM-7(P140)	19.5	24	33	U	3705
DUE-PCL (SRP CE-593)	PM-7(P140)	24.0	18	34	U	3705
DUE-PCL (SRP CE-593)	PM-8(P202)	4.5	12	14	U	#N/A
DUE-PCL (SRP CE-593)	PM-8(P202)	9.5	28	52	U	#N/A
DUE-PCL (SRP CE-593)	PM-8(P202)	19.5	49	53	U	#N/A
DUE-PCL (SRP CE-593)	PM-4(P25A)	4.5	22	26	U	1123
DUE-PCL (SRP CE-593)	PM-4(P25A)	9.5	26	35	U	5243
DUE-PCL (SRP CE-593)	PM-4(P25A)	14.5	42	57	U	5243
DUE-PCL (SRP CE-593)	PM-4(P25A)	19.5	87	120	U	5243
DUE-PCL (SRP CE-593)	PM-4(P25A)	24.5	55	75	U	5243
DUE-PCL (SRP CE-593)	PM-5(P73)	9.5	15	27	U	#N/A
DUE-PCL (SRP CE-593)	PM-5(P73)	14.5	31	42	U	#N/A
PW-DUE (SRP CE-592)	PM-1(P62)	4.5	13	16	U	#N/A
PW-DUE (SRP CE-592)	PM-1(P62)	9.5	10	12	U	#N/A
PW-DUE (SRP CE-592)	PM-1(P62)	14.5	18	33	U	#N/A
PW-DUE (SRP CE-592)	PM-1(P62)	19.5	23	27	U	#N/A
PW-DUE (SRP CE-592)	PM-1(P62)	24.5	19	23	U	#N/A
PW-DUE (SRP CE-592)	PM-2(P88)	4.5	18	21	U	#N/A
PW-DUE (SRP CE-592)	PM-2(P88)	9.5	9	11	U	#N/A
PW-DUE (SRP CE-592)	PM-2(P88)	14.5	40	55	U	#N/A
PW-DUE (SRP CE-592)	PM-2(P88)	19.5	24	33	U	#N/A
BRN-DINO-ABEL (SRP CE-558)	PM-1 (BDA8)	3.0	7	7	S	#N/A
BRN-DINO-ABEL (SRP CE-558)	PM-1 (BDA8)	6.5	14	14	S	#N/A
BRN-DINO-ABEL (SRP CE-558)	PM-1 (BDA8)	12.5	20	20	S	#N/A
BRN-DINO-ABEL (SRP CE-558)	PM-1 (BDA8)	18.5	19	19	S	#N/A
BRN-DINO-ABEL (SRP CE-558)	PM-2 (PCA1)	3.0	16	16	S	#N/A
BRN-DINO-ABEL (SRP CE-558)	PM-2 (PCA1)	8.0	11	11	S	#N/A
BRN-DINO-ABEL (SRP CE-558)	PM-2 (PCA1)	13.0	21	21	S	#N/A
BRN-DINO-ABEL (SRP CE-558)	PM-2 (PCA1)	17.0	43	43	S	#N/A
BRN-DINO-ABEL (SRP CE-558)	PM-3 (PCA-4)	3.0	26	26	S	#N/A
BRN-DINO-ABEL (SRP CE-558)	PM-3 (PCA-4)	7.0	15	14	S	#N/A
BRN-DINO-ABEL (SRP CE-558)	PM-3 (PCA-4)	13.0	25	25	S	#N/A
BRN-DINO-ABEL (SRP CE-558)	PM-3 (PCA-4)	17.0	21	21	S	#N/A
BRN-DINO-ABEL (SRP CE-558)	PM-4 (PCA7)	7.0	19	19	S	#N/A
BRN-DINO-ABEL (SRP CE-558)	PM-4 (PCA7)	13.0	27	27	S	#N/A
BRN-DINO-ABEL (SRP CE-558)	PM-4 (PCA7)	17.0	28	28	S	#N/A
BRN-DINO-ABEL (SRP CE-558)	PM-5 (PCA9)	3.0	12	12	S	#N/A
BRN-DINO-ABEL (SRP CE-558)	PM-5 (PCA9)	7.0	26	26	S	#N/A
BRN-DINO-ABEL (SRP CE-558)	PM-6 (PCA8)	3.0	7	7	S	#N/A
BRN-DINO-ABEL (SRP CE-558)	PM-6 (PCA8)	5.0	7	7	S	#N/A

Appendix A Table 4 Summary of Calculations

Project	Name	Depth (ft)	V_{PMT}*/D	Vs*/D	G_{PMT}/G_0	Dry Unit Weight Est. (pcf)
Duke Substation (SRP CE-584)	PM-3(5A)	4.5	55.7	142.2	0.4	103.1
Duke Substation (SRP CE-584)	PM-3(5A)	9.5	16.7	67.4	0.2	106.7
Duke Substation (SRP CE-584)	PM-3(5A)	14.5	15.9	44.1	0.4	106.7
Duke Substation (SRP CE-584)	PM-3(5A)	19.5	10.8	45.1	0.2	104.1
DUE-PCL (SRP CE-593)	PM-6(P123)	6.5	59.0	123.1	0.5	111.8
DUE-PCL (SRP CE-593)	PM-6(P123)	9.5	49.7	105.3	0.5	115.4
DUE-PCL (SRP CE-593)	PM-6(P123)	14.5	25.8	117.2	0.2	#N/A
DUE-PCL (SRP CE-593)	PM-6(P123)	19.5	13.7	87.2	0.2	#N/A
DUE-PCL (SRP CE-593)	PM-6(P123)	24.5	8.5	21.2	0.4	#N/A
DUE-PCL (SRP CE-593)	PM-7(P140)	5.5	83.8	203.6	0.4	66.2
DUE-PCL (SRP CE-593)	PM-7(P140)	8.5	47.3	188.2	0.3	118.3
DUE-PCL (SRP CE-593)	PM-7(P140)	15.5	23.3	39.4	0.6	#N/A
DUE-PCL (SRP CE-593)	PM-7(P140)	19.5	15.9	31.3	0.5	#N/A
DUE-PCL (SRP CE-593)	PM-7(P140)	24.0	13.2	25.4	0.5	#N/A
DUE-PCL (SRP CE-593)	PM-8(P202)	4.5	64.8	162.2	0.4	102.3
DUE-PCL (SRP CE-593)	PM-8(P202)	9.5	39.7	76.8	0.5	108.5
DUE-PCL (SRP CE-593)	PM-8(P202)	19.5	30.6	87.2	0.4	#N/A
DUE-PCL (SRP CE-593)	PM-4(P25A)	4.5	70.9	202.2	0.4	111.0
DUE-PCL (SRP CE-593)	PM-4(P25A)	9.5	40.3	95.8	0.4	111.0
DUE-PCL (SRP CE-593)	PM-4(P25A)	14.5	22.7	82.8	0.3	106.7
DUE-PCL (SRP CE-593)	PM-4(P25A)	19.5	20.2	92.3	0.2	#N/A
DUE-PCL (SRP CE-593)	PM-4(P25A)	24.5	15.3	29.8	0.5	152.7
DUE-PCL (SRP CE-593)	PM-5(P73)	9.5	33.7	115.8	0.3	118.1
DUE-PCL (SRP CE-593)	PM-5(P73)	14.5	27.6	75.9	0.4	127.7
PW-DUE (SRP CE-592)	PM-1(P62)	4.5	41.0	171.1	0.2	109.8
PW-DUE (SRP CE-592)	PM-1(P62)	9.5	16.5	65.3	0.3	124.8
PW-DUE (SRP CE-592)	PM-1(P62)	14.5	18.0	69.0	0.3	110.5
PW-DUE (SRP CE-592)	PM-1(P62)	19.5	16.9	41.0	0.4	#N/A
PW-DUE (SRP CE-592)	PM-1(P62)	24.5	11.7	32.7	0.4	#N/A
PW-DUE (SRP CE-592)	PM-2(P88)	4.5	61.8	144.4	0.4	113.3
PW-DUE (SRP CE-592)	PM-2(P88)	9.5	26.4	57.9	0.5	124.5
PW-DUE (SRP CE-592)	PM-2(P88)	14.5	25.0	60.7	0.4	98.4
PW-DUE (SRP CE-592)	PM-2(P88)	19.5	11.4	45.1	0.3	98.4
BRN-DINO-ABEL (SRP CE-558)	PM-1 (BDA8)	3.0	93.0	316.7	0.3	111.8
BRN-DINO-ABEL (SRP CE-558)	PM-1 (BDA8)	6.5	14.9	146.2	0.1	111.8
BRN-DINO-ABEL (SRP CE-558)	PM-1 (BDA8)	12.5	17.0	112.0	0.2	121.2
BRN-DINO-ABEL (SRP CE-558)	PM-1 (BDA8)	18.5	25.2	75.7	0.3	#N/A
BRN-DINO-ABEL (SRP CE-558)	PM-2 (PCA1)	3.0	48.7	220.0	0.2	118.6
BRN-DINO-ABEL (SRP CE-558)	PM-2 (PCA1)	8.0	29.9	137.5	0.2	114.1
BRN-DINO-ABEL (SRP CE-558)	PM-2 (PCA1)	13.0	20.3	46.2	0.4	#N/A
BRN-DINO-ABEL (SRP CE-558)	PM-2 (PCA1)	17.0	12.0	82.4	0.1	#N/A
BRN-DINO-ABEL (SRP CE-558)	PM-3 (PCA-4)	3.0	#N/A	193.3	#N/A	110.7
BRN-DINO-ABEL (SRP CE-558)	PM-3 (PCA-4)	7.0	24.1	120.0	0.2	110.4
BRN-DINO-ABEL (SRP CE-558)	PM-3 (PCA-4)	13.0	#N/A	76.9	#N/A	111.8
BRN-DINO-ABEL (SRP CE-558)	PM-3 (PCA-4)	17.0	#N/A	70.6	#N/A	#N/A
BRN-DINO-ABEL (SRP CE-558)	PM-4 (PCA7)	7.0	#N/A	80.0	#N/A	128.6
BRN-DINO-ABEL (SRP CE-558)	PM-4 (PCA7)	13.0	18.9	76.9	0.2	115.4
BRN-DINO-ABEL (SRP CE-558)	PM-4 (PCA7)	17.0	13.7	76.5	0.2	#N/A
BRN-DINO-ABEL (SRP CE-558)	PM-5 (PCA9)	3.0	68.3	200.0	0.3	108.5
BRN-DINO-ABEL (SRP CE-558)	PM-5 (PCA9)	7.0	31.6	136.4	0.2	128.1
BRN-DINO-ABEL (SRP CE-558)	PM-6 (PCA8)	3.0	42.9	170.0	0.3	105.1
BRN-DINO-ABEL (SRP CE-558)	PM-6 (PCA8)	5.0	28.0	126.0	0.2	105.6

APPENDIX B

MFAD RUNS

FOUNDATION ANALYSIS AND DESIGN TOOLS
MFAD VERSION 5.1.20

Project Name:	**PMT Tests**	**Checked By:**	_____
Responsible Engineer:	**A Evans**		
Last Modified Date:	**06/25/2018 06:55:10**	**Date:**	_____
Comments:			

STRUCTURE

Structure ID: P-5a
Description: Str 5a

CASE-DRILLED SHAFT

Case Name: Foundation Estimate
Description: Str 5a

Foundation Data (Str P-5a)

Diameter of Drilled Shaft: [ft]	**7**
Stick up above Ground Level: [ft]	**2**

Model Options

Side Shear Spring:	**On**
Base Shear Spring:	**On**
Base Moment Spring:	**On**

Geotechnical Parameters (PC Est)

Depth to Ground Water: [ft] **50**

All values in table are Nominal Values

Layer No.	Layer Type	Depth to Bottom of Layer [ft]	Total Unit Weight [pcf]	Deformation Modulus [ksi]	Friction Angle [Deg]	Undrained Shear Strength or Rock Cohesion [ksf]	Rock / Concrete Bond Strength [ksf]
1	Soil	4.00	110.0	3.20	30	1.25	0
2	Soil	9.00	106.0	1.90	28	0.60	0
3	Soil	19.00	100.0	2.80	36	0.00	0
4	Soil	26.00	108.0	3.50	40	0.00	0
5	Soil	31.00	123.0	5.00	44	0.00	0

Applied Loads-Top of Shaft (Str 5a x 1.1)

Load Case No.	Load Case Name	Shear Load [kips]	Moment [kip-ft]	Axial Load [kips]	Eccentricity [ft]
1	Str 5a	52.03	6262.74	159.72	122.37

FADTOOLS
Project Name: **PMT Tests**
Structure ID: **P-5a**
Case Name: **Foundation Estimate**

DESIGN RESULTS

Diameter of Drilled Shaft: [ft]	**7**
Stick up above Ground Level: [ft]	**2**
Depth of Embedment: [ft]	**17**
Total Foundation Length: [ft]	**19**
Controlling Applied Load Case Name:	**Str 5a**

Capacity Verification

Loading Mode	Applied Load at Top of Shaft	Applied Load at Groundline	Nominal Capacity at Groundline	Design Capacity at Groundline*	Design Capacity / Applied Load at Groundline
Shear Load [kips]	52.03	52.03	82.78	52.15	1.00
Moment [kip-ft]	6262.74	6366.80	10129.25	6381.43	1.00

Design Capacity is based on a Strength Factor of 0.63

Performance Verification

	Criteria at Groundline	Actual at Groundline	Actual at Top of Shaft
Total Displacement [in]		0.95	1.14
Total Rotation [deg.]	1	0.43	0.43
Nonrecoverable Displacement [in]		0.14	0.17
Nonrecoverable Rotation [deg.]	0.5	0.06	0.06

Maximum Internal Forces

	Maximum Value	Depth of Occurrence
Shear:	407.96 kips	10.50 ft
Moment:	6366.80 kips-ft	0.00 ft

Summary of Results for Controlling Applied Load Case

Depth [ft]	Displacement [in]	Shear Force [kips]	Flexural Moment [kips-ft]	Lateral Pressure [ksf]
Top of Stick (-2)	1.14	52.03	6262.74	0.00
-1	1.05	52.03	6314.77	0.00
Ground Level (0)	0.95	52.03	6366.80	0.00
1	0.86	-18.99	6292.32	11.34
2	0.77	-104.22	6136.58	12.01
3	0.68	-183.97	5897.50	10.88
4	0.59	-255.79	5582.62	9.75
5	0.50	-292.74	5251.94	4.97
6	0.41	-324.90	4886.71	4.29
7	0.32	-352.26	4491.72	3.60
8	0.23	-374.82	4071.77	2.91
9	0.13	-392.58	3631.66	2.23
10	0.04	-405.37	3149.54	1.36
11	-0.05	-404.84	2660.05	-1.37
12	-0.14	-390.50	2179.11	-2.61
13	-0.23	-367.50	1716.86	-3.84

FADTOOLS
Project Name: **PMT Tests**
Structure ID: **P-5a**
Case Name: **Foundation Estimate**

Depth [ft]	Displacement [in]	Shear Force [kips]	Flexural Moment [kips-ft]	Lateral Pressure [ksf]
14	-0.32	-335.85	1281.92	-5.08
15	-0.41	-295.53	882.97	-6.32
16	-0.50	-246.52	528.68	-7.56
17	-0.59	-188.82	227.75	-8.80

Detailed Message:

FOUNDATION ANALYSIS AND DESIGN TOOLS
MFAD VERSION 5.1.20

Project Name:	**PMT Tests**	**Checked By:**	_____
Responsible Engineer:	**A Evans**		
Last Modified Date:	**06/25/2018 06:54:54**	**Date:**	_____
Comments:			

STRUCTURE

Structure ID: P-5a
Description: Str 5a

CASE-DRILLED SHAFT

Case Name: Foundation
Description: Str 5a

Foundation Data (Str P-5a)

Diameter of Drilled Shaft: [ft]	**7**
Stick up above Ground Level: [ft]	**2**

Model Options

Side Shear Spring:	**On**
Base Shear Spring:	**On**
Base Moment Spring:	**On**

Geotechnical Parameters (PC)

Depth to Ground Water: [ft] **50**

All values in table are Nominal Values

Layer No.	Layer Type	Depth to Bottom of Layer [ft]	Total Unit Weight [pcf]	Deformation Modulus [ksi]	Friction Angle [Deg]	Undrained Shear Strength or Rock Cohesion [ksf]	Rock / Concrete Bond Strength [ksf]
1	Soil	4.00	110.0	2.60	30	1.25	0
2	Soil	9.00	106.0	1.30	28	0.60	0
3	Soil	19.00	100.0	2.70	36	0.00	0
4	Soil	26.00	108.0	2.70	40	0.00	0
5	Soil	31.00	123.0	2.70	44	0.00	0

Applied Loads-Top of Shaft (Str 5a x 1.1)

Load Case No.	Load Case Name	Shear Load [kips]	Moment [kip-ft]	Axial Load [kips]	Eccentricity [ft]
1	Str 5a	52.03	6262.74	159.72	122.37

FADTOOLS
Project Name: **PMT Tests**
Structure ID: **P-5a**
Case Name: **Foundation**

DESIGN RESULTS

Diameter of Drilled Shaft: [ft]	**7**
Stick up above Ground Level: [ft]	**2**
Depth of Embedment: [ft]	**17**
Total Foundation Length: [ft]	**19**
Controlling Applied Load Case Name:	**Str 5a**

Capacity Verification

Loading Mode	Applied Load at Top of Shaft	Applied Load at Groundline	Nominal Capacity at Groundline	Design Capacity at Groundline*	Design Capacity / Applied Load at Groundline
Shear Load [kips]	52.03	52.03	82.78	52.15	1.00
Moment [kip-ft]	6262.74	6366.80	10129.25	6381.43	1.00

Design Capacity is based on a Strength Factor of 0.63

Performance Verification

	Criteria at Groundline	Actual at Groundline	Actual at Top of Shaft
Total Displacement [in]		1.17	1.38
Total Rotation [deg.]	1	0.51	0.51
Nonrecoverable Displacement [in]		0.19	0.22
Nonrecoverable Rotation [deg.]	0.5	0.08	0.08

Maximum Internal Forces

	Maximum Value	Depth of Occurrence
Shear:	406.39 kips	10.90 ft
Moment:	6366.80 kips-ft	0.00 ft

Summary of Results for Controlling Applied Load Case

Depth [ft]	Displacement [in]	Shear Force [kips]	Flexural Moment [kips-ft]	Lateral Pressure [ksf]
Top of Stick (-2)	1.38	52.03	6262.74	0.00
-1	1.28	52.03	6314.77	0.00
Ground Level (0)	1.17	52.03	6366.80	0.00
1	1.06	-19.00	6295.02	11.34
2	0.95	-104.26	6143.26	12.04
3	0.85	-184.39	5907.95	10.96
4	0.74	-256.97	5596.29	9.88
5	0.63	-289.40	5277.62	4.39
6	0.52	-318.08	4928.39	3.86
7	0.42	-343.00	4552.36	3.32
8	0.31	-364.17	4153.29	2.78
9	0.20	-381.58	3734.93	2.25
10	0.09	-398.97	3250.13	1.95
11	-0.01	-406.16	2752.38	-0.33
12	-0.12	-394.59	2257.23	-2.32
13	-0.23	-372.96	1778.82	-3.72

FADTOOLS
Project Name: **PMT Tests**
Structure ID: **P-5a**
Case Name: **Foundation**

Depth [ft]	Displacement [in]	Shear Force [kips]	Flexural Moment [kips-ft]	Lateral Pressure [ksf]
14	-0.34	-341.58	1326.90	-5.11
15	-0.44	-300.45	911.25	-6.50
16	-0.55	-249.54	541.61	-7.90
17	-0.66	-188.84	227.78	-9.30

Detailed Message:

FOUNDATION ANALYSIS AND DESIGN TOOLS
MFAD VERSION 5.1.20

Project Name:	**PMT Tests**	**Checked By:**	_____
Responsible Engineer:	**A Evans**		
Last Modified Date:	**06/25/2018 06:53:32**	**Date:**	_____
Comments:			

STRUCTURE

Structure ID: P-25a
Description: Str 25a

CASE-DRILLED SHAFT

Case Name: Foundation Estimate
Description: Str 25a

Foundation Data (Str P-25a)

Diameter of Drilled Shaft: [ft] 7
Stick up above Ground Level: [ft] 3

Model Options

Side Shear Spring: On
Base Shear Spring: On
Base Moment Spring: On

Geotechnical Parameters (1B Est)

Depth to Ground Water: [ft] 50

All values in table are Nominal Values

Layer No.	Layer Type	Depth to Bottom of Layer [ft]	Total Unit Weight [pcf]	Deformation Modulus [ksi]	Friction Angle [Deg]	Undrained Shear Strength or Rock Cohesion [ksf]	Rock / Concrete Bond Strength [ksf]
1	Soil	5.00	110.0	5.80	39	0.50	0
2	Soil	12.00	113.0	6.90	44	1.00	0
3	Soil	19.00	116.0	7.50	55	1.00	0
4	Soil	24.00	116.0	7.30	43	0.75	0

Applied Loads-Top of Shaft (Str 25a x 1.1)

Load Case No.	Load Case Name	Shear Load [kips]	Moment [kip-ft]	Axial Load [kips]	Eccentricity [ft]
1	Str 25a	60.28	6310.92	176.44	107.69

FADTOOLS
Project Name: **PMT Tests**
Structure ID: **P-25a**
Case Name: **Foundation Estimate**

DESIGN RESULTS

Diameter of Drilled Shaft: [ft]	**7**
Stick up above Ground Level: [ft]	**3**
Depth of Embedment: [ft]	**15**
Total Foundation Length: [ft]	**18**
Controlling Applied Load Case Name:	**Str 25a**

Capacity Verification

Loading Mode	Applied Load at Top of Shaft	Applied Load at Groundline	Nominal Capacity at Groundline	Design Capacity at Groundline*	Design Capacity / Applied Load at Groundline
Shear Load [kips]	60.28	60.28	434.67	273.84	4.54
Moment [kip-ft]	6310.92	6491.76	46811.52	29491.26	4.54

Design Capacity is based on a Strength Factor of 0.63

Performance Verification

	Criteria at Groundline	Actual at Groundline	Actual at Top of Shaft
Total Displacement [in]		0.47	0.61
Total Rotation [deg.]	1	0.21	0.21
Nonrecoverable Displacement [in]		0.09	0.11
Nonrecoverable Rotation [deg.]	0.5	0.03	0.03

Maximum Internal Forces

	Maximum Value	Depth of Occurrence
Shear:	547.20 kips	10.40 ft
Moment:	6491.76 kips-ft	0.00 ft

Summary of Results for Controlling Applied Load Case

Depth [ft]	Displacement [in]	Shear Force [kips]	Flexural Moment [kips-ft]	Lateral Pressure [ksf]
Top of Stick (-3)	0.61	60.28	6310.92	0.00
-2	0.56	60.28	6371.20	0.00
-1	0.52	60.28	6431.48	0.00
Ground Level (0)	0.47	60.28	6491.76	0.00
1	0.43	10.05	6445.52	8.38
2	0.38	-59.05	6337.91	11.10
3	0.33	-132.95	6156.63	10.09
4	0.29	-199.59	5905.08	9.05
5	0.24	-259.01	5590.50	8.02
6	0.20	-333.63	5192.87	10.21
7	0.15	-401.30	4724.10	9.23
8	0.11	-462.19	4191.06	8.27
9	0.06	-515.72	3600.48	6.58
10	0.02	-544.49	2967.04	2.09
11	-0.03	-541.84	2320.55	-2.40
12	-0.07	-507.78	1692.41	-6.89

FADTOOLS
Project Name: **PMT Tests**
Structure ID: **P-25a**
Case Name: **Foundation Estimate**

Depth [ft]	Displacement [in]	Shear Force [kips]	Flexural Moment [kips-ft]	Lateral Pressure [ksf]
13	-0.12	-436.60	1107.90	-12.36
14	-0.16	-331.28	611.64	-17.24
15	-0.21	-191.82	237.77	-22.12

Detailed Message:

FOUNDATION ANALYSIS AND DESIGN TOOLS
MFAD VERSION 5.1.20

Project Name:	**PMT Tests**	**Checked By:**	_____
Responsible Engineer:	**A Evans**		
Last Modified Date:	**06/25/2018 06:52:58**	**Date:**	_____
Comments:			

STRUCTURE

Structure ID: P-25a
Description: Str 25a

CASE-DRILLED SHAFT

Case Name: Foundation
Description: Str 25a

Foundation Data (Str P-25a)
Diameter of Drilled Shaft: [ft] 7
Stick up above Ground Level: [ft] 3

Model Options
Side Shear Spring: On
Base Shear Spring: On
Base Moment Spring: On

Geotechnical Parameters (1B)
Depth to Ground Water: [ft] 50
All values in table are Nominal Values

Layer No.	Layer Type	Depth to Bottom of Layer [ft]	Total Unit Weight [pcf]	Deformation Modulus [ksi]	Friction Angle [Deg]	Undrained Shear Strength or Rock Cohesion [ksf]	Rock / Concrete Bond Strength [ksf]
1	Soil	5.00	110.0	6.50	39	0.50	0
2	Soil	12.00	113.0	7.95	44	1.00	0
3	Soil	19.00	116.0	9.10	55	1.00	0
4	Soil	24.00	116.0	8.20	43	0.75	0

Applied Loads-Top of Shaft (Str 25a x 1.1)

Load Case No.	Load Case Name	Shear Load [kips]	Moment [kip-ft]	Axial Load [kips]	Eccentricity [ft]
1	Str 25a	60.28	6310.92	176.44	107.69

FADTOOLS
Project Name: **PMT Tests**
Structure ID: **P-25a**
Case Name: **Foundation**

DESIGN RESULTS

Diameter of Drilled Shaft: [ft]	**7**
Stick up above Ground Level: [ft]	**3**
Depth of Embedment: [ft]	**15**
Total Foundation Length: [ft]	**18**
Controlling Applied Load Case Name:	**Str 25a**

Capacity Verification

Loading Mode	Applied Load at Top of Shaft	Applied Load at Groundline	Nominal Capacity at Groundline	Design Capacity at Groundline*	Design Capacity / Applied Load at Groundline
Shear Load [kips]	60.28	60.28	434.67	273.84	4.54
Moment [kip-ft]	6310.92	6491.76	46811.52	29491.26	4.54

Design Capacity is based on a Strength Factor of 0.63

Performance Verification

	Criteria at Groundline	Actual at Groundline	Actual at Top of Shaft
Total Displacement [in]		0.41	0.52
Total Rotation [deg.]	1	0.18	0.18
Nonrecoverable Displacement [in]		0.08	0.10
Nonrecoverable Rotation [deg.]	0.5	0.03	0.03

Maximum Internal Forces

	Maximum Value	Depth of Occurrence
Shear:	549.65 kips	10.50 ft
Moment:	6491.76 kips-ft	0.00 ft

Summary of Results for Controlling Applied Load Case

Depth [ft]	Displacement [in]	Shear Force [kips]	Flexural Moment [kips-ft]	Lateral Pressure [ksf]
Top of Stick (-3)	0.52	60.28	6310.92	0.00
-2	0.49	60.28	6371.20	0.00
-1	0.45	60.28	6431.48	0.00
Ground Level (0)	0.41	60.28	6491.76	0.00
1	0.37	10.15	6447.76	8.36
2	0.33	-58.66	6343.39	10.87
3	0.29	-130.90	6166.41	9.87
4	0.25	-196.18	5920.68	8.88
5	0.21	-254.55	5613.13	7.89
6	0.18	-329.64	5220.63	10.28
7	0.14	-397.87	4756.49	9.31
8	0.10	-459.38	4227.49	8.37
9	0.06	-514.02	3640.25	6.95
10	0.02	-545.55	3008.07	2.50
11	-0.02	-545.96	2359.92	-1.94
12	-0.06	-515.23	1726.93	-6.39

FADTOOLS
Project Name: **PMT Tests**
Structure ID: **P-25a**
Case Name: **Foundation**

Depth [ft]	Displacement [in]	Shear Force [kips]	Flexural Moment [kips-ft]	Lateral Pressure [ksf]
13	-0.10	-444.43	1129.89	-12.41
14	-0.14	-337.99	621.47	-17.50
15	-0.17	-195.92	237.31	-22.59

Detailed Message:

FOUNDATION ANALYSIS AND DESIGN TOOLS
MFAD VERSION 5.1.20

Project Name:	**PMT Tests**	**Checked By:**	_____
Responsible Engineer:	**A Evans**		
Last Modified Date:	**06/25/2018 06:47:34**	**Date:**	_____
Comments:			

STRUCTURE

Structure ID: PM 2
Description: Str 37

CASE-DRILLED SHAFT

Case Name: Foundation Estimate
Description: Str 37

Foundation Data (Str 37)
Diameter of Drilled Shaft: [ft] 7
Stick up above Ground Level: [ft] 3

Model Options
Side Shear Spring: On
Base Shear Spring: On
Base Moment Spring: On

Geotechnical Parameters (DIN-ABL 1 Est)
Depth to Ground Water: [ft] 50
All values in table are Nominal Values

Layer No.	Layer Type	Depth to Bottom of Layer [ft]	Total Unit Weight [pcf]	Deformation Modulus [ksi]	Friction Angle [Deg]	Undrained Shear Strength or Rock Cohesion [ksf]	Rock / Concrete Bond Strength [ksf]
1	Soil	11.50	110.0	2.00	25	1.00	0
2	Soil	29.00	115.0	5.40	30	1.00	0

Applied Loads-Top of Shaft (Str 37 x 1.05)

Load Case No.	Load Case Name	Shear Load [kips]	Moment [kip-ft]	Axial Load [kips]	Eccentricity [ft]
1	Str 37	61.215	6543.705	79.8	109.90

FADTOOLS
Project Name: **PMT Tests**
Structure ID: **PM 2**
Case Name: **Foundation Estimate**

DESIGN RESULTS

Diameter of Drilled Shaft: [ft]	**7**
Stick up above Ground Level: [ft]	**3**
Depth of Embedment: [ft]	**21**
Total Foundation Length: [ft]	**24**
Controlling Applied Load Case Name:	**Str 37**

Capacity Verification

Loading Mode	Applied Load at Top of Shaft	Applied Load at Groundline	Nominal Capacity at Groundline	Design Capacity at Groundline*	Design Capacity / Applied Load at Groundline
Shear Load [kips]	61.22	61.22	170.22	107.24	1.75
Moment [kip-ft]	6543.71	6727.35	18706.54	11785.12	1.75

Design Capacity is based on a Strength Factor of 0.63

Performance Verification

	Criteria at Groundline	Actual at Groundline	Actual at Top of Shaft
Total Displacement [in]		0.81	0.97
Total Rotation [deg.]	1	0.26	0.26
Nonrecoverable Displacement [in]		0.18	0.21
Nonrecoverable Rotation [deg.]	0.5	0.06	0.06

Maximum Internal Forces

	Maximum Value	Depth of Occurrence
Shear:	431.63 kips	14.80 ft
Moment:	6735.30 kips-ft	0.60 ft

Summary of Results for Controlling Applied Load Case

Depth [ft]	Displacement [in]	Shear Force [kips]	Flexural Moment [kips-ft]	Lateral Pressure [ksf]
Top of Stick (-3)	0.97	61.22	6543.71	0.00
-2	0.92	61.22	6604.92	0.00
-1	0.86	61.22	6666.14	0.00
Ground Level (0)	0.81	61.22	6727.35	0.00
1	0.75	16.13	6731.43	6.68
2	0.70	-29.34	6689.44	6.35
3	0.64	-72.45	6603.15	6.01
4	0.59	-113.17	6474.94	5.66
5	0.54	-151.47	6307.23	5.31
6	0.48	-187.32	6102.44	4.96
7	0.43	-220.71	5863.02	4.61
8	0.37	-251.62	5591.46	4.26
9	0.32	-280.04	5290.22	3.90
10	0.26	-305.95	4961.82	3.54
11	0.21	-329.35	4608.77	3.18
12	0.15	-360.39	4201.08	5.58

FADTOOLS
Project Name: **PMT Tests**
Structure ID: **PM 2**
Case Name: **Foundation Estimate**

Depth [ft]	Displacement [in]	Shear Force [kips]	Flexural Moment [kips-ft]	Lateral Pressure [ksf]
13	0.10	-395.33	3727.58	4.51
14	0.05	-422.63	3222.90	3.27
15	-0.01	-431.29	2698.78	-0.43
16	-0.06	-414.18	2178.94	-3.96
17	-0.12	-381.34	1685.39	-5.29
18	-0.17	-339.22	1229.31	-6.61
19	-0.23	-287.81	820.01	-7.94
20	-0.28	-227.11	466.76	-9.27
21	-0.34	-157.13	178.84	-10.59

Detailed Message:

FOUNDATION ANALYSIS AND DESIGN TOOLS
MFAD VERSION 5.1.20

Project Name:	**PMT Tests**	**Checked By:**	_____
Responsible Engineer:	**A Evans**		
Last Modified Date:	**06/25/2018 06:47:09**	**Date:**	_____
Comments:			

STRUCTURE

Structure ID: PM 2
Description: Str 37

CASE-DRILLED SHAFT

Case Name: Foundation
Description: Str 37

Foundation Data (Str 37)
Diameter of Drilled Shaft: [ft] 7
Stick up above Ground Level: [ft] 3

Model Options
Side Shear Spring: On
Base Shear Spring: On
Base Moment Spring: On

Geotechnical Parameters (DIN-ABL 1)
Depth to Ground Water: [ft] 50
All values in table are Nominal Values

Layer No.	Layer Type	Depth to Bottom of Layer [ft]	Total Unit Weight [pcf]	Deformation Modulus [ksi]	Friction Angle [Deg]	Undrained Shear Strength or Rock Cohesion [ksf]	Rock / Concrete Bond Strength [ksf]
1	Soil	12.50	110.0	2.10	25	1.00	0
2	Soil	29.00	115.0	3.40	30	1.00	0

Applied Loads-Top of Shaft (Str 37 x 1.05)

Load Case No.	Load Case Name	Shear Load [kips]	Moment [kip-ft]	Axial Load [kips]	Eccentricity [ft]
1	Str 37	61.215	6543.705	79.8	109.90

FADTOOLS
Project Name: **PMT Tests**
Structure ID: **PM 2**
Case Name: **Foundation**

DESIGN RESULTS

Diameter of Drilled Shaft: [ft]	**7**
Stick up above Ground Level: [ft]	**3**
Depth of Embedment: [ft]	**21**
Total Foundation Length: [ft]	**24**
Controlling Applied Load Case Name:	**Str 37**

Capacity Verification

Loading Mode	Applied Load at Top of Shaft	Applied Load at Groundline	Nominal Capacity at Groundline	Design Capacity at Groundline*	Design Capacity / Applied Load at Groundline
Shear Load [kips]	61.22	61.22	168.09	105.90	1.73
Moment [kip-ft]	6543.71	6727.35	18472.37	11637.59	1.73

Design Capacity is based on a Strength Factor of 0.63

Performance Verification

	Criteria at Groundline	Actual at Groundline	Actual at Top of Shaft
Total Displacement [in]		0.89	1.08
Total Rotation [deg.]	1	0.30	0.30
Nonrecoverable Displacement [in]		0.17	0.20
Nonrecoverable Rotation [deg.]	0.5	0.06	0.06

Maximum Internal Forces

	Maximum Value	Depth of Occurrence
Shear:	420.85 kips	14.20 ft
Moment:	6731.38 kips-ft	0.40 ft

Summary of Results for Controlling Applied Load Case

Depth [ft]	Displacement [in]	Shear Force [kips]	Flexural Moment [kips-ft]	Lateral Pressure [ksf]
Top of Stick (-3)	1.08	61.22	6543.71	0.00
-2	1.02	61.22	6604.92	0.00
-1	0.96	61.22	6666.14	0.00
Ground Level (0)	0.89	61.22	6727.35	0.00
1	0.83	15.15	6723.72	7.34
2	0.77	-36.78	6669.89	7.24
3	0.71	-85.76	6565.57	6.80
4	0.64	-131.67	6413.80	6.36
5	0.58	-174.49	6217.66	5.92
6	0.52	-214.19	5980.27	5.47
7	0.45	-250.75	5704.74	5.02
8	0.39	-284.17	5394.22	4.57
9	0.33	-314.42	5051.87	4.12
10	0.26	-341.49	4680.85	3.66
11	0.20	-365.37	4284.36	3.21
12	0.14	-386.07	3865.58	2.75

FADTOOLS
Project Name: **PMT Tests**
Structure ID: **PM 2**
Case Name: **Foundation**

Depth [ft]	Displacement [in]	Shear Force [kips]	Flexural Moment [kips-ft]	Lateral Pressure [ksf]
13	0.08	-407.44	3413.45	3.34
14	0.01	-420.51	2928.63	0.65
15	-0.05	-414.69	2440.18	-2.05
16	-0.11	-390.97	1966.85	-4.14
17	-0.18	-358.13	1522.43	-5.14
18	-0.24	-318.26	1114.36	-6.15
19	-0.30	-271.37	749.67	-7.15
20	-0.37	-217.47	435.38	-8.15
21	-0.43	-156.56	178.49	-9.15

Detailed Message:

FOUNDATION ANALYSIS AND DESIGN TOOLS
MFAD VERSION 5.1.20

Project Name:	**PMT Tests**	**Checked By:**	_____
Responsible Engineer:	**A Evans**		
Last Modified Date:	**06/25/2018 06:54:40**	**Date:**	_____
Comments:			

STRUCTURE

Structure ID: P-62
Description: Str 62

CASE-DRILLED SHAFT

Case Name: Foundation Estimate
Description: Str 62

Foundation Data (Str P-62)
Diameter of Drilled Shaft: [ft] 7
Stick up above Ground Level: [ft] 3

Model Options
Side Shear Spring: On
Base Shear Spring: On
Base Moment Spring: On

Geotechnical Parameters (1A/2A/1C Est)
Depth to Ground Water: [ft] 50
All values in table are Nominal Values

Layer No.	Layer Type	Depth to Bottom of Layer [ft]	Total Unit Weight [pcf]	Deformation Modulus [ksi]	Friction Angle [Deg]	Undrained Shear Strength or Rock Cohesion [ksf]	Rock / Concrete Bond Strength [ksf]
1	Soil	6.00	107.0	2.80	33	0.65	0
2	Soil	21.00	111.0	4.20	42	1.00	0
3	Soil	26.00	118.0	4.60	33	0.75	0

Applied Loads-Top of Shaft (Str 62 x 1.1)

Load Case No.	Load Case Name	Shear Load [kips]	Moment [kip-ft]	Axial Load [kips]	Eccentricity [ft]
1	Str 62	50.38	6114.46	144.43	124.37

FADTOOLS
Project Name: **PMT Tests**
Structure ID: **P-62**
Case Name: **Foundation Estimate**

DESIGN RESULTS

Diameter of Drilled Shaft: [ft]	**7**
Stick up above Ground Level: [ft]	**3**
Depth of Embedment: [ft]	**18**
Total Foundation Length: [ft]	**21**
Controlling Applied Load Case Name:	**Str 62**

Capacity Verification

Loading Mode	Applied Load at Top of Shaft	Applied Load at Groundline	Nominal Capacity at Groundline	Design Capacity at Groundline*	Design Capacity / Applied Load at Groundline
Shear Load [kips]	50.38	50.38	259.36	163.40	3.24
Moment [kip-ft]	6114.46	6265.60	32255.97	20321.26	3.24

Design Capacity is based on a Strength Factor of 0.63

Performance Verification

	Criteria at Groundline	Actual at Groundline	Actual at Top of Shaft
Total Displacement [in]		0.63	0.78
Total Rotation [deg.]	1	0.24	0.24
Nonrecoverable Displacement [in]		0.10	0.13
Nonrecoverable Rotation [deg.]	0.5	0.03	0.03

Maximum Internal Forces

	Maximum Value	Depth of Occurrence
Shear:	473.11 kips	12.10 ft
Moment:	6265.75 kips-ft	0.10 ft

Summary of Results for Controlling Applied Load Case

Depth [ft]	Displacement [in]	Shear Force [kips]	Flexural Moment [kips-ft]	Lateral Pressure [ksf]
Top of Stick (-3)	0.78	50.38	6114.46	0.00
-2	0.73	50.38	6164.84	0.00
-1	0.68	50.38	6215.22	0.00
Ground Level (0)	0.63	50.38	6265.60	0.00
1	0.58	5.78	6247.89	7.27
2	0.52	-45.02	6181.04	7.03
3	0.47	-92.35	6065.12	6.54
4	0.42	-136.18	5903.63	6.04
5	0.37	-176.53	5700.04	5.54
6	0.32	-213.40	5457.83	5.04
7	0.26	-273.22	5143.77	8.29
8	0.21	-329.01	4771.91	7.71
9	0.16	-380.82	4346.25	7.15
10	0.11	-428.42	3870.76	6.25
11	0.06	-460.93	3353.98	3.33
12	0.00	-473.02	2814.91	0.42

FADTOOLS
Project Name: **PMT Tests**
Structure ID: **P-62**
Case Name: **Foundation Estimate**

Depth [ft]	Displacement [in]	Shear Force [kips]	Flexural Moment [kips-ft]	Lateral Pressure [ksf]
13	-0.05	-464.70	2273.94	-2.50
14	-0.10	-435.96	1751.51	-5.42
15	-0.15	-386.81	1268.02	-8.33
16	-0.20	-319.38	843.44	-10.35
17	-0.25	-241.74	491.68	-11.70
18	-0.31	-154.67	222.28	-13.04

Detailed Message:

FOUNDATION ANALYSIS AND DESIGN TOOLS
MFAD VERSION 5.1.20

Project Name:	**PMT Tests**	**Checked By:**	_____
Responsible Engineer:	**A Evans**		
Last Modified Date:	**06/25/2018 06:54:26**	**Date:**	_____
Comments:			

STRUCTURE

Structure ID: P-62
Description: Str 62

CASE-DRILLED SHAFT

Case Name: Foundation
Description: Str 62

Foundation Data (Str P-62)
Diameter of Drilled Shaft: [ft] 7
Stick up above Ground Level: [ft] 3

Model Options
Side Shear Spring: On
Base Shear Spring: On
Base Moment Spring: On

Geotechnical Parameters (1A/2A/1C)
Depth to Ground Water: [ft] 50
All values in table are Nominal Values

Layer No.	Layer Type	Depth to Bottom of Layer [ft]	Total Unit Weight [pcf]	Deformation Modulus [ksi]	Friction Angle [Deg]	Undrained Shear Strength or Rock Cohesion [ksf]	Rock / Concrete Bond Strength [ksf]
1	Soil	6.00	107.0	1.80	33	0.65	0
2	Soil	21.00	111.0	5.20	42	1.00	0
3	Soil	26.00	118.0	4.60	33	0.75	0

Applied Loads-Top of Shaft (Str 62 x 1.1)

Load Case No.	Load Case Name	Shear Load [kips]	Moment [kip-ft]	Axial Load [kips]	Eccentricity [ft]
1	Str 62	50.38	6114.46	144.43	124.37

FADTOOLS
Project Name: **PMT Tests**
Structure ID: **P-62**
Case Name: **Foundation**

DESIGN RESULTS

Diameter of Drilled Shaft: [ft]	**7**
Stick up above Ground Level: [ft]	**3**
Depth of Embedment: [ft]	**18**
Total Foundation Length: [ft]	**21**
Controlling Applied Load Case Name:	**Str 62**

Capacity Verification

Loading Mode	Applied Load at Top of Shaft	Applied Load at Groundline	Nominal Capacity at Groundline	Design Capacity at Groundline*	Design Capacity / Applied Load at Groundline
Shear Load [kips]	50.38	50.38	259.36	163.40	3.24
Moment [kip-ft]	6114.46	6265.60	32255.97	20321.26	3.24

Design Capacity is based on a Strength Factor of 0.63

Performance Verification

	Criteria at Groundline	Actual at Groundline	Actual at Top of Shaft
Total Displacement [in]		0.67	0.84
Total Rotation [deg.]	1	0.25	0.25
Nonrecoverable Displacement [in]		0.13	0.16
Nonrecoverable Rotation [deg.]	0.5	0.04	0.04

Maximum Internal Forces

	Maximum Value	Depth of Occurrence
Shear:	497.43 kips	12.60 ft
Moment:	6270.38 kips-ft	0.50 ft

Summary of Results for Controlling Applied Load Case

Depth [ft]	Displacement [in]	Shear Force [kips]	Flexural Moment [kips-ft]	Lateral Pressure [ksf]
Top of Stick (-3)	0.84	50.38	6114.46	0.00
-2	0.78	50.38	6164.84	0.00
-1	0.73	50.38	6215.22	0.00
Ground Level (0)	0.67	50.38	6265.60	0.00
1	0.62	11.97	6265.53	5.38
2	0.57	-24.58	6227.93	5.09
3	0.51	-59.13	6154.77	4.81
4	0.46	-91.68	6048.06	4.52
5	0.41	-122.22	5909.81	4.23
6	0.35	-150.76	5742.02	3.95
7	0.30	-225.17	5463.61	10.25
8	0.25	-293.67	5113.75	9.41
9	0.19	-356.31	4698.32	8.57
10	0.14	-413.14	4223.16	7.75
11	0.09	-463.34	3694.14	6.21
12	0.03	-492.47	3124.13	2.49

FADTOOLS
Project Name: **PMT Tests**
Structure ID: **P-62**
Case Name: **Foundation**

Depth [ft]	Displacement [in]	Shear Force [kips]	Flexural Moment [kips-ft]	Lateral Pressure [ksf]
13	-0.02	-495.52	2538.03	-1.24
14	-0.07	-472.50	1961.91	-4.97
15	-0.13	-423.39	1421.86	-8.69
16	-0.18	-353.64	942.40	-10.71
17	-0.23	-272.47	538.47	-12.32
18	-0.29	-180.04	221.33	-13.93

Detailed Message:

FOUNDATION ANALYSIS AND DESIGN TOOLS
MFAD VERSION 5.1.20

Project Name:	**PMT Tests**	**Checked By:**	_____
Responsible Engineer:	**A Evans**		
Last Modified Date:	**06/25/2018 06:48:06**	**Date:**	_____
Comments:			

STRUCTURE

Structure ID: PM 3
Description: Str 73

CASE-DRILLED SHAFT

Case Name: Foundation Estimate
Description: Str 73

Foundation Data (Str 73)
Diameter of Drilled Shaft: [ft] 7
Stick up above Ground Level: [ft] 3

Model Options
Side Shear Spring: On
Base Shear Spring: On
Base Moment Spring: On

Geotechnical Parameters (DIN-ABL 3C Est)
Depth to Ground Water: [ft] 50
All values in table are Nominal Values

Layer No.	Layer Type	Depth to Bottom of Layer [ft]	Total Unit Weight [pcf]	Deformation Modulus [ksi]	Friction Angle [Deg]	Undrained Shear Strength or Rock Cohesion [ksf]	Rock / Concrete Bond Strength [ksf]
1	Soil	6.00	104.0	1.40	35	0.45	0
2	Soil	16.00	120.0	2.80	36	0.50	0
3	Soil	29.00	127.0	4.00	40	0.00	0

Applied Loads-Top of Shaft (Str 73 x1.1)

Load Case No.	Load Case Name	Shear Load [kips]	Moment [kip-ft]	Axial Load [kips]	Eccentricity [ft]
1	Str 73 x 1.1	75.57	8368.36	92.07	113.74

FADTOOLS
Project Name: **PMT Tests**
Structure ID: **PM 3**
Case Name: **Foundation Estimate**

DESIGN RESULTS

Diameter of Drilled Shaft: [ft]	**7**
Stick up above Ground Level: [ft]	**3**
Depth of Embedment: [ft]	**19**
Total Foundation Length: [ft]	**22**
Controlling Applied Load Case Name:	**Str 73 x 1.1**

Capacity Verification

Loading Mode	Applied Load at Top of Shaft	Applied Load at Groundline	Nominal Capacity at Groundline	Design Capacity at Groundline*	Design Capacity / Applied Load at Groundline
Shear Load [kips]	75.57	75.57	138.98	87.56	1.16
Moment [kip-ft]	8368.36	8595.07	15806.81	9958.29	1.16

Design Capacity is based on a Strength Factor of 0.63

Performance Verification

	Criteria at Groundline	Actual at Groundline	Actual at Top of Shaft
Total Displacement [in]		1.83	2.26
Total Rotation [deg.]	1	0.68	0.68
Nonrecoverable Displacement [in]		0.50	0.64
Nonrecoverable Rotation [deg.]	0.5	0.21	0.21

Maximum Internal Forces

	Maximum Value	Depth of Occurrence
Shear:	579.49 kips	12.70 ft
Moment:	8603.05 kips-ft	0.60 ft

Summary of Results for Controlling Applied Load Case

Depth [ft]	Displacement [in]	Shear Force [kips]	Flexural Moment [kips-ft]	Lateral Pressure [ksf]
Top of Stick (-3)	2.26	75.57	8368.36	0.00
-2	2.12	75.57	8443.93	0.00
-1	1.97	75.57	8519.50	0.00
Ground Level (0)	1.83	75.57	8595.07	0.00
1	1.69	40.93	8597.95	5.75
2	1.54	-6.21	8551.35	7.54
3	1.40	-65.68	8451.33	9.02
4	1.26	-125.98	8290.09	8.28
5	1.11	-181.15	8071.11	7.55
6	0.97	-231.22	7799.51	6.82
7	0.82	-314.75	7395.63	11.23
8	0.68	-387.39	6913.68	9.68
9	0.54	-449.16	6364.51	8.13
10	0.39	-500.08	5759.01	6.58
11	0.25	-540.17	5108.00	5.03
12	0.11	-569.51	4422.29	3.51

FADTOOLS
Project Name: **PMT Tests**
Structure ID: **PM 3**
Case Name: **Foundation Estimate**

Depth [ft]	Displacement [in]	Shear Force [kips]	Flexural Moment [kips-ft]	Lateral Pressure [ksf]
13	-0.04	-578.34	3715.44	-1.08
14	-0.18	-554.80	3017.11	-4.48
15	-0.32	-516.13	2350.56	-6.38
16	-0.47	-464.23	1729.30	-8.26
17	-0.61	-384.85	1117.54	-12.53
18	-0.75	-287.01	594.39	-15.17
19	-0.90	-170.67	178.33	-17.81

Detailed Message:

FOUNDATION ANALYSIS AND DESIGN TOOLS
MFAD VERSION 5.1.20

Project Name:	**PMT Tests**	**Checked By:**	_____
Responsible Engineer:	**A Evans**		
Last Modified Date:	**06/25/2018 06:47:48**	**Date:**	_____
Comments:			

STRUCTURE

Structure ID: PM 3
Description: Str 73

CASE-DRILLED SHAFT

Case Name: Foundation
Description: Str 73

Foundation Data (Str 73)
Diameter of Drilled Shaft: [ft] 7
Stick up above Ground Level: [ft] 3

Model Options
Side Shear Spring: On
Base Shear Spring: On
Base Moment Spring: On

Geotechnical Parameters (DIN-ABL 3C)
Depth to Ground Water: [ft] 50
All values in table are Nominal Values

Layer No.	Layer Type	Depth to Bottom of Layer [ft]	Total Unit Weight [pcf]	Deformation Modulus [ksi]	Friction Angle [Deg]	Undrained Shear Strength or Rock Cohesion [ksf]	Rock / Concrete Bond Strength [ksf]
1	Soil	6.00	104.0	3.15	35	0.45	0
2	Soil	16.00	120.0	4.95	36	0.50	0
3	Soil	29.00	127.0	6.60	40	0.00	0

Applied Loads-Top of Shaft (Str 73 x1.1)

Load Case No.	Load Case Name	Shear Load [kips]	Moment [kip-ft]	Axial Load [kips]	Eccentricity [ft]
1	Str 73 x 1.1	75.57	8368.36	92.07	113.74

FADTOOLS
Project Name: **PMT Tests**
Structure ID: **PM 3**
Case Name: **Foundation**

DESIGN RESULTS

Diameter of Drilled Shaft: [ft]	**7**
Stick up above Ground Level: [ft]	**3**
Depth of Embedment: [ft]	**19**
Total Foundation Length: [ft]	**22**
Controlling Applied Load Case Name:	**Str 73 x 1.1**

Capacity Verification

Loading Mode	Applied Load at Top of Shaft	Applied Load at Groundline	Nominal Capacity at Groundline	Design Capacity at Groundline*	Design Capacity / Applied Load at Groundline
Shear Load [kips]	75.57	75.57	138.98	87.56	1.16
Moment [kip-ft]	8368.36	8595.07	15806.81	9958.29	1.16

Design Capacity is based on a Strength Factor of 0.63

Performance Verification

	Criteria at Groundline	Actual at Groundline	Actual at Top of Shaft
Total Displacement [in]		0.98	1.21
Total Rotation [deg.]	1	0.37	0.37
Nonrecoverable Displacement [in]		0.30	0.37
Nonrecoverable Rotation [deg.]	0.5	0.12	0.12

Maximum Internal Forces

	Maximum Value	Depth of Occurrence
Shear:	574.28 kips	12.50 ft
Moment:	8603.03 kips-ft	0.60 ft

Summary of Results for Controlling Applied Load Case

Depth [ft]	Displacement [in]	Shear Force [kips]	Flexural Moment [kips-ft]	Lateral Pressure [ksf]
Top of Stick (-3)	1.21	75.57	8368.36	0.00
-2	1.13	75.57	8443.93	0.00
-1	1.05	75.57	8519.50	0.00
Ground Level (0)	0.98	75.57	8595.07	0.00
1	0.90	40.91	8597.90	5.75
2	0.82	-6.26	8542.91	7.55
3	0.74	-66.06	8428.42	9.36
4	0.66	-135.31	8248.41	9.72
5	0.59	-199.77	8000.96	8.79
6	0.51	-257.79	7692.27	7.87
7	0.43	-335.70	7269.92	10.46
8	0.35	-403.21	6774.87	8.98
9	0.27	-460.33	6217.50	7.49
10	0.20	-507.08	5608.21	6.01
11	0.12	-543.50	4957.32	4.54
12	0.04	-569.53	4275.16	2.88

FADTOOLS
Project Name: **PMT Tests**
Structure ID: **PM 3**
Case Name: **Foundation**

Depth [ft]	Displacement [in]	Shear Force [kips]	Flexural Moment [kips-ft]	Lateral Pressure [ksf]
13	-0.04	-570.19	3577.65	-2.18
14	-0.12	-542.92	2895.12	-4.78
15	-0.19	-502.47	2246.64	-6.60
16	-0.27	-449.28	1644.97	-8.42
17	-0.35	-373.13	1066.07	-11.95
18	-0.43	-280.30	571.65	-14.33
19	-0.51	-170.76	178.42	-16.72

Detailed Message:

FOUNDATION ANALYSIS AND DESIGN TOOLS
MFAD VERSION 5.1.20

Project Name:	**PMT Tests**	**Checked By:**	_____
Responsible Engineer:	**A Evans**		
Last Modified Date:	**06/25/2018 06:49:36**	**Date:**	_____
Comments:			

STRUCTURE

Structure ID: PM 6
Description: Str 84

CASE-DRILLED SHAFT

Case Name: Foundation Estimate
Description: Str PM 6

Foundation Data (Str 84)

Diameter of Drilled Shaft: [ft]	**6**
Stick up above Ground Level: [ft]	**2**

Model Options

Side Shear Spring:	**On**
Base Shear Spring:	**On**
Base Moment Spring:	**On**

Geotechnical Parameters (DIN-ABL 3B 0 ft Est)
Depth to Ground Water: [ft] **50**
All values in table are Nominal Values

Layer No.	Layer Type	Depth to Bottom of Layer [ft]	Total Unit Weight [pcf]	Deformation Modulus [ksi]	Friction Angle [Deg]	Undrained Shear Strength or Rock Cohesion [ksf]	Rock / Concrete Bond Strength [ksf]
1	Soil	17.00	105.0	1.50	34	0.30	0
2	Soil	30.00	127.0	5.00	45	0.00	0

Applied Loads-Top of Shaft (Str 84 x 1.1)

Load Case No.	Load Case Name	Shear Load [kips]	Moment [kip-ft]	Axial Load [kips]	Eccentricity [ft]
1	Str 84	64.35	6409.7	176.55	101.61

FADTOOLS
Project Name: **PMT Tests**
Structure ID: **PM 6**
Case Name: **Foundation Estimate**

DESIGN RESULTS

Diameter of Drilled Shaft: [ft]	**6**
Stick up above Ground Level: [ft]	**2**
Depth of Embedment: [ft]	**20**
Total Foundation Length: [ft]	**22**
Controlling Applied Load Case Name:	**Str 84**

Capacity Verification

Loading Mode	Applied Load at Top of Shaft	Applied Load at Groundline	Nominal Capacity at Groundline	Design Capacity at Groundline*	Design Capacity / Applied Load at Groundline
Shear Load [kips]	64.35	64.35	134.68	84.85	1.32
Moment [kip-ft]	6409.70	6538.40	13684.08	8620.97	1.32

Design Capacity is based on a Strength Factor of 0.63

Performance Verification

	Criteria at Groundline	Actual at Groundline	Actual at Top of Shaft
Total Displacement [in]		1.75	1.97
Total Rotation [deg.]	1	0.53	0.53
Nonrecoverable Displacement [in]		0.53	0.60
Nonrecoverable Rotation [deg.]	0.5	0.15	0.15

Maximum Internal Forces

	Maximum Value	Depth of Occurrence
Shear:	459.92 kips	15.60 ft
Moment:	6568.79 kips-ft	1.30 ft

Summary of Results for Controlling Applied Load Case

Depth [ft]	Displacement [in]	Shear Force [kips]	Flexural Moment [kips-ft]	Lateral Pressure [ksf]
Top of Stick (-2)	1.97	64.35	6409.70	0.00
-1	1.86	64.35	6474.05	0.00
Ground Level (0)	1.75	64.35	6538.40	0.00
1	1.64	44.44	6566.61	3.98
2	1.53	15.65	6560.67	5.47
3	1.41	-22.16	6518.24	6.99
4	1.30	-69.17	6433.42	8.53
5	1.19	-123.20	6297.39	8.90
6	1.08	-174.39	6108.34	8.23
7	0.97	-221.63	5870.07	7.58
8	0.85	-264.91	5586.56	6.92
9	0.74	-304.25	5261.73	6.26
10	0.63	-339.66	4899.53	5.61
11	0.52	-371.16	4503.87	4.96
12	0.41	-398.76	4078.67	4.31
13	0.29	-422.48	3627.81	3.66

FADTOOLS
Project Name: **PMT Tests**
Structure ID: **PM 6**
Case Name: **Foundation Estimate**

Depth [ft]	Displacement [in]	Shear Force [kips]	Flexural Moment [kips-ft]	Lateral Pressure [ksf]
14	0.18	-442.36	3155.15	3.03
15	0.07	-457.12	2664.74	1.61
16	-0.04	-458.95	2165.61	-0.76
17	-0.15	-446.62	1671.75	-3.05
18	-0.27	-396.13	1115.85	-9.73
19	-0.38	-328.16	619.18	-12.64
20	-0.49	-242.70	199.23	-15.56

Detailed Message:

FOUNDATION ANALYSIS AND DESIGN TOOLS
MFAD VERSION 5.1.20

Project Name:	**PMT Tests**	**Checked By:**	_____
Responsible Engineer:	**A Evans**		
Last Modified Date:	**06/25/2018 06:49:23**	**Date:**	_____
Comments:			

STRUCTURE

Structure ID: PM 6
Description: Str 84

CASE-DRILLED SHAFT

Case Name: Foundation
Description: Str 84

Foundation Data (Str 84)
Diameter of Drilled Shaft: [ft] 6
Stick up above Ground Level: [ft] 2

Model Options
Side Shear Spring: On
Base Shear Spring: On
Base Moment Spring: On

Geotechnical Parameters (DIN-ABL 3B 0 ft)
Depth to Ground Water: [ft] 50
All values in table are Nominal Values

Layer No.	Layer Type	Depth to Bottom of Layer [ft]	Total Unit Weight [pcf]	Deformation Modulus [ksi]	Friction Angle [Deg]	Undrained Shear Strength or Rock Cohesion [ksf]	Rock / Concrete Bond Strength [ksf]
1	Soil	17.00	105.0	1.10	34	0.30	0
2	Soil	30.00	127.0	5.00	45	0.00	0

Applied Loads-Top of Shaft (Str 84 x 1.1)

Load Case No.	Load Case Name	Shear Load [kips]	Moment [kip-ft]	Axial Load [kips]	Eccentricity [ft]
1	Str 84	64.35	6409.7	176.55	101.61

FADTOOLS
Project Name: **PMT Tests**
Structure ID: **PM 6**
Case Name: **Foundation**

DESIGN RESULTS

Diameter of Drilled Shaft: [ft]	**6**
Stick up above Ground Level: [ft]	**2**
Depth of Embedment: [ft]	**20**
Total Foundation Length: [ft]	**22**
Controlling Applied Load Case Name:	**Str 84**

Capacity Verification

Loading Mode	Applied Load at Top of Shaft	Applied Load at Groundline	Nominal Capacity at Groundline	Design Capacity at Groundline*	Design Capacity / Applied Load at Groundline
Shear Load [kips]	64.35	64.35	134.68	84.85	1.32
Moment [kip-ft]	6409.70	6538.40	13684.08	8620.97	1.32

Design Capacity is based on a Strength Factor of 0.63

Performance Verification

	Criteria at Groundline	Actual at Groundline	Actual at Top of Shaft
Total Displacement [in]		2.22	2.49
Total Rotation [deg.]	1	0.64	0.64
Nonrecoverable Displacement [in]		0.67	0.75
Nonrecoverable Rotation [deg.]	0.5	0.19	0.19

Maximum Internal Forces

	Maximum Value	Depth of Occurrence
Shear:	462.17 kips	16.20 ft
Moment:	6568.82 kips-ft	1.30 ft

Summary of Results for Controlling Applied Load Case

Depth [ft]	Displacement [in]	Shear Force [kips]	Flexural Moment [kips-ft]	Lateral Pressure [ksf]
Top of Stick (-2)	2.49	64.35	6409.70	0.00
-1	2.36	64.35	6474.05	0.00
Ground Level (0)	2.22	64.35	6538.40	0.00
1	2.08	44.46	6566.63	3.98
2	1.94	15.69	6562.42	5.47
3	1.81	-22.09	6524.19	6.98
4	1.67	-69.06	6443.60	8.52
5	1.53	-121.06	6312.57	8.44
6	1.40	-169.78	6131.08	7.86
7	1.26	-215.01	5902.62	7.28
8	1.12	-256.78	5630.66	6.70
9	0.99	-295.08	5318.66	6.12
10	0.85	-329.93	4970.10	5.55
11	0.71	-361.34	4588.40	4.98
12	0.58	-389.33	4177.00	4.41
13	0.44	-413.91	3739.32	3.84

FADTOOLS
Project Name: **PMT Tests**
Structure ID: **PM 6**
Case Name: **Foundation**

Depth [ft]	Displacement [in]	Shear Force [kips]	Flexural Moment [kips-ft]	Lateral Pressure [ksf]
14	0.30	-435.11	3278.75	3.28
15	0.16	-452.93	2798.66	2.66
16	0.03	-461.90	2304.42	0.54
17	-0.11	-458.15	1807.57	-1.58
18	-0.25	-412.22	1208.01	-9.23
19	-0.38	-345.32	664.89	-12.72
20	-0.52	-257.50	199.12	-16.21

Detailed Message:

FOUNDATION ANALYSIS AND DESIGN TOOLS
MFAD VERSION 5.1.20

Project Name:	**PMT Tests**	**Checked By:**	_____
Responsible Engineer:	**A Evans**		
Last Modified Date:	**06/25/2018 06:54:08**	**Date:**	_____
Comments:			

STRUCTURE

Structure ID: P-88
Description: Str 88

CASE-DRILLED SHAFT

Case Name: Foundation Estimate
Description: Str 88

Foundation Data (Str P-88)
Diameter of Drilled Shaft: [ft] 7
Stick up above Ground Level: [ft] 3

Model Options
Side Shear Spring: On
Base Shear Spring: On
Base Moment Spring: On

Geotechnical Parameters (1A/1B/1D Est)
Depth to Ground Water: [ft] 50
All values in table are Nominal Values

Layer No.	Layer Type	Depth to Bottom of Layer [ft]	Total Unit Weight [pcf]	Deformation Modulus [ksi]	Friction Angle [Deg]	Undrained Shear Strength or Rock Cohesion [ksf]	Rock / Concrete Bond Strength [ksf]
1	Soil	6.00	107.0	3.70	33	0.65	0
2	Soil	19.00	114.0	4.10	40	0.55	0
3	Soil	24.00	113.0	4.10	45	0.30	0

Applied Loads-Top of Shaft (Str 88 x 1.1)

Load Case No.	Load Case Name	Shear Load [kips]	Moment [kip-ft]	Axial Load [kips]	Eccentricity [ft]
1	Str 88	48.29	5302.33	139.59	112.80

FADTOOLS
Project Name: **PMT Tests**
Structure ID: **P-88**
Case Name: **Foundation Estimate**

DESIGN RESULTS

Diameter of Drilled Shaft: [ft]	**7**
Stick up above Ground Level: [ft]	**3**
Depth of Embedment: [ft]	**17**
Total Foundation Length: [ft]	**20**
Controlling Applied Load Case Name:	**Str 88**

Capacity Verification

Loading Mode	Applied Load at Top of Shaft	Applied Load at Groundline	Nominal Capacity at Groundline	Design Capacity at Groundline*	Design Capacity / Applied Load at Groundline
Shear Load [kips]	48.29	48.29	157.56	99.26	2.06
Moment [kip-ft]	5302.33	5447.20	17772.67	11196.78	2.06

Design Capacity is based on a Strength Factor of 0.63

Performance Verification

	Criteria at Groundline	Actual at Groundline	Actual at Top of Shaft
Total Displacement [in]		0.57	0.72
Total Rotation [deg.]	1	0.24	0.24
Nonrecoverable Displacement [in]		0.11	0.13
Nonrecoverable Rotation [deg.]	0.5	0.04	0.04

Maximum Internal Forces

	Maximum Value	Depth of Occurrence
Shear:	395.87 kips	11.10 ft
Moment:	5447.20 kips-ft	0.00 ft

Summary of Results for Controlling Applied Load Case

Depth [ft]	Displacement [in]	Shear Force [kips]	Flexural Moment [kips-ft]	Lateral Pressure [ksf]
Top of Stick (-3)	0.72	48.29	5302.33	0.00
-2	0.67	48.29	5350.62	0.00
-1	0.62	48.29	5398.91	0.00
Ground Level (0)	0.57	48.29	5447.20	0.00
1	0.51	4.02	5413.39	7.22
2	0.46	-52.73	5328.55	8.30
3	0.41	-108.07	5186.63	7.59
4	0.36	-158.46	4991.84	6.88
5	0.31	-203.88	4749.14	6.17
6	0.26	-244.34	4463.51	5.46
7	0.21	-286.81	4129.81	5.75
8	0.16	-324.35	3756.10	5.05
9	0.11	-357.02	3347.30	4.36
10	0.05	-384.38	2908.28	3.21
11	0.00	-395.83	2448.80	0.34
12	-0.05	-387.18	1987.92	-2.53

FADTOOLS
Project Name: **PMT Tests**
Structure ID: **P-88**
Case Name: **Foundation Estimate**

Depth [ft]	Displacement [in]	Shear Force [kips]	Flexural Moment [kips-ft]	Lateral Pressure [ksf]
13	-0.10	-358.93	1545.67	-5.00
14	-0.15	-319.32	1138.14	-6.19
15	-0.20	-271.40	774.37	-7.38
16	-0.25	-215.16	462.68	-8.57
17	-0.30	-150.61	211.39	-9.76

Detailed Message:

FOUNDATION ANALYSIS AND DESIGN TOOLS
MFAD VERSION 5.1.20

Project Name:	**PMT Tests**	**Checked By:**	_____
Responsible Engineer:	**A Evans**		
Last Modified Date:	**06/25/2018 06:53:48**	**Date:**	_____
Comments:			

STRUCTURE

Structure ID: P-88
Description: Str 88

CASE-DRILLED SHAFT

Case Name: Foundation
Description: Str 88

Foundation Data (Str P-88)
Diameter of Drilled Shaft: [ft] 7
Stick up above Ground Level: [ft] 3

Model Options
Side Shear Spring: On
Base Shear Spring: On
Base Moment Spring: On

Geotechnical Parameters (1A/1B/1D)
Depth to Ground Water: [ft] 50
All values in table are Nominal Values

Layer No.	Layer Type	Depth to Bottom of Layer [ft]	Total Unit Weight [pcf]	Deformation Modulus [ksi]	Friction Angle [Deg]	Undrained Shear Strength or Rock Cohesion [ksf]	Rock / Concrete Bond Strength [ksf]
1	Soil	6.00	107.0	5.20	33	0.65	0
2	Soil	19.00	114.0	5.55	40	0.55	0
3	Soil	24.00	113.0	3.00	45	0.30	0

Applied Loads-Top of Shaft (Str 88 x 1.1)

Load Case No.	Load Case Name	Shear Load [kips]	Moment [kip-ft]	Axial Load [kips]	Eccentricity [ft]
1	Str 88	48.29	5302.33	139.59	112.80

FADTOOLS
Project Name: **PMT Tests**
Structure ID: **P-88**
Case Name: **Foundation**

DESIGN RESULTS

Diameter of Drilled Shaft: [ft]	**7**
Stick up above Ground Level: [ft]	**3**
Depth of Embedment: [ft]	**17**
Total Foundation Length: [ft]	**20**
Controlling Applied Load Case Name:	**Str 88**

Capacity Verification

Loading Mode	Applied Load at Top of Shaft	Applied Load at Groundline	Nominal Capacity at Groundline	Design Capacity at Groundline*	Design Capacity / Applied Load at Groundline
Shear Load [kips]	48.29	48.29	157.56	99.26	2.06
Moment [kip-ft]	5302.33	5447.20	17772.67	11196.78	2.06

Design Capacity is based on a Strength Factor of 0.63

Performance Verification

	Criteria at Groundline	Actual at Groundline	Actual at Top of Shaft
Total Displacement [in]		0.41	0.52
Total Rotation [deg.]	1	0.17	0.17
Nonrecoverable Displacement [in]		0.08	0.10
Nonrecoverable Rotation [deg.]	0.5	0.03	0.03

Maximum Internal Forces

	Maximum Value	Depth of Occurrence
Shear:	395.11 kips	11.00 ft
Moment:	5447.20 kips-ft	0.00 ft

Summary of Results for Controlling Applied Load Case

Depth [ft]	Displacement [in]	Shear Force [kips]	Flexural Moment [kips-ft]	Lateral Pressure [ksf]
Top of Stick (-3)	0.52	48.29	5302.33	0.00
-2	0.48	48.29	5350.62	0.00
-1	0.45	48.29	5398.91	0.00
Ground Level (0)	0.41	48.29	5447.20	0.00
1	0.37	3.98	5412.18	7.22
2	0.34	-53.14	5325.91	8.42
3	0.30	-109.31	5181.84	7.70
4	0.26	-160.39	4984.15	6.97
5	0.22	-206.38	4737.93	6.24
6	0.19	-247.28	4448.25	5.52
7	0.15	-289.00	4113.08	5.65
8	0.11	-325.90	3738.61	4.96
9	0.08	-358.03	3329.63	4.29
10	0.04	-384.72	2890.95	3.04
11	0.00	-395.11	2432.78	0.21
12	-0.04	-385.73	1974.10	-2.61

FADTOOLS
Project Name: **PMT Tests**
Structure ID: **P-88**
Case Name: **Foundation**

Depth [ft]	Displacement [in]	Shear Force [kips]	Flexural Moment [kips-ft]	Lateral Pressure [ksf]
13	-0.07	-357.13	1534.63	-5.02
14	-0.11	-317.48	1130.01	-6.19
15	-0.15	-269.62	769.16	-7.36
16	-0.18	-213.56	460.27	-8.54
17	-0.22	-149.27	211.55	-9.71

Detailed Message:

FOUNDATION ANALYSIS AND DESIGN TOOLS
MFAD VERSION 5.1.20

Project Name:	**PMT Tests**	**Checked By:**	_____
Responsible Engineer:	**A Evans**		
Last Modified Date:	**06/25/2018 06:49:09**	**Date:**	_____
Comments:			

STRUCTURE

Structure ID: PM 5
Description: Str 89

CASE-DRILLED SHAFT

Case Name: Foundation Estimate
Description: Str 89

Foundation Data (Str 89)

Diameter of Drilled Shaft: [ft]	**6**
Stick up above Ground Level: [ft]	**2**

Model Options

Side Shear Spring:	**On**
Base Shear Spring:	**On**
Base Moment Spring:	**On**

Geotechnical Parameters (DIN-ABL 3B -2 ft Est)
Depth to Ground Water: [ft] **50**
All values in table are Nominal Values

Layer No.	Layer Type	Depth to Bottom of Layer [ft]	Total Unit Weight [pcf]	Deformation Modulus [ksi]	Friction Angle [Deg]	Undrained Shear Strength or Rock Cohesion [ksf]	Rock / Concrete Bond Strength [ksf]
1	Soil	15.00	105.0	3.60	34	0.30	0
2	Soil	28.00	127.0	5.00	45	0.00	0

Applied Loads-Top of Shaft (Str 89 x 1.1)

Load Case No.	Load Case Name	Shear Load [kips]	Moment [kip-ft]	Axial Load [kips]	Eccentricity [ft]
1	Str 89	65.12	6771.6	178.42	105.99

FADTOOLS
Project Name: **PMT Tests**
Structure ID: **PM 5**
Case Name: **Foundation Estimate**

DESIGN RESULTS

Diameter of Drilled Shaft: [ft]	**6**
Stick up above Ground Level: [ft]	**2**
Depth of Embedment: [ft]	**22**
Total Foundation Length: [ft]	**24**
Controlling Applied Load Case Name:	**Str 89**

Capacity Verification

Loading Mode	Applied Load at Top of Shaft	Applied Load at Groundline	Nominal Capacity at Groundline	Design Capacity at Groundline*	Design Capacity / Applied Load at Groundline
Shear Load [kips]	65.12	65.12	179.02	112.78	1.73
Moment [kip-ft]	6771.60	6901.84	18973.81	11953.50	1.73

Design Capacity is based on a Strength Factor of 0.63

Performance Verification

	Criteria at Groundline	Actual at Groundline	Actual at Top of Shaft
Total Displacement [in]		0.76	0.85
Total Rotation [deg.]	1	0.23	0.23
Nonrecoverable Displacement [in]		0.22	0.25
Nonrecoverable Rotation [deg.]	0.5	0.07	0.07

Maximum Internal Forces

	Maximum Value	Depth of Occurrence
Shear:	449.65 kips	15.40 ft
Moment:	6933.13 kips-ft	1.40 ft

Summary of Results for Controlling Applied Load Case

Depth [ft]	Displacement [in]	Shear Force [kips]	Flexural Moment [kips-ft]	Lateral Pressure [ksf]
Top of Stick (-2)	0.85	65.12	6771.60	0.00
-1	0.80	65.12	6836.72	0.00
Ground Level (0)	0.76	65.12	6901.84	0.00
1	0.71	45.15	6930.72	3.99
2	0.66	16.26	6925.13	5.49
3	0.61	-21.68	6881.18	7.01
4	0.56	-68.85	6794.70	8.56
5	0.51	-122.69	6656.94	8.82
6	0.46	-173.39	6466.59	8.15
7	0.41	-220.08	6227.53	7.48
8	0.36	-262.76	5943.79	6.81
9	0.31	-301.45	5619.37	6.15
10	0.26	-336.16	5258.25	5.49
11	0.22	-366.90	4864.41	4.83
12	0.17	-393.70	4441.79	4.17
13	0.12	-416.58	3994.34	3.52

FADTOOLS
Project Name: **PMT Tests**
Structure ID: **PM 5**
Case Name: **Foundation Estimate**

Depth [ft]	Displacement [in]	Shear Force [kips]	Flexural Moment [kips-ft]	Lateral Pressure [ksf]
14	0.07	-435.59	3525.95	2.88
15	0.02	-448.07	3041.11	1.07
16	-0.03	-446.01	2534.10	-1.84
17	-0.08	-423.98	2039.14	-5.17
18	-0.13	-388.12	1574.06	-6.62
19	-0.18	-343.65	1149.15	-8.06
20	-0.23	-290.56	773.01	-9.50
21	-0.28	-228.82	454.29	-10.94
22	-0.32	-158.38	201.65	-12.39

Detailed Message:

FOUNDATION ANALYSIS AND DESIGN TOOLS
MFAD VERSION 5.1.20

Project Name:	**PMT Tests**	**Checked By:**	_____
Responsible Engineer:	**A Evans**		
Last Modified Date:	**06/25/2018 06:48:53**	**Date:**	_____
Comments:			

STRUCTURE

Structure ID: PM 5
Description: Str 89

CASE-DRILLED SHAFT

Case Name: Fondation
Description: Str 89

Foundation Data (Str 89)

Diameter of Drilled Shaft: [ft]	**6**
Stick up above Ground Level: [ft]	**2**

Model Options

Side Shear Spring:	**On**
Base Shear Spring:	**On**
Base Moment Spring:	**On**

Geotechnical Parameters (DIN-ABL 3B -2 ft)
Depth to Ground Water: [ft] **50**
All values in table are Nominal Values

Layer No.	Layer Type	Depth to Bottom of Layer [ft]	Total Unit Weight [pcf]	Deformation Modulus [ksi]	Friction Angle [Deg]	Undrained Shear Strength or Rock Cohesion [ksf]	Rock / Concrete Bond Strength [ksf]
1	Soil	15.00	105.0	2.50	34	0.30	0
2	Soil	28.00	127.0	5.00	45	0.00	0

Applied Loads-Top of Shaft (Str 89 x 1.1)

Load Case No.	Load Case Name	Shear Load [kips]	Moment [kip-ft]	Axial Load [kips]	Eccentricity [ft]
1	Str 89	65.12	6771.6	178.42	105.99

FADTOOLS
Project Name: **PMT Tests**
Structure ID: **PM 5**
Case Name: **Fondation**

DESIGN RESULTS

Diameter of Drilled Shaft: [ft]	**6**
Stick up above Ground Level: [ft]	**2**
Depth of Embedment: [ft]	**22**
Total Foundation Length: [ft]	**24**
Controlling Applied Load Case Name:	**Str 89**

Capacity Verification

Loading Mode	Applied Load at Top of Shaft	Applied Load at Groundline	Nominal Capacity at Groundline	Design Capacity at Groundline*	Design Capacity / Applied Load at Groundline
Shear Load [kips]	65.12	65.12	179.02	112.78	1.73
Moment [kip-ft]	6771.60	6901.84	18973.81	11953.50	1.73

Design Capacity is based on a Strength Factor of 0.63

Performance Verification

	Criteria at Groundline	Actual at Groundline	Actual at Top of Shaft
Total Displacement [in]		0.97	1.09
Total Rotation [deg.]	1	0.28	0.28
Nonrecoverable Displacement [in]		0.27	0.30
Nonrecoverable Rotation [deg.]	0.5	0.08	0.08

Maximum Internal Forces

	Maximum Value	Depth of Occurrence
Shear:	452.56 kips	16.10 ft
Moment:	6933.12 kips-ft	1.40 ft

Summary of Results for Controlling Applied Load Case

Depth [ft]	Displacement [in]	Shear Force [kips]	Flexural Moment [kips-ft]	Lateral Pressure [ksf]
Top of Stick (-2)	1.09	65.12	6771.60	0.00
-1	1.03	65.12	6836.72	0.00
Ground Level (0)	0.97	65.12	6901.84	0.00
1	0.91	45.15	6930.72	3.99
2	0.85	16.28	6927.00	5.49
3	0.79	-21.66	6889.12	7.01
4	0.73	-68.81	6808.71	8.56
5	0.67	-118.98	6678.60	8.11
6	0.61	-165.80	6499.99	7.55
7	0.55	-209.27	6276.24	6.99
8	0.49	-249.41	6010.68	6.44
9	0.43	-286.22	5706.65	5.89
10	0.37	-319.73	5367.46	5.34
11	0.31	-349.94	4996.41	4.79
12	0.25	-376.87	4596.79	4.24
13	0.19	-400.53	4171.88	3.70

FADTOOLS
Project Name: **PMT Tests**
Structure ID: **PM 5**
Case Name: **Fondation**

Depth [ft]	Displacement [in]	Shear Force [kips]	Flexural Moment [kips-ft]	Lateral Pressure [ksf]
14	0.13	-420.95	3724.93	3.16
15	0.07	-437.93	3259.17	2.34
16	0.01	-452.46	2740.06	0.57
17	-0.06	-442.37	2218.73	-3.53
18	-0.12	-410.15	1719.30	-6.34
19	-0.18	-366.55	1258.23	-8.03
20	-0.24	-312.80	845.83	-9.72
21	-0.30	-248.88	492.27	-11.42
22	-0.36	-174.74	207.73	-13.12

Detailed Message:

FOUNDATION ANALYSIS AND DESIGN TOOLS
MFAD VERSION 5.1.20

Project Name:	**PMT Tests**	**Checked By:**	_____
Responsible Engineer:	**A Evans**		
Last Modified Date:	**06/25/2018 06:48:38**	**Date:**	_____
Comments:			

STRUCTURE

Structure ID: PM 4
Description: Str 90

CASE-DRILLED SHAFT

Case Name: Foundation Estimate
Description: Str 90

Foundation Data (Str 90)
Diameter of Drilled Shaft: [ft] 7
Stick up above Ground Level: [ft] 5

Model Options
Side Shear Spring: On
Base Shear Spring: On
Base Moment Spring: On

Geotechnical Parameters (DIN-ABL 3B -3 ft Est)
Depth to Ground Water: [ft] 50
All values in table are Nominal Values

Layer No.	Layer Type	Depth to Bottom of Layer [ft]	Total Unit Weight [pcf]	Deformation Modulus [ksi]	Friction Angle [Deg]	Undrained Shear Strength or Rock Cohesion [ksf]	Rock / Concrete Bond Strength [ksf]
1	Soil	14.00	105.0	1.40	34	0.30	0
2	Soil	27.00	127.0	5.10	45	0.00	0

Applied Loads-Top of Shaft (Str 90 x 1.15)

Load Case No.	Load Case Name	Shear Load [kips]	Moment [kip-ft]	Axial Load [kips]	Eccentricity [ft]
1	DIN-ABL 3B	108.445	14030.805	119.14	134.38

FADTOOLS
Project Name: **PMT Tests**
Structure ID: **PM 4**
Case Name: **Foundation Estimate**

DESIGN RESULTS

Diameter of Drilled Shaft: [ft]	**7**
Stick up above Ground Level: [ft]	**5**
Depth of Embedment: [ft]	**26.5**
Total Foundation Length: [ft]	**31.5**
Controlling Applied Load Case Name:	**DIN-ABL 3B**

Capacity Verification

Loading Mode	Applied Load at Top of Shaft	Applied Load at Groundline	Nominal Capacity at Groundline	Design Capacity at Groundline*	Design Capacity / Applied Load at Groundline
Shear Load [kips]	108.45	108.45	300.31	189.19	1.74
Moment [kip-ft]	14030.81	14573.03	40355.68	25424.08	1.74

Design Capacity is based on a Strength Factor of 0.63

Performance Verification

	Criteria at Groundline	Actual at Groundline	Actual at Top of Shaft
Total Displacement [in]		2.08	2.62
Total Rotation [deg.]	1	0.50	0.50
Nonrecoverable Displacement [in]		0.64	0.80
Nonrecoverable Rotation [deg.]	0.5	0.16	0.16

Maximum Internal Forces

	Maximum Value	Depth of Occurrence
Shear:	866.29 kips	19.60 ft
Moment:	14657.85 kips-ft	2.10 ft

Summary of Results for Controlling Applied Load Case

Depth [ft]	Displacement [in]	Shear Force [kips]	Flexural Moment [kips-ft]	Lateral Pressure [ksf]
Top of Stick (-5)	2.62	108.45	14030.81	0.00
-4	2.51	108.45	14139.25	0.00
-3	2.40	108.45	14247.70	0.00
-2	2.30	108.45	14356.14	0.00
-1	2.19	108.45	14464.59	0.00
Ground Level (0)	2.08	108.45	14573.03	0.00
1	1.98	85.52	14634.49	3.89
2	1.87	52.97	14657.56	5.28
3	1.76	10.61	14641.98	6.69
4	1.66	-41.75	14579.06	8.13
5	1.55	-102.76	14458.95	8.78
6	1.45	-162.45	14277.90	8.32
7	1.34	-218.95	14038.75	7.87
8	1.23	-272.29	13744.68	7.42
9	1.13	-322.47	13398.85	6.97
10	1.02	-369.51	13004.41	6.52

FADTOOLS
Project Name: **PMT Tests**
Structure ID: **PM 4**
Case Name: **Foundation Estimate**

Depth [ft]	Displacement [in]	Shear Force [kips]	Flexural Moment [kips-ft]	Lateral Pressure [ksf]
11	0.91	-413.43	12564.50	6.07
12	0.81	-454.22	12082.23	5.63
13	0.70	-491.90	11560.73	5.18
14	0.59	-526.49	11003.09	4.74
15	0.49	-617.61	10254.50	12.23
16	0.38	-696.57	9420.88	10.50
17	0.27	-763.43	8514.34	8.78
18	0.17	-818.25	7546.98	7.06
19	0.06	-858.98	6531.05	3.92
20	-0.04	-862.44	5491.20	-2.31
21	-0.15	-823.64	4469.55	-7.51
22	-0.26	-761.93	3499.86	-9.88
23	-0.36	-683.62	2600.17	-12.26
24	-0.47	-588.65	1787.12	-14.64
25	-0.58	-476.96	1077.40	-17.03
26	-0.68	-348.49	487.75	-19.43
26.5	-0.74	-277.95	243.20	-20.64

Detailed Message:

FOUNDATION ANALYSIS AND DESIGN TOOLS
MFAD VERSION 5.1.20

Project Name:	**PMT Tests**	**Checked By:**	_____
Responsible Engineer:	**A Evans**		
Last Modified Date:	**06/25/2018 06:48:22**	**Date:**	_____
Comments:			

STRUCTURE

Structure ID: PM 4
Description: Str 90

CASE-DRILLED SHAFT

Case Name: Foundation
Description: Str 90

Foundation Data (Str 90)
Diameter of Drilled Shaft: [ft] 7
Stick up above Ground Level: [ft] 5

Model Options
Side Shear Spring: On
Base Shear Spring: On
Base Moment Spring: On

Geotechnical Parameters (DIN-ABL 3B -3 ft)
Depth to Ground Water: [ft] 50
All values in table are Nominal Values

Layer No.	Layer Type	Depth to Bottom of Layer [ft]	Total Unit Weight [pcf]	Deformation Modulus [ksi]	Friction Angle [Deg]	Undrained Shear Strength or Rock Cohesion [ksf]	Rock / Concrete Bond Strength [ksf]
1	Soil	14.00	105.0	4.00	34	0.30	0
2	Soil	27.00	127.0	3.50	45	0.00	0

Applied Loads-Top of Shaft (Str 90 x 1.15)

Load Case No.	Load Case Name	Shear Load [kips]	Moment [kip-ft]	Axial Load [kips]	Eccentricity [ft]
1	DIN-ABL 3B	108.445	14030.805	119.14	134.38

FADTOOLS
Project Name: **PMT Tests**
Structure ID: **PM 4**
Case Name: **Foundation**

DESIGN RESULTS

Diameter of Drilled Shaft: [ft]	**7**
Stick up above Ground Level: [ft]	**5**
Depth of Embedment: [ft]	**26.5**
Total Foundation Length: [ft]	**31.5**
Controlling Applied Load Case Name:	**DIN-ABL 3B**

Capacity Verification

Loading Mode	Applied Load at Top of Shaft	Applied Load at Groundline	Nominal Capacity at Groundline	Design Capacity at Groundline*	Design Capacity / Applied Load at Groundline
Shear Load [kips]	108.45	108.45	300.31	189.19	1.74
Moment [kip-ft]	14030.81	14573.03	40355.68	25424.08	1.74

Design Capacity is based on a Strength Factor of 0.63

Performance Verification

	Criteria at Groundline	Actual at Groundline	Actual at Top of Shaft
Total Displacement [in]		1.31	1.68
Total Rotation [deg.]	1	0.35	0.35
Nonrecoverable Displacement [in]		0.46	0.58
Nonrecoverable Rotation [deg.]	0.5	0.12	0.12

Maximum Internal Forces

	Maximum Value	Depth of Occurrence
Shear:	816.98 kips	17.60 ft
Moment:	14655.13 kips-ft	1.90 ft

Summary of Results for Controlling Applied Load Case

Depth [ft]	Displacement [in]	Shear Force [kips]	Flexural Moment [kips-ft]	Lateral Pressure [ksf]
Top of Stick (-5)	1.68	108.45	14030.81	0.00
-4	1.61	108.45	14139.25	0.00
-3	1.53	108.45	14247.70	0.00
-2	1.46	108.45	14356.14	0.00
-1	1.38	108.45	14464.59	0.00
Ground Level (0)	1.31	108.45	14573.03	0.00
1	1.24	85.41	14634.37	3.91
2	1.16	52.69	14655.09	5.30
3	1.09	10.09	14625.17	6.73
4	1.01	-42.57	14534.41	8.18
5	0.94	-105.48	14372.39	9.65
6	0.86	-178.84	14135.00	11.16
7	0.79	-262.83	13818.95	12.69
8	0.72	-347.91	13416.90	11.70
9	0.64	-425.97	12933.28	10.70
10	0.57	-497.04	12375.10	9.70

FADTOOLS
Project Name: **PMT Tests**
Structure ID: **PM 4**
Case Name: **Foundation**

Depth [ft]	Displacement [in]	Shear Force [kips]	Flexural Moment [kips-ft]	Lateral Pressure [ksf]
11	0.49	-561.13	11749.33	8.71
12	0.42	-618.24	11062.97	7.71
13	0.34	-668.41	10322.97	6.72
14	0.27	-711.66	9536.26	5.73
15	0.20	-752.52	8719.70	5.54
16	0.12	-788.82	7864.58	4.91
17	0.05	-812.69	6978.01	2.07
18	-0.03	-815.67	6078.02	-0.92
19	-0.10	-797.76	5185.49	-3.90
20	-0.18	-759.33	4321.29	-6.55
21	-0.25	-708.36	3502.59	-7.88
22	-0.32	-648.10	2739.50	-9.21
23	-0.40	-578.54	2041.33	-10.54
24	-0.47	-499.66	1417.37	-11.87
25	-0.55	-411.40	876.98	-13.21
26	-0.62	-313.71	429.55	-14.56
26.5	-0.66	-261.32	243.66	-15.24

Detailed Message:

FOUNDATION ANALYSIS AND DESIGN TOOLS
MFAD VERSION 5.1.20

Project Name:	**PMT Tests**	**Checked By:**	_____
Responsible Engineer:	**A Evans**		
Last Modified Date:	**06/25/2018 06:51:26**	**Date:**	_____
Comments:			

STRUCTURE

Structure ID: P-123
Description: Str 123

CASE-DRILLED SHAFT

Case Name: Foundation Estimate
Description: Str 123

Foundation Data (Str P-123)

Diameter of Drilled Shaft: [ft]	**7**
Stick up above Ground Level: [ft]	**2**

Model Options

Side Shear Spring:	**On**
Base Shear Spring:	**On**
Base Moment Spring:	**On**

Geotechnical Parameters (3A Est)

Depth to Ground Water: [ft] **50**

All values in table are Nominal Values

Layer No.	Layer Type	Depth to Bottom of Layer [ft]	Total Unit Weight [pcf]	Deformation Modulus [ksi]	Friction Angle [Deg]	Undrained Shear Strength or Rock Cohesion [ksf]	Rock / Concrete Bond Strength [ksf]
1	Soil	4.00	105.0	6.10	35	1.00	0
2	Soil	10.00	106.0	9.70	45	1.00	0
3	Soil	20.00	108.0	10.00	53	0.50	0
4	Soil	25.00	106.0	2.20	36	0.40	0

Applied Loads-Top of Shaft (Str 123 x 1.1)

Load Case No.	Load Case Name	Shear Load [kips]	Moment [kip-ft]	Axial Load [kips]	Eccentricity [ft]
1	Str 123	61.27	6643.12	178.53	110.42

FADTOOLS
Project Name: **PMT Tests**
Structure ID: **P-123**
Case Name: **Foundation Estimate**

DESIGN RESULTS

Diameter of Drilled Shaft: [ft]	**7**
Stick up above Ground Level: [ft]	**2**
Depth of Embedment: [ft]	**14**
Total Foundation Length: [ft]	**16**
Controlling Applied Load Case Name:	**Str 123**

Capacity Verification

Loading Mode	Applied Load at Top of Shaft	Applied Load at Groundline	Nominal Capacity at Groundline	Design Capacity at Groundline*	Design Capacity / Applied Load at Groundline
Shear Load [kips]	61.27	61.27	312.84	197.09	3.22
Moment [kip-ft]	6643.12	6765.66	34545.44	21763.63	3.22

Design Capacity is based on a Strength Factor of 0.63

Performance Verification

	Criteria at Groundline	Actual at Groundline	Actual at Top of Shaft
Total Displacement [in]		0.41	0.49
Total Rotation [deg.]	1	0.20	0.20
Nonrecoverable Displacement [in]		0.07	0.08
Nonrecoverable Rotation [deg.]	0.5	0.03	0.03

Maximum Internal Forces

	Maximum Value	Depth of Occurrence
Shear:	592.60 kips	9.70 ft
Moment:	6765.66 kips-ft	0.00 ft

Summary of Results for Controlling Applied Load Case

Depth [ft]	Displacement [in]	Shear Force [kips]	Flexural Moment [kips-ft]	Lateral Pressure [ksf]
Top of Stick (-2)	0.49	61.27	6643.12	0.00
-1	0.45	61.27	6704.39	0.00
Ground Level (0)	0.41	61.27	6765.66	0.00
1	0.36	-13.03	6708.95	11.55
2	0.32	-89.93	6574.46	10.53
3	0.28	-159.68	6366.64	9.50
4	0.24	-222.26	6092.65	8.48
5	0.20	-315.79	5691.71	12.69
6	0.15	-398.97	5202.42	11.22
7	0.11	-471.88	4635.09	9.76
8	0.07	-534.67	3999.92	8.33
9	0.03	-582.27	3307.94	4.51
10	-0.01	-590.72	2586.91	-1.49
11	-0.05	-556.12	1874.80	-7.73
12	-0.10	-478.20	1218.95	-13.92
13	-0.14	-362.17	661.49	-18.07

FADTOOLS
Project Name: **PMT Tests**
Structure ID: **P-123**
Case Name: **Foundation Estimate**

Depth [ft]	Displacement [in]	Shear Force [kips]	Flexural Moment [kips-ft]	Lateral Pressure [ksf]
14	-0.18	-224.26	231.45	-21.03

Detailed Message:

FOUNDATION ANALYSIS AND DESIGN TOOLS
MFAD VERSION 5.1.20

Project Name:	**PMT Tests**	**Checked By:**	_____
Responsible Engineer:	**A Evans**		
Last Modified Date:	**06/25/2018 06:51:08**	**Date:**	_____
Comments:			

STRUCTURE

Structure ID: P-123
Description: Str 123

CASE-DRILLED SHAFT

Case Name: Foundation
Description: Str 123

Foundation Data (Str P-123)

Diameter of Drilled Shaft: [ft]	**7**
Stick up above Ground Level: [ft]	**2**

Model Options

Side Shear Spring:	**On**
Base Shear Spring:	**On**
Base Moment Spring:	**On**

Geotechnical Parameters (3A)

Depth to Ground Water: [ft] **50**

All values in table are Nominal Values

Layer No.	Layer Type	Depth to Bottom of Layer [ft]	Total Unit Weight [pcf]	Deformation Modulus [ksi]	Friction Angle [Deg]	Undrained Shear Strength or Rock Cohesion [ksf]	Rock / Concrete Bond Strength [ksf]
1	Soil	4.00	105.0	8.20	35	1.00	0
2	Soil	10.00	106.0	12.50	45	1.00	0
3	Soil	20.00	108.0	5.95	53	0.50	0
4	Soil	25.00	106.0	3.10	36	0.40	0

Applied Loads-Top of Shaft (Str 123 x 1.1)

Load Case No.	Load Case Name	Shear Load [kips]	Moment [kip-ft]	Axial Load [kips]	Eccentricity [ft]
1	Str 123	61.27	6643.12	178.53	110.42

FADTOOLS
Project Name: **PMT Tests**
Structure ID: **P-123**
Case Name: **Foundation**

DESIGN RESULTS

Diameter of Drilled Shaft: [ft]	**7**
Stick up above Ground Level: [ft]	**2**
Depth of Embedment: [ft]	**14**
Total Foundation Length: [ft]	**16**
Controlling Applied Load Case Name:	**Str 123**

Capacity Verification

Loading Mode	Applied Load at Top of Shaft	Applied Load at Groundline	Nominal Capacity at Groundline	Design Capacity at Groundline*	Design Capacity / Applied Load at Groundline
Shear Load [kips]	61.27	61.27	312.84	197.09	3.22
Moment [kip-ft]	6643.12	6765.66	34545.44	21763.63	3.22

Design Capacity is based on a Strength Factor of 0.63

Performance Verification

	Criteria at Groundline	Actual at Groundline	Actual at Top of Shaft
Total Displacement [in]		0.37	0.46
Total Rotation [deg.]	1	0.20	0.20
Nonrecoverable Displacement [in]		0.05	0.06
Nonrecoverable Rotation [deg.]	0.5	0.02	0.02

Maximum Internal Forces

	Maximum Value	Depth of Occurrence
Shear:	567.30 kips	8.70 ft
Moment:	6765.66 kips-ft	0.00 ft

Summary of Results for Controlling Applied Load Case

Depth [ft]	Displacement [in]	Shear Force [kips]	Flexural Moment [kips-ft]	Lateral Pressure [ksf]
Top of Stick (-2)	0.46	61.27	6643.12	0.00
-1	0.41	61.27	6704.39	0.00
Ground Level (0)	0.37	61.27	6765.66	0.00
1	0.33	-13.38	6680.11	12.04
2	0.28	-102.62	6508.56	12.34
3	0.24	-183.32	6251.33	10.86
4	0.20	-253.62	5918.61	9.38
5	0.16	-351.10	5442.16	12.98
6	0.11	-433.94	4875.57	10.90
7	0.07	-502.28	4233.40	8.85
8	0.03	-555.24	3530.08	5.63
9	-0.01	-564.15	2792.94	-2.29
10	-0.06	-519.47	2074.40	-8.87
11	-0.10	-470.95	1494.73	-8.63
12	-0.14	-396.05	976.76	-12.40
13	-0.19	-294.78	546.88	-16.16

FADTOOLS
Project Name: **PMT Tests**
Structure ID: **P-123**
Case Name: **Foundation**

Depth [ft]	Displacement [in]	Shear Force [kips]	Flexural Moment [kips-ft]	Lateral Pressure [ksf]
14	-0.23	-169.63	230.91	-18.94

Detailed Message:

FOUNDATION ANALYSIS AND DESIGN TOOLS
MFAD VERSION 5.1.20

Project Name:	**PMT Tests**	**Checked By:**	_____
Responsible Engineer:	**A Evans**		
Last Modified Date:	**06/25/2018 06:50:47**	**Date:**	_____
Comments:			

STRUCTURE

Structure ID: P-140
Description: Str 140

CASE-DRILLED SHAFT

Case Name: Foundation Estimate
Description: Str 140

Foundation Data (Str P-140)
Diameter of Drilled Shaft: [ft] 7
Stick up above Ground Level: [ft] 3

Model Options
Side Shear Spring: On
Base Shear Spring: On
Base Moment Spring: On

Geotechnical Parameters (3B/2B Est)
Depth to Ground Water: [ft] 50
All values in table are Nominal Values

Layer No.	Layer Type	Depth to Bottom of Layer [ft]	Total Unit Weight [pcf]	Deformation Modulus [ksi]	Friction Angle [Deg]	Undrained Shear Strength or Rock Cohesion [ksf]	Rock / Concrete Bond Strength [ksf]
1	Soil	9.00	118.0	9.90	40	1.00	0
2	Soil	17.00	111.0	4.40	45	0.25	0
3	Soil	21.00	107.0	3.80	42	1.00	0
4	Soil	26.50	112.0	3.80	48	0.00	0
5	Soil	29.00	114.0	3.80	50	1.25	0

Applied Loads-Top of Shaft (Str 140 x 1.1)

Load Case No.	Load Case Name	Shear Load [kips]	Moment [kip-ft]	Axial Load [kips]	Eccentricity [ft]
1	Str 140	62.59	7647.2	185.24	125.18

FADTOOLS
Project Name: **PMT Tests**
Structure ID: **P-140**
Case Name: **Foundation Estimate**

DESIGN RESULTS

Diameter of Drilled Shaft: [ft]	**7**
Stick up above Ground Level: [ft]	**3**
Depth of Embedment: [ft]	**18**
Total Foundation Length: [ft]	**21**
Controlling Applied Load Case Name:	**Str 140**

Capacity Verification

Loading Mode	Applied Load at Top of Shaft	Applied Load at Groundline	Nominal Capacity at Groundline	Design Capacity at Groundline*	Design Capacity / Applied Load at Groundline
Shear Load [kips]	62.59	62.59	266.13	167.66	2.68
Moment [kip-ft]	7647.20	7834.97	33314.38	20988.06	2.68

Design Capacity is based on a Strength Factor of 0.63

Performance Verification

	Criteria at Groundline	Actual at Groundline	Actual at Top of Shaft
Total Displacement [in]		0.33	0.44
Total Rotation [deg.]	1	0.16	0.16
Nonrecoverable Displacement [in]		0.05	0.07
Nonrecoverable Rotation [deg.]	0.5	0.02	0.02

Maximum Internal Forces

	Maximum Value	Depth of Occurrence
Shear:	536.82 kips	9.40 ft
Moment:	7834.97 kips-ft	0.00 ft

Summary of Results for Controlling Applied Load Case

Depth [ft]	Displacement [in]	Shear Force [kips]	Flexural Moment [kips-ft]	Lateral Pressure [ksf]
Top of Stick (-3)	0.44	62.59	7647.20	0.00
-2	0.40	62.59	7709.79	0.00
-1	0.37	62.59	7772.38	0.00
Ground Level (0)	0.33	62.59	7834.97	0.00
1	0.30	-33.47	7738.49	13.91
2	0.26	-126.18	7545.95	12.70
3	0.23	-210.46	7264.93	11.50
4	0.19	-286.34	6903.83	10.30
5	0.16	-353.83	6471.04	9.10
6	0.12	-412.96	5974.94	7.91
7	0.09	-463.77	5423.88	6.73
8	0.05	-506.35	4826.13	5.56
9	0.02	-535.45	4191.06	2.26
10	-0.02	-534.54	3605.09	-1.06
11	-0.05	-519.20	3027.25	-3.12
12	-0.09	-489.46	2471.96	-5.13

FADTOOLS
Project Name: **PMT Tests**
Structure ID: **P-140**
Case Name: **Foundation Estimate**

Depth [ft]	Displacement [in]	Shear Force [kips]	Flexural Moment [kips-ft]	Lateral Pressure [ksf]
13	-0.12	-449.76	1952.00	-6.11
14	-0.16	-403.15	1475.19	-7.11
15	-0.19	-349.58	1048.46	-8.10
16	-0.23	-289.02	678.80	-9.10
17	-0.26	-221.43	373.20	-10.11
18	-0.30	-136.89	150.49	-12.51

Detailed Message:

FOUNDATION ANALYSIS AND DESIGN TOOLS
MFAD VERSION 5.1.20

Project Name:	**PMT Tests**	**Checked By:**	_____
Responsible Engineer:	**A Evans**		
Last Modified Date:	**06/25/2018 06:50:30**	**Date:**	_____
Comments:			

STRUCTURE

Structure ID: P-140
Description: Str 140

CASE-DRILLED SHAFT

Case Name: Foundation
Description: Str 140

Foundation Data (Str P-140)
Diameter of Drilled Shaft: [ft] 7
Stick up above Ground Level: [ft] 3

Model Options
Side Shear Spring: On
Base Shear Spring: On
Base Moment Spring: On

Geotechnical Parameters (3B/2B)
Depth to Ground Water: [ft] 50
All values in table are Nominal Values

Layer No.	Layer Type	Depth to Bottom of Layer [ft]	Total Unit Weight [pcf]	Deformation Modulus [ksi]	Friction Angle [Deg]	Undrained Shear Strength or Rock Cohesion [ksf]	Rock / Concrete Bond Strength [ksf]
1	Soil	9.00	118.0	11.70	40	1.00	0
2	Soil	17.00	111.0	8.80	45	0.25	0
3	Soil	21.00	107.0	5.70	42	1.00	0
4	Soil	26.50	112.0	6.00	48	0.00	0
5	Soil	29.00	114.0	6.00	50	1.25	0

Applied Loads-Top of Shaft (Str 140 x 1.1)

Load Case No.	Load Case Name	Shear Load [kips]	Moment [kip-ft]	Axial Load [kips]	Eccentricity [ft]
1	Str 140	62.59	7647.2	185.24	125.18

FADTOOLS
Project Name: **PMT Tests**
Structure ID: **P-140**
Case Name: **Foundation**

DESIGN RESULTS

Diameter of Drilled Shaft: [ft]	**7**
Stick up above Ground Level: [ft]	**3**
Depth of Embedment: [ft]	**18**
Total Foundation Length: [ft]	**21**
Controlling Applied Load Case Name:	**Str 140**

Capacity Verification

Loading Mode	Applied Load at Top of Shaft	Applied Load at Groundline	Nominal Capacity at Groundline	Design Capacity at Groundline*	Design Capacity / Applied Load at Groundline
Shear Load [kips]	62.59	62.59	266.13	167.66	2.68
Moment [kip-ft]	7647.20	7834.97	33314.38	20988.06	2.68

Design Capacity is based on a Strength Factor of 0.63

Performance Verification

	Criteria at Groundline	Actual at Groundline	Actual at Top of Shaft
Total Displacement [in]		0.25	0.33
Total Rotation [deg.]	1	0.12	0.12
Nonrecoverable Displacement [in]		0.04	0.06
Nonrecoverable Rotation [deg.]	0.5	0.02	0.02

Maximum Internal Forces

	Maximum Value	Depth of Occurrence
Shear:	545.02 kips	10.20 ft
Moment:	7834.97 kips-ft	0.00 ft

Summary of Results for Controlling Applied Load Case

Depth [ft]	Displacement [in]	Shear Force [kips]	Flexural Moment [kips-ft]	Lateral Pressure [ksf]
Top of Stick (-3)	0.33	62.59	7647.20	0.00
-2	0.30	62.59	7709.79	0.00
-1	0.28	62.59	7772.38	0.00
Ground Level (0)	0.25	62.59	7834.97	0.00
1	0.23	-28.86	7757.40	12.86
2	0.20	-115.18	7590.30	11.90
3	0.18	-194.72	7340.26	10.93
4	0.15	-267.50	7014.06	9.96
5	0.13	-333.54	6618.45	9.00
6	0.10	-392.84	6160.18	8.04
7	0.08	-445.44	5645.96	7.08
8	0.05	-491.38	5082.46	6.14
9	0.03	-530.46	4476.35	4.85
10	0.00	-544.66	3865.99	0.70
11	-0.02	-538.24	3251.74	-2.24
12	-0.05	-511.25	2654.22	-5.13

FADTOOLS
Project Name: **PMT Tests**
Structure ID: **P-140**
Case Name: **Foundation**

Depth [ft]	Displacement [in]	Shear Force [kips]	Flexural Moment [kips-ft]	Lateral Pressure [ksf]
13	-0.07	-470.43	2091.54	-6.41
14	-0.10	-420.67	1574.15	-7.68
15	-0.12	-361.94	1111.01	-8.97
16	-0.15	-294.20	711.09	-10.26
17	-0.17	-217.42	383.43	-11.55
18	-0.20	-133.76	161.20	-12.41

Detailed Message:

FOUNDATION ANALYSIS AND DESIGN TOOLS
MFAD VERSION 5.1.20

Project Name:	**PMT Tests**	**Checked By:**	_____
Responsible Engineer:	**A Evans**		
Last Modified Date:	**06/25/2018 06:50:12**	**Date:**	_____
Comments:			

STRUCTURE

Structure ID: P-202
Description: Str 202

CASE-DRILLED SHAFT

Case Name: Foundation Estimate
Description: Str 202

Foundation Data (Str P-202)
Diameter of Drilled Shaft: [ft] 7
Stick up above Ground Level: [ft] 3

Model Options
Side Shear Spring: On
Base Shear Spring: On
Base Moment Spring: On

Geotechnical Parameters (1A/3B Est)
Depth to Ground Water: [ft] 50
All values in table are Nominal Values

Layer No.	Layer Type	Depth to Bottom of Layer [ft]	Total Unit Weight [pcf]	Deformation Modulus [ksi]	Friction Angle [Deg]	Undrained Shear Strength or Rock Cohesion [ksf]	Rock / Concrete Bond Strength [ksf]
1	Soil	6.00	104.0	3.90	35	0.75	0
2	Soil	10.00	111.0	5.30	45	0.25	0
3	Soil	21.00	107.0	20.30	42	1.00	0
4	Soil	24.00	114.0	20.30	50	1.25	0

Applied Loads-Top of Shaft (Str 202 x 1.1)

Load Case No.	Load Case Name	Shear Load [kips]	Moment [kip-ft]	Axial Load [kips]	Eccentricity [ft]
1	Str 202	61.27	6643.12	178.53	111.42

FADTOOLS
Project Name: **PMT Tests**
Structure ID: **P-202**
Case Name: **Foundation Estimate**

DESIGN RESULTS

Diameter of Drilled Shaft: [ft]	**7**
Stick up above Ground Level: [ft]	**3**
Depth of Embedment: [ft]	**17**
Total Foundation Length: [ft]	**20**
Controlling Applied Load Case Name:	**Str 202**

Capacity Verification

Loading Mode	Applied Load at Top of Shaft	Applied Load at Groundline	Nominal Capacity at Groundline	Design Capacity at Groundline*	Design Capacity / Applied Load at Groundline
Shear Load [kips]	61.27	61.27	223.46	140.78	2.30
Moment [kip-ft]	6643.12	6826.93	24899.28	15686.55	2.30

Design Capacity is based on a Strength Factor of 0.63

Performance Verification

	Criteria at Groundline	Actual at Groundline	Actual at Top of Shaft
Total Displacement [in]		0.39	0.48
Total Rotation [deg.]	1	0.14	0.14
Nonrecoverable Displacement [in]		0.09	0.10
Nonrecoverable Rotation [deg.]	0.5	0.03	0.03

Maximum Internal Forces

	Maximum Value	Depth of Occurrence
Shear:	551.79 kips	13.20 ft
Moment:	6832.88 kips-ft	0.50 ft

Summary of Results for Controlling Applied Load Case

Depth [ft]	Displacement [in]	Shear Force [kips]	Flexural Moment [kips-ft]	Lateral Pressure [ksf]
Top of Stick (-3)	0.48	61.27	6643.12	0.00
-2	0.45	61.27	6704.39	0.00
-1	0.42	61.27	6765.66	0.00
Ground Level (0)	0.39	61.27	6826.93	0.00
1	0.36	12.24	6826.53	6.87
2	0.33	-34.56	6778.14	6.53
3	0.30	-78.94	6684.16	6.19
4	0.27	-120.91	6547.00	5.84
5	0.24	-160.46	6369.08	5.50
6	0.21	-197.60	6152.82	5.15
7	0.18	-242.67	5882.11	6.24
8	0.15	-284.74	5567.83	5.82
9	0.12	-323.89	5212.94	5.41
10	0.09	-360.17	4820.35	5.00
11	0.07	-443.33	4224.52	10.86
12	0.04	-510.63	3553.47	8.60

FADTOOLS
Project Name: **PMT Tests**
Structure ID: **P-202**
Case Name: **Foundation Estimate**

Depth [ft]	Displacement [in]	Shear Force [kips]	Flexural Moment [kips-ft]	Lateral Pressure [ksf]
13	0.01	-550.45	2825.95	2.18
14	-0.02	-534.28	2086.10	-5.99
15	-0.05	-469.78	1388.91	-10.82
16	-0.08	-382.28	768.35	-13.87
17	-0.11	-273.46	245.95	-16.92

Detailed Message:

FOUNDATION ANALYSIS AND DESIGN TOOLS
MFAD VERSION 5.1.20

Project Name:	**PMT Tests**	**Checked By:**	_____
Responsible Engineer:	**A Evans**		
Last Modified Date:	**06/25/2018 06:49:51**	**Date:**	_____
Comments:			

STRUCTURE

Structure ID: P-202
Description: Str 202

CASE-DRILLED SHAFT

Case Name: Foundation
Description: Str 202

Foundation Data (Str P-202)
Diameter of Drilled Shaft: [ft] 7
Stick up above Ground Level: [ft] 3

Model Options
Side Shear Spring: On
Base Shear Spring: On
Base Moment Spring: On

Geotechnical Parameters (1A/3B)
Depth to Ground Water: [ft] 50
All values in table are Nominal Values

Layer No.	Layer Type	Depth to Bottom of Layer [ft]	Total Unit Weight [pcf]	Deformation Modulus [ksi]	Friction Angle [Deg]	Undrained Shear Strength or Rock Cohesion [ksf]	Rock / Concrete Bond Strength [ksf]
1	Soil	6.00	104.0	5.30	35	0.75	0
2	Soil	10.00	111.0	9.00	45	0.25	0
3	Soil	21.00	107.0	20.90	42	1.00	0
4	Soil	24.00	114.0	20.90	50	1.25	0

Applied Loads-Top of Shaft (Str 202 x 1.1)

Load Case No.	Load Case Name	Shear Load [kips]	Moment [kip-ft]	Axial Load [kips]	Eccentricity [ft]
1	Str 202	61.27	6643.12	178.53	111.42

FADTOOLS
Project Name: **PMT Tests**
Structure ID: **P-202**
Case Name: **Foundation**

DESIGN RESULTS

Diameter of Drilled Shaft: [ft]	**7**
Stick up above Ground Level: [ft]	**3**
Depth of Embedment: [ft]	**17**
Total Foundation Length: [ft]	**20**
Controlling Applied Load Case Name:	**Str 202**

Capacity Verification

Loading Mode	Applied Load at Top of Shaft	Applied Load at Groundline	Nominal Capacity at Groundline	Design Capacity at Groundline*	Design Capacity / Applied Load at Groundline
Shear Load [kips]	61.27	61.27	223.46	140.78	2.30
Moment [kip-ft]	6643.12	6826.93	24899.28	15686.55	2.30

Design Capacity is based on a Strength Factor of 0.63

Performance Verification

	Criteria at Groundline	Actual at Groundline	Actual at Top of Shaft
Total Displacement [in]		0.31	0.38
Total Rotation [deg.]	1	0.11	0.11
Nonrecoverable Displacement [in]		0.06	0.08
Nonrecoverable Rotation [deg.]	0.5	0.02	0.02

Maximum Internal Forces

	Maximum Value	Depth of Occurrence
Shear:	542.08 kips	12.80 ft
Moment:	6831.10 kips-ft	0.40 ft

Summary of Results for Controlling Applied Load Case

Depth [ft]	Displacement [in]	Shear Force [kips]	Flexural Moment [kips-ft]	Lateral Pressure [ksf]
Top of Stick (-3)	0.38	61.27	6643.12	0.00
-2	0.35	61.27	6704.39	0.00
-1	0.33	61.27	6765.66	0.00
Ground Level (0)	0.31	61.27	6826.93	0.00
1	0.28	9.82	6821.76	7.31
2	0.26	-39.81	6765.67	6.91
3	0.23	-86.67	6661.33	6.51
4	0.21	-130.73	6511.53	6.12
5	0.19	-172.01	6319.05	5.72
6	0.16	-210.50	6086.70	5.32
7	0.14	-265.38	5778.95	7.53
8	0.12	-315.43	5418.75	6.84
9	0.09	-360.70	5010.90	6.16
10	0.07	-401.26	4560.13	5.49
11	0.04	-470.26	3962.14	9.03
12	0.02	-525.18	3301.68	6.09

FADTOOLS
Project Name: **PMT Tests**
Structure ID: **P-202**
Case Name: **Foundation**

Depth [ft]	Displacement [in]	Shear Force [kips]	Flexural Moment [kips-ft]	Lateral Pressure [ksf]
13	0.00	-541.52	2603.22	-0.74
14	-0.03	-510.06	1912.32	-7.57
15	-0.05	-442.24	1273.40	-10.90
16	-0.08	-355.90	711.67	-13.51
17	-0.10	-251.31	245.40	-16.11

Detailed Message:

FOUNDATION ANALYSIS AND DESIGN TOOLS
MFAD VERSION 5.1.20

Project Name:	**PMT Tests**	**Checked By:**	_____
Responsible Engineer:	**A Evans**		
Last Modified Date:	**06/25/2018 06:52:00**	**Date:**	_____
Comments:			

STRUCTURE

Structure ID: P-73
Description: Str 73

CASE-DRILLED SHAFT

Case Name: Foundation Estimate
Description: Str 73

Foundation Data (Str P-73)

Diameter of Drilled Shaft: [ft]	7
Stick up above Ground Level: [ft]	2

Model Options

Side Shear Spring:	On
Base Shear Spring:	On
Base Moment Spring:	On

Geotechnical Parameters (2A/3A/1B Est)
Depth to Ground Water: [ft] 50
All values in table are Nominal Values

Layer No.	Layer Type	Depth to Bottom of Layer [ft]	Total Unit Weight [pcf]	Deformation Modulus [ksi]	Friction Angle [Deg]	Undrained Shear Strength or Rock Cohesion [ksf]	Rock / Concrete Bond Strength [ksf]
1	Soil	8.00	102.0	7.40	30	0.00	0
2	Soil	23.00	105.0	10.00	37	0.40	0
3	Soil	27.00	106.0	2.20	36	0.40	0
4	Soil	30.00	123.0	7.50	36	1.30	0

Applied Loads-Top of Shaft (Str 73 x 1.1)

Load Case No.	Load Case Name	Shear Load [kips]	Moment [kip-ft]	Axial Load [kips]	Eccentricity [ft]
1	Str 73	61.27	6643.12	178.53	110.42

FADTOOLS
Project Name: **PMT Tests**
Structure ID: **P-73**
Case Name: **Foundation Estimate**

DESIGN RESULTS

Diameter of Drilled Shaft: [ft]	**7**
Stick up above Ground Level: [ft]	**2**
Depth of Embedment: [ft]	**20**
Total Foundation Length: [ft]	**22**
Controlling Applied Load Case Name:	**Str 73**

Capacity Verification

Loading Mode	Applied Load at Top of Shaft	Applied Load at Groundline	Nominal Capacity at Groundline	Design Capacity at Groundline*	Design Capacity / Applied Load at Groundline
Shear Load [kips]	61.27	61.27	116.12	73.15	1.19
Moment [kip-ft]	6643.12	6765.66	12822.06	8077.90	1.19

Design Capacity is based on a Strength Factor of 0.63

Performance Verification

	Criteria at Groundline	Actual at Groundline	Actual at Top of Shaft
Total Displacement [in]		0.75	0.85
Total Rotation [deg.]	1	0.24	0.24
Nonrecoverable Displacement [in]		0.31	0.35
Nonrecoverable Rotation [deg.]	0.5	0.09	0.09

Maximum Internal Forces

	Maximum Value	Depth of Occurrence
Shear:	519.65 kips	15.00 ft
Moment:	6939.63 kips-ft	4.60 ft

Summary of Results for Controlling Applied Load Case

Depth [ft]	Displacement [in]	Shear Force [kips]	Flexural Moment [kips-ft]	Lateral Pressure [ksf]
Top of Stick (-2)	0.85	61.27	6643.12	0.00
-1	0.80	61.27	6704.39	0.00
Ground Level (0)	0.75	61.27	6765.66	0.00
1	0.70	59.49	6824.32	0.49
2	0.65	53.96	6875.12	1.04
3	0.60	44.41	6913.87	1.63
4	0.55	30.59	6936.13	2.26
5	0.50	12.24	6937.22	2.92
6	0.45	-10.87	6912.24	3.62
7	0.40	-38.97	6856.05	4.34
8	0.35	-72.28	6763.31	5.10
9	0.30	-177.59	6474.82	14.17
10	0.25	-269.29	6087.83	12.23
11	0.20	-347.40	5615.93	10.29
12	0.15	-411.94	5072.71	8.35
13	0.10	-462.97	4471.71	6.42

FADTOOLS
Project Name: **PMT Tests**
Structure ID: **P-73**
Case Name: **Foundation Estimate**

Depth [ft]	Displacement [in]	Shear Force [kips]	Flexural Moment [kips-ft]	Lateral Pressure [ksf]
14	0.05	-500.58	3826.40	4.52
15	0.00	-519.65	3151.12	0.22
16	-0.05	-499.33	2476.50	-4.57
17	-0.10	-458.50	1833.83	-6.86
18	-0.15	-401.70	1239.98	-9.14
19	-0.20	-329.00	710.88	-11.41
20	-0.25	-240.39	262.44	-13.68

Detailed Message:

FOUNDATION ANALYSIS AND DESIGN TOOLS
MFAD VERSION 5.1.20

Project Name:	**PMT Tests**	**Checked By:**	_____
Responsible Engineer:	**A Evans**		
Last Modified Date:	**06/25/2018 06:51:40**	**Date:**	_____
Comments:			

STRUCTURE

Structure ID: P-73
Description: Str 73

CASE-DRILLED SHAFT

Case Name: Foundation
Description: Str 73

Foundation Data (Str P-73)

Diameter of Drilled Shaft: [ft]	**7**
Stick up above Ground Level: [ft]	**2**

Model Options

Side Shear Spring:	**On**
Base Shear Spring:	**On**
Base Moment Spring:	**On**

Geotechnical Parameters (2A/3A/1B)

Depth to Ground Water: [ft] **50**

All values in table are Nominal Values

Layer No.	Layer Type	Depth to Bottom of Layer [ft]	Total Unit Weight [pcf]	Deformation Modulus [ksi]	Friction Angle [Deg]	Undrained Shear Strength or Rock Cohesion [ksf]	Rock / Concrete Bond Strength [ksf]
1	Soil	8.00	102.0	6.00	30	0.00	0
2	Soil	23.00	105.0	8.90	37	0.40	0
3	Soil	27.00	106.0	8.90	36	0.40	0
4	Soil	30.00	123.0	8.90	36	1.30	0

Applied Loads-Top of Shaft (Str 73 x 1.1)

Load Case No.	Load Case Name	Shear Load [kips]	Moment [kip-ft]	Axial Load [kips]	Eccentricity [ft]
1	Str 73	61.27	6643.12	178.53	110.42

FADTOOLS
Project Name: **PMT Tests**
Structure ID: **P-73**
Case Name: **Foundation**

DESIGN RESULTS

Diameter of Drilled Shaft: [ft]	**7**
Stick up above Ground Level: [ft]	**2**
Depth of Embedment: [ft]	**20**
Total Foundation Length: [ft]	**22**
Controlling Applied Load Case Name:	**Str 73**

Capacity Verification

Loading Mode	Applied Load at Top of Shaft	Applied Load at Groundline	Nominal Capacity at Groundline	Design Capacity at Groundline*	Design Capacity / Applied Load at Groundline
Shear Load [kips]	61.27	61.27	116.12	73.15	1.19
Moment [kip-ft]	6643.12	6765.66	12822.06	8077.90	1.19

Design Capacity is based on a Strength Factor of 0.63

Performance Verification

	Criteria at Groundline	Actual at Groundline	Actual at Top of Shaft
Total Displacement [in]		0.85	0.96
Total Rotation [deg.]	1	0.26	0.26
Nonrecoverable Displacement [in]		0.34	0.39
Nonrecoverable Rotation [deg.]	0.5	0.10	0.10

Maximum Internal Forces

	Maximum Value	Depth of Occurrence
Shear:	519.64 kips	15.00 ft
Moment:	6939.58 kips-ft	4.60 ft

Summary of Results for Controlling Applied Load Case

Depth [ft]	Displacement [in]	Shear Force [kips]	Flexural Moment [kips-ft]	Lateral Pressure [ksf]
Top of Stick (-2)	0.96	61.27	6643.12	0.00
-1	0.90	61.27	6704.39	0.00
Ground Level (0)	0.85	61.27	6765.66	0.00
1	0.79	59.49	6824.32	0.49
2	0.73	53.95	6875.12	1.04
3	0.68	44.40	6913.85	1.63
4	0.62	30.57	6936.09	2.26
5	0.56	12.21	6937.15	2.92
6	0.51	-10.91	6912.12	3.62
7	0.45	-39.03	6855.87	4.35
8	0.39	-72.37	6763.04	5.11
9	0.34	-177.64	6474.51	14.16
10	0.28	-269.32	6087.51	12.22
11	0.22	-347.41	5615.63	10.28
12	0.17	-411.94	5072.43	8.35
13	0.11	-462.96	4471.47	6.42

FADTOOLS
Project Name: **PMT Tests**
Structure ID: **P-73**
Case Name: **Foundation**

Depth [ft]	Displacement [in]	Shear Force [kips]	Flexural Moment [kips-ft]	Lateral Pressure [ksf]
14	0.06	-500.58	3826.19	4.52
15	0.00	-519.64	3150.95	0.21
16	-0.06	-499.30	2476.39	-4.56
17	-0.11	-458.48	1833.77	-6.86
18	-0.17	-401.69	1239.97	-9.14
19	-0.23	-328.98	710.93	-11.41
20	-0.28	-240.37	262.54	-13.68

Detailed Message: